

Security Cost Analysis in Electricity Markets Based on Voltage Security Criteria and Web-based Implementation

by

Hong Chen

A thesis
presented to the University of Waterloo
in fulfillment of the
thesis requirement for the degree of
Doctor of Philosophy
in
Electrical and Computer Engineering

Waterloo, Ontario, Canada, 2002

© Hong Chen 2002

I hereby declare that I am the sole author of this thesis.

I authorize the University of Waterloo to lend this thesis to other institutions or individuals for the purpose of scholarly research.

I further authorize the University of Waterloo to reproduce this thesis by photocopying or by other means, in total or in part, at the request of other institutions or individuals for the purpose of scholarly research.

The University of Waterloo requires the signatures of all persons using or photocopying this thesis. Please sign below, and give address and date.

ABSTRACT

For a simple auction market model, this thesis presents an efficient and transparent approach for transaction security cost analysis to quantify the correlation between market operation and power system operation, which is an important and challenging issue in electricity markets.

Two different strategies, namely, rescheduling and take-risk, are proposed and discussed in detail based on adequate “System-wide” ATC (SATC) and transaction impact computations, considering thermal and voltage limits, as well as voltage stability criteria. The rescheduling technique is associated with an iterative generation redispatch and/or load curtailment procedure to minimize the amount of rescheduling; whereas the take-risk technique is based on the idea of taking a less conservative approach to consider operating risks to facilitate transactions. In this thesis, the SATC concept is proposed to accurately evaluate transmission congestion. The transactions’ impact is computed using novel sensitivity formulas to find the most effective rescheduling direction, as well as for cost distribution. A novel pricing method, i.e. Nodal Congestion Price (NCP), is also proposed to generate proper price signals.

An Artificial Neural Network (ANN) based Short Term Load Forecasting (STLF) method considering the effect of price on the load is presented for a distributed computational scheme, to provide proper load prediction. To facilitate the access of all market participants to the proposed analysis and pricing techniques, a web-based prototype is implemented using a three-tier client/server architecture and up-to-date web technologies.

The results of several case studies on various test systems show the effectiveness and applicability of the proposed techniques, which would help Independent System

Operators (ISOs) determine congestion prices, coordinate and manage transactions, and also help market participants make profitable market decisions.

ACKNOWLEDGMENTS

I would like to sincerely thank Prof. Claudio Cañizares and Prof. Ajit Singh, for their guidance, support and continuous encouragement throughout these years of my Ph.D. study in Waterloo.

Also acknowledged is the invaluable suggestion provided by Prof. David Fuller, Prof. Victor Quintana, Prof. Magdy Salama and Prof. Gordon Agnew.

During this research topic development, I was greatly helped by Dr. Chi Tang, Mr. Derek Beamer, Mr. Andrew Zulawski, Mr. Mike Falvo and Mr. Mike Isber from IMO, and Dr. Deqiang Gan from NewEngland ISO. I very much appreciate their enlightening discussions and information. I also would like to thank Prof. Roy Billinton from University of Saskatchewan and Mr. John Kehler from EAL Alberta for the information provided for my research.

A group of people I have to mention are my office-mates, Edvina, Lily, Bill, Mithulan, Cavalo, Federico, Sameh, Hassan, Warren and Valery. They created friendly work environment. I always enjoy being colleague with Mithulan for all these years; and thank Federico for providing the Italian system data.

A very special thank should go to my husband, colleague, Jianwei Liu, for his love, support and help ever since we met. Without him, my dreams will never become true.

Last but not least, I would like to thank the invaluable support of my family. My beloved father and mother have undergone all the hardships in bringing up and educating their daughter. They gave me the great love for all my life. My parents-in-law also gave me their encouragement and support for my study and life as much as they can.

This thesis is dedicated to my very special daughter, Sophia!

GLOSSARY

AC	Altenate Current
ANN	Artificial Neural Network
ATC	Available Transfer Capability
CBM	Capacity Benefit Margin
CPF	Continuation Power Flow
DAE	Differential Algebraic Equation
DBMS	DataBase Management System
DC	Direct Current
DISCO	Distribution Company
ESCO	Electrical Service Company
ETC	Existing Transmission Commitment
FCTTC	First Contingency Total Transfer Capability
GENCO	Generation Company
GUI	Graphic User Interface
HTML	HyperText Markup Language
HTTP	Hyper-Text Transfer Protocol
IMO	Independent Market Operator
IPC	Inter-Process Communication
ISO	Independent System Operator
JVM	Java Virtual Machine
LAN	Local Area Network
LIB	Limit-Induced Bifurcation
LMP	Locational Marginal Price
MAPE	Mean Absolute Percentage Error

MCP	Market Clearing Price
MO	Market Operator
NCP	Nodal Congestion Price
OASIS	Open Access Same time Information System
OLB	Operating Limit Boundary
OPF	Optimal Power Flow
RMI	Remote Method Invocation
RMSE	Root Mean Square Error
SATC	“System-wide” Available Transfer Capability
SCOPF	Security Constrained Optimal Power Flow
SCADA	Supervisory Control And Data Acquisition
SETC	“System-wide” Existing Transmission Commitment
SNB	Saddle-Node Bifurcation
STLF	Short Term Load Forecasting
STRM	“System-wide” Transmission Reliability Margin
STTC	“System-wide” Total Transfer Capability
TCF	Transaction Contribution Factor
TI	Transaction Impact
TOF	Transaction Operational Feasibility
TRM	Transmission Reliability Margin
TSC	Transaction Security Cost
TTC	Total Transfer Capability
WWW	World Wide Web

Contents

1	Introduction	1
1.1	Electricity Markets	1
1.1.1	Energy Brokerage	5
1.1.2	Transmission Congestion	7
1.1.3	Security Cost and Pricing Analysis	8
1.2	Motivation and Objectives	10
1.3	Thesis Outline	13
2	TOF and TI Analysis	14
2.1	Introduction	15
2.2	Voltage Stability	16
2.2.1	Basic Concepts	16
2.2.2	Continuation Power Flow	21
2.3	ATC Definitions and Computations	25
2.3.1	ATC Definitions	27

2.3.2	“System-wide” ATC (SATC) Computation	28
2.4	Transaction Operational Feasibility (TOF) Analysis	31
2.5	Transaction Impact (TI) on SATC	33
2.6	Case Studies	37
2.6.1	Case 1: With Demand-side Bidding	37
2.6.2	Case 2: Inelastic Demand	41
2.7	Summary	44
3	TSC Analysis by Rescheduling Strategy	45
3.1	Introduction	45
3.2	Rescheduling Procedure	47
3.3	Case Studies	54
3.3.1	Three-area Electricity Market	54
3.3.2	Six-bus System	59
3.3.3	129-bus Model of Italian HV Transmission System	64
3.4	Summary	65
4	TSC Analysis by Take-risk Strategy	71
4.1	Introduction	71
4.2	Analysis Procedure	72
4.3	Case Studies	77
4.3.1	Three-area Electricity Market	77

4.3.2	Six-bus System	80
4.3.3	129-bus Model of Italian HV Transmission System	81
4.4	Summary	83
5	STLF in Electricity Markets	85
5.1	Introduction	86
5.2	Load Characteristics	87
5.3	An ANN-based STLF	89
5.3.1	Forecasting Model	89
5.3.2	Forecasting Procedure	93
5.4	Case Study	95
5.5	Summary	102
6	Web-based Implementation	105
6.1	Introduction	105
6.2	Web-based TSC Analysis	108
6.2.1	Requirements	108
6.2.2	Architecture	112
6.2.3	Implementation	114
6.3	Implementation of the STLF Module	118
6.3.1	Architecture	124
6.3.2	Implementation	124
6.4	Summary	127

7	Conclusions	129
7.1	Summary	129
7.2	Contributions	131
7.3	Future Work	132
	Bibliography	133
A	Three-area Electricity Market	149
B	Six-bus Test System	151
C	129-bus Model of Italian HV Transmission System	154

List of Figures

1.1	A wholesale electricity market.	2
2.1	A PV curve showing loading margin.	20
2.2	The main procedure of CPF.	22
2.3	CPF shown in a PV curve.	23
2.4	TOF analysis procedure.	32
2.5	Six-bus test system.	38
2.6	High-low bid matching with demand-side bidding, six-bus system. .	39
2.7	High-low bid matching for inelastic demand, six-bus system. . . .	42
3.1	Rescheduling procedure.	48
3.2	Three-area electricity market.	55
3.3	Generation redispatching results, three-area electricity market. . .	57
3.4	Load curtailment results, three-area electricity market.	58
3.5	129-bus model of the Italian HV transmission system.	66
3.6	Some NCPs by rescheduling technique, 129-bus Italian system. . . .	67

4.1	Probability distribution of collapse, six-bus test system.	74
4.2	Probabilistic density of system collapse, six-bus test system.	75
4.3	Security cost comparison, three-area electricity market	79
4.4	Some NCPs by take-risk technique, 129-bus Italian system.	83
5.1	Mathematical model of an ANN neuron.	90
5.2	Schematic of the three layer feed-forward ANN for STLF.	91
5.3	ANN-based demand forecasting procedure.	94
5.4	Training performance of the chosen ANN.	97
5.5	Forecasting results for Monday May 24, 1999.	98
5.6	Forecasting results for Thursday May 27, 1999.	99
5.7	Forecasting results for Saturday May 29, 1999.	100
5.8	Absolute percentage errors for the May 1999 load data set.	101
5.9	Comparison of the forecasting results for June 1, 1999. This data is not used for the ANN training.	103
6.1	Web-based distributed computational network.	107
6.2	Level-0 data flow diagram of the TSC analysis.	109
6.3	Data dependence between the web-based TSC modules.	110
6.4	Three-tier client/server architecture.	113
6.5	Pseudocode of <code>basecon</code> servlet.	116
6.6	Pseudocode of <code>atc</code> servlet.	117
6.7	Database interface.	119

6.8	Part of the input GUI.	120
6.9	SATC results.	121
6.10	Rescheduling results.	122
6.11	Take-risk results.	123
6.12	Distributed STLF architecture.	125
6.13	Remote interface and remote object.	126

List of Tables

1.1	Electricity market comparison	4
2.1	Load and generation increase direction with demand-side bidding, six-bus system	40
2.2	Loading margin results with demand-side bidding, six-bus system .	40
2.3	Load and generation increase direction for inelastic demand, six-bus system	43
2.4	Loading margin results for inelastic demand, six-bus system	43
3.1	Price-quantity bids, three-area electricity market	55
3.2	Loading margin results, three-area electricity market	56
3.3	Rescheduling results with demand-side bidding, six-bus system . . .	60
3.4	TCFs with demand-side bidding, six-bus system	60
3.5	NCPs with demand-side bidding, six-bus system	61
3.6	Curtailement bids for inelastic demand, six-bus system	62
3.7	Generation redispatch results for inelastic demand, six-bus system .	62
3.8	Load curtailement results for inelastic demand, six-bus system	63

3.9	TCFs for inelastic demand, six-bus system.	63
3.10	NCPs for inelastic demand, six-bus system.	64
3.11	Generation increase direction, 129-bus Italian system	67
3.12	Load increase direction, 129-bus Italian system	68
3.13	Loading margin results, 129-bus Italian system	69
3.14	Rescheduling results, 129-bus Italian system	69
4.1	Security costs vs. probability distribution, three-area electricity market	78
4.2	TCFs, three-area electricity market	78
4.3	NCPs, three-area electricity market	78
4.4	TCFs with demand-side bidding, six-bus system.	80
4.5	Security costs vs. probability distribution with demand-side bidding, six-bus system.	81
4.6	NCPs with demand-side bidding, six-bus system	82
4.7	Security costs vs. probability distribution, 129-bus Italian system .	82
5.1	Comparison of the number of iterations	102
6.1	Execution times	127
B.1	Price-quantity bids	153
C.1	Supply bids: I	161
C.2	Supply bids: II	162
C.3	Demand bids: I	163

C.4	Demand bids: II	164
C.5	Demand bids: III	165
C.6	Demand bids: IV	166

Chapter 1

Introduction

1.1 Electricity Markets

Worldwide power industries are changing from traditional monopolies to competitive markets, from vertically integrated utilities to deregulated electricity markets, with the original purpose to achieve higher efficiency and lower price. In electricity markets, as shown in Figure 1.1, generation, transmission and distribution are separated and deregulated; competition is introduced in both the generation side and the consumption side, whereas the transmission of power from suppliers to customers is integrated to provide open and equal access to all market participants to ensure fair competition [1, 2, 3, 4].

The implementation of electricity markets varies throughout the world. However, market models can be categorized into three main groups, i.e. centralized markets, decentralized markets, and hybrid markets [4]. Centralized markets can be viewed as unit commitment and Optimal Power Flow (OPF) problems, where a “central” operator, such as Independent System Operator (ISO), takes care of cen-

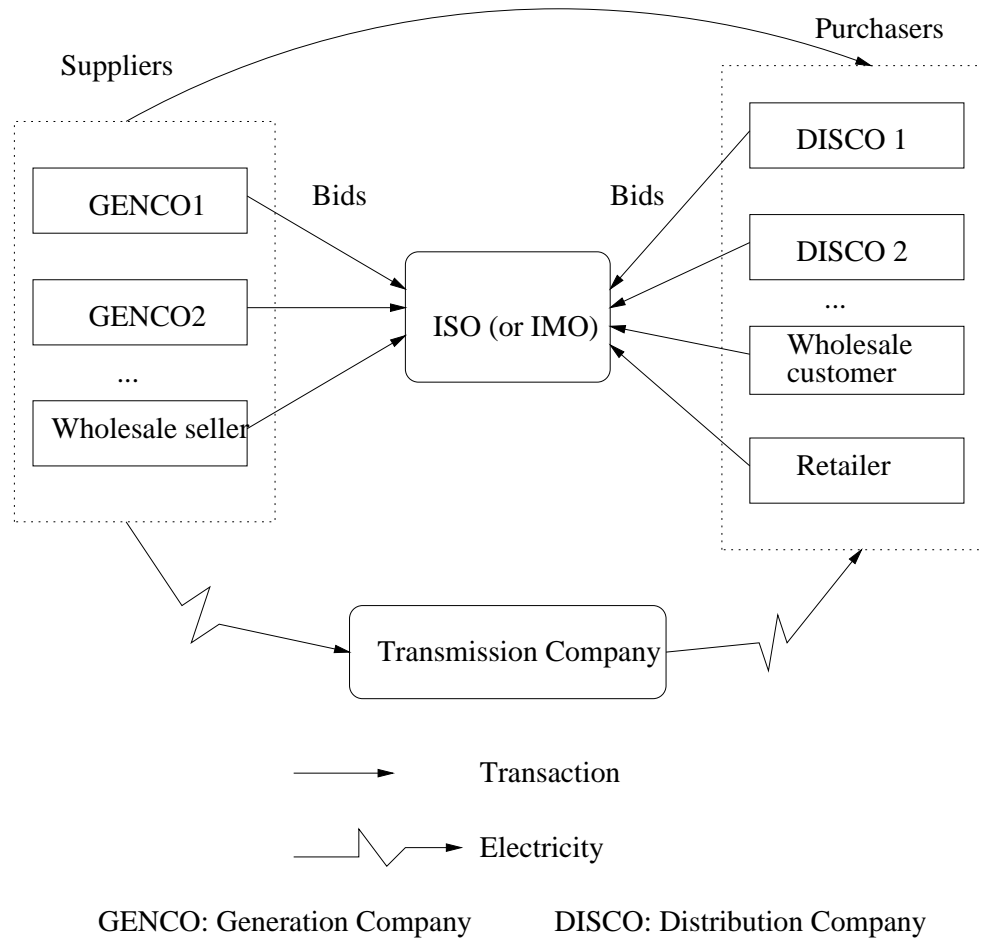


Figure 1.1: A wholesale electricity market.

tral market operation and transmission system operation. In decentralized markets, Market Operator (MO) is in charge of determining market schedules and the Market Clearing Price (MCP) based on participants' bids, and using a simple auction mechanism. In this case, the transmission security and congestion management are performed by an ISO. Hybrid markets are based on spot pricing theory [5] and OPF methods. Among these market models, decentralized markets are considered as "transparent" to all market participants and are purely market oriented. However, market operation and system operation are decoupled.

Two types of pricing schemes, i.e. uniform pricing and locational pricing, are generally used. Under uniform pricing, all participants receive the same price, while, locational pricing accounts for locational differences in the costs of transmission losses and transmission congestion, and thus is able to generate proper price signals for both orderly market operation and secure system operation. Locational Marginal Prices (LMP), which are typically used in locational pricing schemes, are typically associated with the Lagrange multipliers of OPF process.

Table 1.1 summarizes the most recent structures of some typical electricity markets in the world.

In competitive electricity markets, the demand, i.e. the load, has both elastic and inelastic components which are associated with their responses to price changes. Thus, if the demand changes as price changes, the load is said to be elastic; for inelastic load, on the other hand, the demand does not directly respond to price changes. For the online operation, the demand information comes from demand bids and load forecasting; load forecasting considering market price is a new challenge that is expected to provide more accurate forecasting results for market and system operation.

Table 1.1: Electricity market comparison

Market	Market Opening Year	Central Market/System Operator	Market Model	Price Scheme
Chile [6, 7]	1982	CDEC	centralized	node price
UK [8]	1990	NGC	from centralized to decentralized	from uniform to pay-as-bid
Alberta [9]	1996	Power Pool/ EAL	decentralized	uniform pricing
PJM [10]	1997	PJMISO	centralized	LMP
Spain [11]	1998	MO/ISO	decentralized	uniform pricing
California [12]	1998- 2001	PX/ Cal-ISO	decentralized	locational pricing
New York [13]	1998	NYISO	centralized	LMP
New England [14]	1999	ISO New England	centralized	uniform(now)/ LMP(future)
Ontario [15]	2002	IMO	hybrid	uniform(now)/ LMP(future)

In a successful electricity market, the correlation between efficient market operation and secure system operation is very important. Because of the lack of large quantity energy storage, in today's markets, the generation and consumption must be balanced at all times. The transaction and price determination are usually coordinated by energy brokerage systems within the physical constraints of electric power systems. Only transactions that do not violate system security limits are operationally feasible; those that violate the limits lead to congestion problems, which require the intervention of system operators to relieve them. Facing the complexities of power transactions, congestion management and pricing is a key issue in the daily operation of electricity markets [16, 17, 18, 19]. Security cost analysis, which basically consists on figuring out the cost of congestion relief, provides the proper market signals to market participants for competitive decision-making [5].

1.1.1 Energy Brokerage

Energy brokerage is a centralized trading process important for market operation. Impartial central brokers, such as NGC in UK [8], NYISO in New York [13], PJMISO in PJM [10], ISO New England in New England [14], the IMO in Ontario [15], etc. are in charge of matching bids sent by market participants and thus determine market schedules and transaction prices considering economic efficiency and transmission security [15, 20]. Energy brokerage is also referred to as bid-clearing [21, 22, 23], auction [20, 21, 22, 24, 25], trading [26], etc.

Energy brokerage is essentially an optimization problem. The energy brokerage methods can be categorized into two classes: high-low bid matching and Security Constrained Optimal Power Flow (SCOPF).

The high-low bid matching method [27], which matches highest buying bids

with lowest selling bids, is the most widely used method in practical markets. It is also known as simple bid energy auction, since participants only submit the power quantity and its unitary price [21, 22]. This method provides a simple mechanism to determine transaction schedules and energy prices. However, security constraints are not considered in this process.

SCOPF methods implement more complex energy brokerage mechanisms in which the bids are matched in such a way to achieve maximum social benefit (or minimum social cost) while satisfying certain security constraints at the same time. Social benefit is expressed here as the benefit of energy consumption minus the cost of energy production. To solve the market scheduling problems, some linear programming approaches have been proposed [20, 21, 22, 28, 29, 30]. Valuable observations and discussions on different optimization models and techniques for simple-bid format and multi-part bid format auctions can be found in [21, 22]. Transmission security constraints usually are highly nonlinear and are difficult to include in the optimization model, especially for large practical systems. Therefore, most approaches use simplified security constraints, such as thermal limits in DC models of the networks, or simple voltage and transmission power limits in AC models, which do not accurately represent actual system constraints.

It is obvious that the more accurate the system operation constraints considered in the brokerage process, the more feasible the bid matching results will be, i.e. the power transactions that result from this process will meet system security constraints corresponding to actual operating conditions associated with these transaction levels. This problem remains unresolved, due to the complexity of accounting for accurate security constraints in the energy brokerage process.

1.1.2 Transmission Congestion

Transmission congestion occurs when the dispatching of transactions violates transmission security constraints, which are set by thermal limits, voltage limits and stability limits [31]. Congestion leads to cheaper generation not being delivered through the transmission network to the desired load, thus increasing the cost of energy for the users. In competitive electricity markets, transmission congestion affects the feasibility of transactions yielding variations in prices associated with the location of the participants; in some cases, it may even lead to price spikes [18, 19].

Congestion management is the process of managing generators and loads to maintain an acceptable level of power system security in both short-term and long-term, while maximizing market efficiency. Generation re-dispatch and load curtailment are two essential ways to relieve congestion [18]. In the deregulated/privatized environment, with the increasing complexity of potential transactions, the impact on system and market operation caused by congestion management need to be carefully investigated [32, 33].

Congestion pricing addresses the issue of first determining the cost of congestion management, and then trying to price these costs in electricity markets. It bridges economic and security concerns in electricity markets, and can be applied as a functional feedback signal to relieve congestion in real-time or pre-dispatch periods, and motivate market participants to adjust their behaviors in the short and long term [34].

Congestion management and pricing is one of the most important and challenging tasks of an ISO, and has been at the center of the debate of how to facilitate greater competition in power generation and consumption [31]. If the congestion

problem has been identified, and hence the associated security problem has been resolved, then the task left is to find an optimal or sub-optimal solution to different system or market operation objectives. Examples of these objectives are: minimizing the total production cost [31, 35, 36]; maximizing social surplus [37]; minimizing congestion relief cost [38]; minimizing the absolute MW of rescheduling [39]; minimizing the deviations from transaction requirement [40]; or minimizing the total system ancillary energy service [41]. Linear DC power flow models or AC power flow models are extensively used to represent transmission security constraints, by means of power flow, voltage and current limits. Highly nonlinear stability constraints are still difficult to be included in these optimization or sub-optimization processes. A common practice is to express stability limits as power flow limits obtained through “off-line” computation, as suggested in [42]. However, these limits are not accurate, as they do not represent the actual stability limits of the network.

In [43], the authors discuss the effect of dynamic security in congestion management, using the sensitivity of transient energy margins with respect to changes in generation. The relief of congestion using voltage security concepts is discussed in [44], where certain heuristics are used to minimize costs based on constrained-on and constrained-off generators, and interruptible loads.

1.1.3 Security Cost and Pricing Analysis

System security, an important concern in power system planning and operation, is the ability of the electric system to withstand sudden disturbances [42]. It is an issue related to all generation, load and transmission. In this thesis, only transmission security is considered. Security issues on generation and load, such as frequency control, are out of the scope of this work. Hence, security here will be closely

associated with transmission congestion, and security costs will represent in this thesis the cost of congestion relief.

Since an efficient economical solution requires prices based on costs [5, 34], in competitive electricity markets, transaction costs are unbundled into several components [45], which vary as functions of time, location, load and generation patterns, and system configuration. Accurate knowledge of unbundled cost components is vital for pricing transactions correctly, especially for locational pricing, thus helping market participants make adequate operation and business decisions. In order to set that prices efficiently, security costs, a component of the total unbundled costs that ensure the operational feasibility of the transactions, needs to be properly determined.

Determining the costs associated with system security has been of great interest in power systems, especially under the framework of competitive electricity markets [45, 46, 47, 48, 49, 50]. In these papers, optimization techniques are extensively used, and the Lagrange multipliers associated with the given security constraints are used to represent security costs. This idea of pricing security was first advanced in [5] by means of representing system security through line flow constraints. Contingency pricing is studied in [51], based on a probabilistic framework to achieve a social optimal level of security. In all of these references, rather conservative limits on the transmission system power flows and bus voltage magnitudes are usually used to represent system security, where these power flow and voltage limits being typically determined through off-line studies and by making fairly conservative assumptions to account for operating uncertainties.

A series of engineering approaches not based on optimization techniques to analyze security costs are reported in [33, 52, 53]. In [52], the authors determine the outage cost based on probabilistic measures, using the distance to an Operation

Limit Boundary (OLB) defined by means of point of collapse methods. In [53], a geometric approach is used to consider pricing near any security constraints.

The objective of security cost-based pricing is to fairly distribute security costs among all market participants, as well as give incentives for using the transmission system efficiently. Different cost allocation strategies have been proposed. Locational Marginal Pricing (LMP), which is based on the marginal cost of supplying the next MWh at a particular location, is being proposed as an efficient technique to price security [5, 18, 35, 51, 54, 55, 56]. LMP is usually associated with Lagrange multipliers obtained from security constrained optimal power flow problems, and is designed to generate revenue for future transmission enhancement. A “usage” based method, proposed in [31], is a two step process in which the total congestion cost is first allocated to the congested facilities, and then to the bilateral transactions involved in the use of these facilities. A similar approach is proposed in [38], where “usage” is measured by complex power flows; it is designed to fully recover costs. A “responsibility” based allocation method is discussed in [36], to overcome some asymmetries of LMP methods, using a hypothetical load reduction on the system nodes. How to price security based on costs depends on different market rules. In this thesis, a novel pricing method that could be categorized as a “responsibility” based technique is proposed based on transaction impact analysis.

1.2 Motivation and Objectives

In electricity markets, generation must be matched with demand at any time, considering that transmission systems have certain security requirements. Therefore, efficient market operation must be coordinated with secure system operation. Because of system security requirements, transactions determined by market forces

are feasible only when they are within the systems' transmission transfer capabilities. Thus, transactions in electricity markets need to be evaluated and analyzed based on system security to make sure of their operational feasibility, in this thesis it is basically associated with transmission congestion management. The correct cost information for congestion relief, which ensures feasibility of transactions and referred to as "security costs" in this thesis, can help ISOs determine congestion prices, coordinate and manage transactions, and also help market participants make profitable market decisions for themselves and maintain system security by properly responding to the given price signals.

Based on the assumption that system configuration has already been set to maximize security limits, typical way to relieve transmission congestion is redispatching generators and/or curtailing loads to bring the system back to limits [18], which is a common practice for system operators and is one of the techniques used in this work. Another novel option, proposed here, is to ease security constraints based on the observation that security limits are usually rather conservative to account for unexpected disturbances. In such a scenario, certain risks are taken to facilitate transactions, driven by potential market profits.

As the overall system load increases, voltage stability becomes the limiting security constraints among all thermal, voltage and stability limits [57]. Hence, for the purpose of this thesis, transfer capability computations considering thermal, voltage and voltage stability limits will be used for detecting transmission congestion, and thus determining transaction feasibility and transaction security costs. Determining a realistic load increase direction is important for the transfer capability computations, thus Short-Term Load Forecasting (STLF) can be used for this task. In order to obtain high forecasting accuracy in an electricity market environment, price factors need also to be considered in the forecasting procedure, besides

traditional load affecting factors [58]. In this thesis, an Artificial Neural Network (ANN) based STLF methodology will be proposed for load forecasting in electricity markets.

Effective methods to analyze transaction feasibility, transaction impact and transaction security costs based on voltage security criteria in a simple bid auction market are proposed in this research. The purpose is to generate adequate feedback signals to market participants for an orderly market operation and secure system operation. An efficient way in which all market participants, which are geographically widely distributed and have heterogeneous hardware and software platforms, can easily and widely carry out this analysis is to implement the proposed techniques on a web-based platform, which is user friendly and installation/configuration free.

Based on all of the above, the objectives of this research are as follows:

1. Analyze transaction operational feasibility and transaction impact considering thermal limits, voltage limits and voltage stability limits, based on a proposed “System-wide” ATC (SATC) computation and sensitivity analysis.
2. Analyze transaction security costs and pricing by means of rescheduling strategy, based on an iterative procedure of generation re-dispatching and/or load curtailment.
3. Analyze transaction security costs and pricing by means of a take-risk strategy based on a probabilistic view of the proposed SATC.
4. Develop an efficient STLF computational method to provide proper load information for the proposed Transaction Security Cost (TSC) and pricing analysis.

5. Implement the above analysis using web-based computing, based on a three-tier client/server architecture and up-to-date web technologies.

1.3 Thesis Outline

This thesis is organized as follows: Chapter 2 discusses the analyses of Transaction Operational Feasibility (TOF) and Transaction Impact (TI), associated with the proposed SATC computation. These analyses are all based on voltage security concepts and tools. Chapter 3 presents the proposed rescheduling techniques used for transaction security cost and pricing analysis, from a deterministic view; whereas, Chapter 4 discusses similar issues from a probabilistic and take-risk point of view.

In Chapter 5, an ANN-based STLF method that can be used to determine load patterns for the SATC computation in electricity markets is presented. The prototype implementation of all of the proposed analyses with web-based computing techniques is discussed in Chapter 6. Finally, Chapter 7 provides the main contribution of this thesis and discusses possible future research directions.

Chapter 2

Transaction Operational Feasibility and Impact Analysis

Chapter Synopsis

Transaction Operational Feasibility (TOF) analysis is the process by which system operators check if the dispatching of transactions violates operating limits, i.e. whether the potential transactions create congestion problems. On the other hand, Transaction Impact (TI) analysis consists of determining how the changes of transactions affect transmission congestion. Hence, in this thesis, this impact analysis is used to determine the most efficient rescheduling option, as well as to distribute total security costs among market participants.

The TOF and TI analyses are based on voltage security concepts and tools. Thus, in this Chapter, the basic concepts of voltage stability are first reviewed, followed by a discussion of the definition and computation of Available Transfer Capability (ATC). Then, TOF and TI analysis procedures based on the computation of “System-wide” ATC (SATC) are proposed and discussed in detail. A case

study based on a six-bus test system is used to illustrate the concepts and analysis techniques presented in this Chapter.

2.1 Introduction

Because of power system security requirements, the transfer capabilities of transmission systems are limited. In electricity markets, transactions proposed by the market forces are hence limited by these security requirements. Thus, transactions are operational feasible only when they are within the transfer capabilities of the network, so that these are dispatched without violating transmission security limits. After bid matching, potential transactions need to be checked by market/system operators for their operational feasibility [59, 60]; market participants can also use this feasibility analysis to estimate the possibilities of the acceptances of their bids for strategic bidding to achieve higher profits [61].

ATC, which defines the extent of the usage of transmission networks by transmission services customers, is an important market signal of the capability of transmission systems to securely and reliably deliver energy [62]. The knowledge of accurate ATC values and the associated speedy computation become more important with increasing energy use and open access. Its calculation has become a challenging task for ISOs [63, 64]. For example, in US, the calculations of ATC for each control area is mandated and the value is required to be posted on Open Access Same-time Information System (OASIS) for transmission access [65].

Due to the physical characteristics of transmission networks, each transaction has an impact on the voltages and power flows of the whole transmission networks, thus affects the value of ATC. The information of transaction impact is important to provide guidance to relieve transmission congestion and determine transaction

security costs [32, 33]. TI analysis basically consists on determining how changes of transactions affect transmission networks, such as power flow, losses, voltages etc. so that thermal limits, voltage limits and stability limits can be respected.

Most of the reported efforts have been put on determining the contributions of generators to line flows, losses, reactive powers, which can be used for power flow tracing, transmission service allocation, as well as transmission load relief [66, 67, 68, 69, 70, 71]. However, so far, stability limits have not been properly accounted for, due to their high non-linearity. Thus, TI analysis is a challenging issue, especially for real-time operation [32, 33, 43, 72, 73].

In the current market environment, the increase of load demand and power transfers may force power systems to operate under increasingly stressed conditions, and hence make them more prone to stability problems, in view of the current status of transmission networks. Under these conditions, system stability can be approximately studied through voltage stability analysis. In this thesis, bifurcation-based techniques, especially Continuation Power Flow (CPF) methods [74, 75, 76, 77], are used for voltage stability analysis to efficiently provide the required information for TOF and TI analysis.

2.2 Voltage Stability

2.2.1 Basic Concepts

A power system is typically modelled using the following generic set of Differential-Algebraic Equations (DAE) for stability studies, with “slowly” changing bifurcation

parameter λ that is typically used to represent loading level [57]:

$$\begin{aligned}\dot{x} &= f(x, y, \lambda, p) \\ 0 &= g(x, y, \lambda, p)\end{aligned}\tag{2.1}$$

where x corresponds to the system state variables, y represents the “algebraic” variables, and p corresponds to “controllable” system parameters. An equilibrium point $(x_0, y_0, \lambda_0, p_0)$ corresponds to the solution of the steady-state equations

$$\begin{aligned}f(x_0, y_0, \lambda_0, p_0) &= 0 \\ g(x_0, y_0, \lambda_0, p_0) &= 0\end{aligned}\tag{2.2}$$

With changes in the parameter λ , the system typically moves from one equilibrium point to another until reaching the collapse point.

By defining $z = [x \ y]^T$, equation (2.1) can be rewritten as

$$\begin{bmatrix} \dot{x} \\ 0 \end{bmatrix} = F(z, \lambda, p)\tag{2.3}$$

Thus an equilibrium point (z_0, λ_0, p_0) of equation (2.3) is defined by $F(z_0, \lambda_0, p_0) = 0$.

Static analysis consists on the study of system equilibrium points as the parameters λ and p change. Typically, these analysis are based on the power flow equations

$$\begin{bmatrix} \Delta P(u, \lambda, \tilde{p}) \\ \Delta Q(u, \lambda, \tilde{p}) \end{bmatrix} = G(u, \lambda, \tilde{p}) = 0\tag{2.4}$$

where ΔP and ΔQ are active and reactive power mismatches, and $G(u, \lambda, \tilde{p})$ can be seen as a subset of $F(z, \lambda, p)$, where the control parameters p may not be necessarily the same (e.g. AVR set points are assumed variable, so that generators can be treated as PV buses). Typically, u represents bus voltage phasors, denoted as $V\angle\delta$.

Saddle-Node Bifurcation

Saddle-Node Bifurcations (SNB) have been shown to be one of the primary causes for voltage collapse [57, 74, 78, 79, 80, 81]. This phenomenon is characterized by a pair of equilibrium points locally coalescing and disappearing as the bifurcation parameter λ “slowly” changes. Mathematically, the SNB point is an equilibrium point (z_c, λ_c, p_c) with corresponding Jacobian $D_z F(z_c, \lambda_c, p_c)$ that presents a simple and unique zero eigenvalue associated with nonzero right eigenvector v and left eigenvector w [74]. These conditions can be summarized as follows [78]:

$$\begin{aligned} F(z, \lambda, p) &= 0 \\ D_z F(z, \lambda, p)v &= 0 \\ \|v\| &\neq 0 \end{aligned} \tag{2.5}$$

or

$$\begin{aligned} F(z, \lambda, p) &= 0 \\ D_z^T F(z, \lambda, p)w &= 0 \\ \|w\| &\neq 0 \end{aligned} \tag{2.6}$$

For certain dynamic power system models, singularities of the related power flow Jacobians have been shown to be associated with actual singular bifurcations of the corresponding dynamic systems [78, 79, 82]. Therefore, in certain cases, a SNB point can be detected by checking for singularities of power flow Jacobians [79].

Limit-Induced Bifurcation

In some cases, voltage collapse may also be caused by Limit-Induced Bifurcation (LIB), which is produced by control limits being reached, especially generator re-

active power limits [57, 83]. A LIB is characterized by a “jump” on the eigenvalue of Jacobian $D_z F$, i.e. eigenvalues change instantaneously when system hits limits. At a LIB, the system model changes; for example, when generator reactive power limits are reached, generator models are changed from constant voltage and active power models (PV buses) to constant active and reactive power models (PQ buses). Both the original model and the “limit induced” model have the same equilibrium point when the limit is reached but have different bifurcation diagrams. These bifurcations can also be detected using power flow equations, if the control limits are properly modeled, and are also characterized by two solution points locally coalescing and disappearing as the bifurcation parameter λ “slowly” changes.

Loading Margin

Loading margin is the most basic and widely accepted voltage collapse index. For a particular operating point, the loading margin is the amount of additional load for a given load increase pattern that may cause voltage collapse [57]. It indicates how much the system may be stressed before reaching its voltage stability limits on a given direction of load increase.

The loading margin is expressed as

$$L = L_c - L_0 \quad (2.7)$$

where L_0 represents the current system loading and L_c represents the system loading at the voltage collapse point. This loading margin is depicted in the PV curve of Figure 2.1, where it represents the load change between the operating point and the “nose” of the curve.

When thermal limits and voltage limits are also considered to obtain the maximum system loading L_c , the loading margin, L , becomes an adequate index that

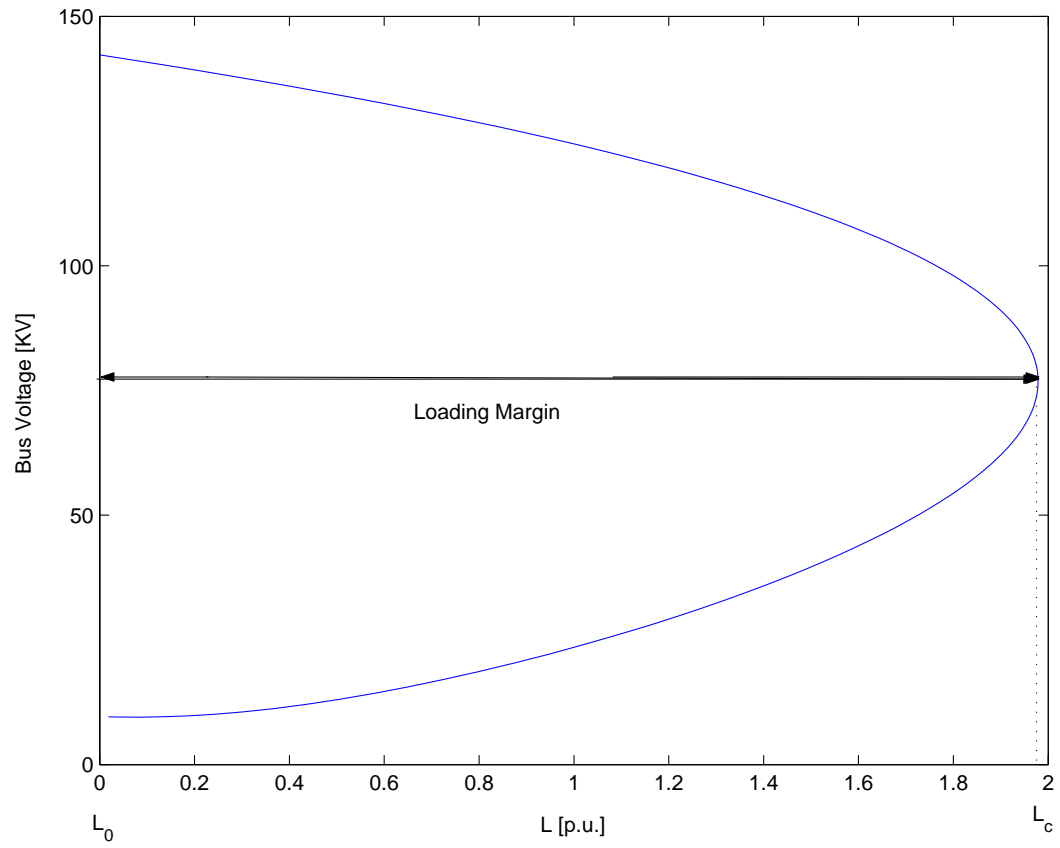


Figure 2.1: A PV curve showing loading margin.

takes full account of power system non-linearity and various limits. In this research, the steady state loading margin is used to determine the proposed SATC on the known or forecasted load and generation patterns for TOF and TI analysis, and to determine security costs associated with each transaction.

2.2.2 Continuation Power Flow

The well-known conventional power flow equations may be expressed as

$$P_{Gi} - P_{Li} - \sum_{j=1}^n V_i V_j (G_{ij} \cos \theta_{ij} + B_{ij} \sin \theta_{ij}) = 0 \quad (2.8)$$

$$Q_{Gi} - Q_{Li} - \sum_{j=1}^n V_i V_j (G_{ij} \sin \theta_{ij} - B_{ij} \cos \theta_{ij}) = 0 \quad (2.9)$$

where P_{Gi} and Q_{Gi} are the real and reactive power generation on bus i ; P_{Li} and Q_{Li} are the corresponding real and reactive load; V_i and θ_i are the bus voltage magnitude and angle; and G_{ij} and B_{ij} represent real and imaginary parts of the ij element of the bus admittance matrix. When it is used for voltage stability analysis, the Jacobian may become singular at the voltage collapse point. Therefore, these equations are prone to convergence problems at operating points near the collapse point.

For constant power load models, changes in P_{Li} , Q_{Li} and P_{Gi} may be represented as

$$P_{Li} = P_{Li0}(1 + \lambda K_{LPi}) \quad (2.10)$$

$$Q_{Li} = Q_{Li0}(1 + \lambda K_{LQi})$$

$$P_{Gi} = P_{Gi0}(1 + \lambda K_{Gi}) \quad (2.11)$$

where P_{Li0} , Q_{Li0} , P_{Gi0} are the base load and generation at bus i , and K_{LPi} , K_{LQi} , K_{Gi} determine the direction of the load and generation increase as the scale parameter λ changes.

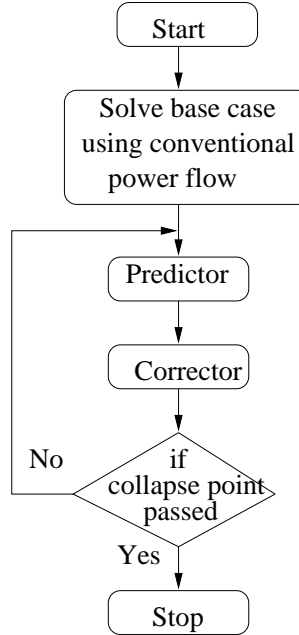


Figure 2.2: The main procedure of CPF.

CPF methods reformulate the power flow equations by adding an additional equation, typically associated with the varying parameter λ , so that the power flow equations remain well-conditioned at all possible loading levels [74, 75]. They are iterative numerical techniques used to detect bifurcations by tracing the bifurcation diagram. A typical CPF procedure is shown in Figure 2.2. It starts from a known solution, and then uses an iterative process involving predictor and corrector steps, as shown in Figure 2.3, to find subsequent solutions at different load levels.

Predictor Step

The predictor provides an initial estimation of the state variables of the power flow solution for the next step increase in λ , in a tangent direction to the solution path [57, 74, 75]. This tangent direction is computed using the power flow Jacobian. Thus, a known equilibrium point (z_1, λ_1) , as shown in Figure 2.3, is used to compute

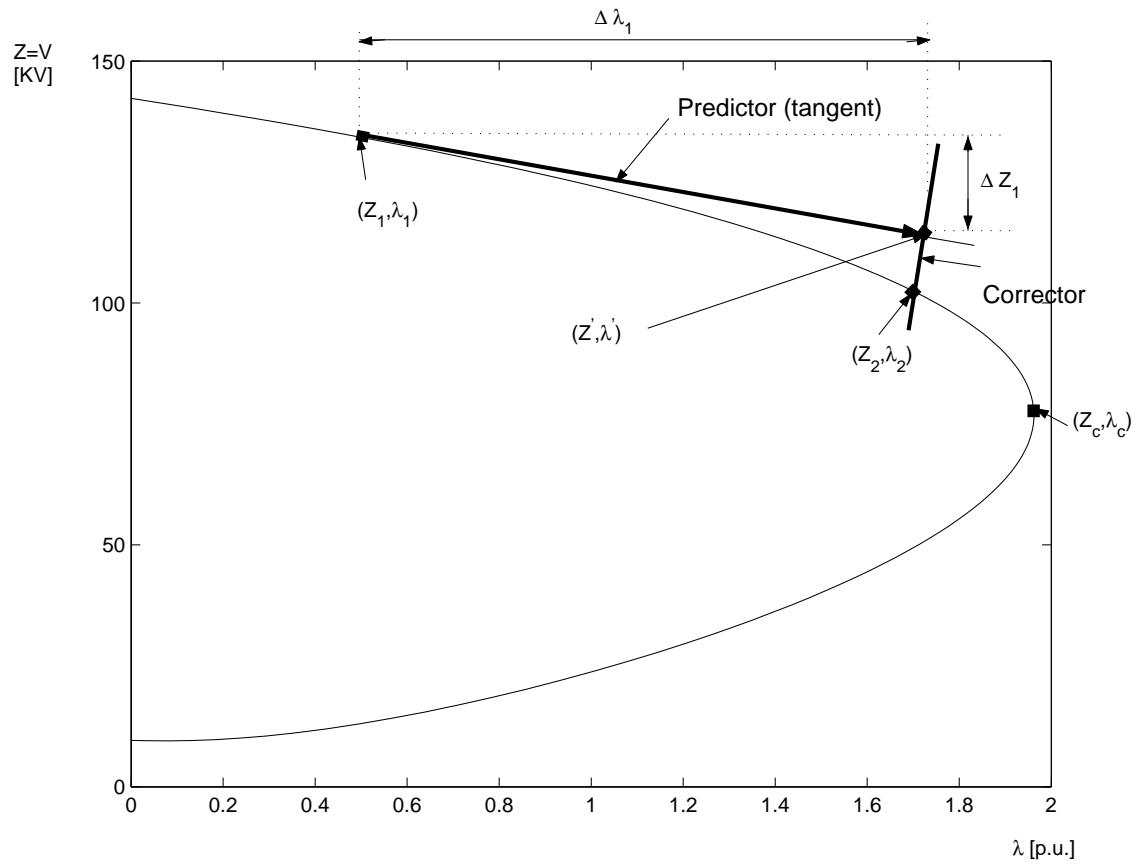


Figure 2.3: CPF shown in a PV curve.

the direction vector Δz_1 and a change $\Delta \lambda_1$ of the system parameter, as follows:

$$\frac{\Delta z_1}{\Delta \lambda_1} \approx \left. \frac{dz}{d\lambda} \right|_1 = -[D_z F|_1]^{-1} D_\lambda F|_1 \quad (2.12)$$

By defining the step $\Delta \lambda_1$, the change Δz_1 can be calculated as

$$\begin{aligned} \Delta \lambda_1 &= \frac{\alpha}{\|dz/d\lambda|_1\|} \\ \Delta z_1 &= \Delta \lambda_1 \left. \frac{dz}{d\lambda} \right|_1 \end{aligned} \quad (2.13)$$

where α is a positive scalar that is chosen to control the “length” of the step; typically, an $\alpha = 1$ is chosen [57]. Therefore, the predictor yields a new point (z', λ') , as shown in Figure 2.3,

$$\begin{bmatrix} z' \\ \lambda' \end{bmatrix} = \begin{bmatrix} z_1 \\ \lambda_1 \end{bmatrix} + \begin{bmatrix} \Delta z_1 \\ \Delta \lambda_1 \end{bmatrix} \quad (2.14)$$

Once the CPF moves past a SNB or a LIB, the sign of $\Delta \lambda_1$ may be changed to trace the lower portion of the P-V curve.

Corrector Step

The actual equilibrium point (z_2, λ_2) , as shown in Figure 2.3, is determined by solving a modified power flow based on the approximate point (z', λ') predicted by the predictor step. An additional equation is used to solve the problem, i.e.

$$F(z, \lambda) = 0 \quad (2.15)$$

$$\varphi(z, \lambda) = 0$$

The simplest approach for choosing $\varphi(z, \lambda)$ is to just fix one of the variables in z or λ at the value calculated from the predictor step [57]. The idea is to pick $\varphi(z, \lambda)$

as to avoid convergence problems at operating conditions near the voltage collapse point.

CPF methods can fully compute complete voltage profiles, allowing to reliably determine the maximum loading point, and thus the loading margin associated with λ_c by automatically changing the value of λ , while readily enforcing system limits [57]. In this thesis, it is used for a determination of SATC, and to obtain data for TI and security cost analyses.

2.3 ATC Definitions and Computations

System security is the ability of the electric system to withstand sudden disturbances [42], by imposing transmission constraints that lead to operating limits, such as thermal limits, voltage limits, and stability limits [42].

Thermal limits are set by the capabilities of lines and apparatus to absorb and dissipate the heat created by the current flowing in the various elements. It is required that

$$I_{ij} \leq I_{ijmax} \quad (2.16)$$

where, I_{ij} is the current in an element connecting nodes i and j , I_{ijmax} is its thermal limit.

Voltage limits arise because voltage magnitudes in the system must remain within a bandwidth that is set by the voltage tolerances of both system and customer equipment. It is expressed for a bus i as

$$V_{imin} \leq V_i \leq V_{imax} \quad (2.17)$$

where V_i is the voltage magnitude at bus i , and V_{imin} and V_{imax} are the corresponding low and high limits.

Stability limits are set because a system must be capable of surviving expected disturbances. Time-domain simulation is usually used for detailed stability analyses when large disturbances are studied[84]. For on-line applications, different direct methods have been developed for limited system models to determine these stability limits [85, 86, 87]. Hybrid methods, which take advantage of the merits of the above two methods, have been proposed for these types of studies [88, 89]. For small disturbances, eigenvalue analysis approaches are extensively used [84]. Given the computational costs associated with these analysis techniques, off-line studies are used to set stability limits that are then used on-line to define the transfer capability of the network [42].

All these operating limits vary with time and are used to define acceptable operating boundaries. Thermal limits are easy to be considered, and are typically used as the operating limits in simple DC power flow-based models. To include voltage limits, AC power flows are necessary. Stability limits, on the other hand, are more difficult to obtain, especially when considering that stability problems become more significant as the system loading increases, as various stability limits need to be quickly found by analyzing the network under increasing loading conditions. In this case, off-line computation of these limits is not appropriate, and hence there is a need for approximate on-line estimations of these limits.

To account for possible system disturbances or contingencies, an N-1 contingency analysis is commonly used to obtain all of these limits, so that the system is “secure” even if it loses *one* of its major components.

2.3.1 ATC Definitions

ATC is “the remaining transfer capability of the transmission system for further commercial activity over and above already committed uses” [62]. It is commonly expressed as

$$ATC = TTC - TRM - ETC \quad (2.18)$$

where TRM stands for Transmission Reliability Margin and ETC stands for Existing Transmission Commitments, which includes a Capacity Benefit Margin (CBM). TRM and CBM are included to account for uncertainties in system operation. TTC stands for Total Transfer Capability, i.e. the total amount of electric power that can be transferred in a reliable manner. The TTC between any two areas or across particular paths or interfaces is less or equal to the First Contingency Total Transfer Capability (FCTTC) [62], and can be expressed as

$$TTC = \text{Min}\{P_{Max_{Thermal}}, P_{Max_{Voltage}}, P_{Max_{Stability}}\}$$

where $P_{Max_{Thermal}}$, $P_{Max_{Voltage}}$ and $P_{Max_{Stability}}$ represent the maximum powers considering thermal limits, voltage limits and stability limits respectively, typically based on an (N-1) contingency criterion. As system operating conditions vary, critical system contingencies vary, and hence the most restrictive limit on TTC may move from one system limit to another.

The above definition of ATC has been extensively applied in market operation to analyze potential transactions between two areas. The ATC value of the power exchange paths between the two areas provides an indication of the amount of additional electric power that can be exchanged for a specific time frame and a specific set of conditions. It is dynamic and needs to be calculated periodically.

With the increase of complexity of power transactions, which may not be limited

only within the “area domain”, but may occur in anywhere in the system, any transmission facility could become the critical transaction path. Hence, the basic ATC concept is extended in this thesis from the “area domain” to a “system domain” [90], and will be referred as “System-wide” ATC (SATC) using the same concept defined in (2.18), since the SATC is computed for a whole system, as opposed to a given interchange path. It is important to highlight the fact that the SATC concept is only used to properly represent system security, for congestion management and pricing. Its value continuously changes with system operating condition, and cannot be used in the way ATC values are currently being utilized by market/system operators in OASIS. This concept is consistent with the physical characteristics of security problems, as stability problems can not always be associated with a given set of transmission corridors, these would depend on system operating conditions, which continuously change. Hence, the SATC should be computed on-line.

2.3.2 “System-wide” ATC (SATC) Computation

Accurate ATC values are critical for maintaining system security and reliability while maximising economic gains from the market trades. The computation of ATC generally requires a set of simulations of the transmission network under specific operating conditions. As the system operating conditions change over time, the limiting factor can shift among thermal, voltage and stability limits. For “large” systems, the stability limits tend to be the main limiting factor, due to the intensive use of transmission facilities. In this sense, the ATC is basically a stability margin. In heavy loaded systems, voltage stability limits usually become dominant, especially in the market environments where transmission systems are operating under more stressed conditions.

ATC computations must be accurate, speedy and updated with changes in system operating conditions. Overestimation could threaten system security by making the system “risky” to operate; however, this would “facilitate” transactions. Underestimation could result in lose of benefit by making the system “expensive” to operate; however, system security increases in this case. Thus, the ATC needs to be calculated periodically to reflect changing system conditions. Therefore, the current practice of using off-line computations to determine ATC values is not adequate for real-time market operation.

In most of the current implementations of electricity markets, the ATC is determined in off-line studies, and is represented in the bidding process as rather conservative limits on the power flowing through the transmission lines or main transmission “corridors” [62]. Furthermore, these transmission corridors might not necessarily be the ones that could be associated with system security problem for all given operating conditions. This could easily lead to “fictitious” congestion problems. These issues are addressed here by basing security on a SATC value computed every time the operating conditions change. However, the proper on-line computation of a SATC is a challenge, as the actual determination of stability limits requires costly time domain simulations.

In this thesis, the stability limits are approximately represented using voltage stability limits, which can be readily computed, giving a good idea of the “relative” stability of the network in stressed systems [57]. Thus, a bifurcation-based CPF method [74], which can quickly and reliably calculate “System-wide” TTC (STTC) values considering all system limits, based on a given load and generation pattern, is used for “adequate” and fast SATC computations, using the loading margin L defined in (2.7) as an approximation of the $STTC - SETC$ value [32, 33, 90, 91, 92], considering thermal limits, voltage limits and voltage stability limits, where

SETC represents “System-wide” ETC and is represented through the base system conditions. Hence, the SATC is then defined here as

$$SATC \approx L - STRM \quad (2.19)$$

where STRM represents “System-wide” TRM, and is assumed to be a known value, as is typically done nowadays in industry. Thus, the SATC can be readily computed on-line.

The procedure of SATC computations based on a CPF is as follows.

1. Model the basic operating condition associated with the SETC, i.e. define P_{G0} and P_{L0} in (2.11) and (2.10).
2. Obtain load and generation increase direction from market schedule and load forecasting.
3. Perform an N-1 contingency analysis to identify the most critical contingencies.
4. Calculate the loading margins $L_0, L_1, L_2, \dots, L_m$ using a CPF for normal conditions and each critical contingency, based on the load and generation increase direction defined in Step 2.
5. The SATC is then approximated using the minimum value of the loading margins computed in Step 4, i.e.

$$SATC = \min(L_0, L_1, \dots, L_i, \dots, L_m) - STRM \quad (2.20)$$

The above procedure quickly gives “adequate” SATC value. Observe that the proposed SATC computation procedure accounts for all transmission paths in the system.

2.4 Transaction Operational Feasibility (TOF) Analysis

TOF analysis consists of checking if the dispatching of transactions violates system operating limits, including thermal limits, voltage limits and stability limits. The acceptance, rejection and adjustment of transactions are based on this analysis.

A TOF analysis procedure based on the proposed SATC computations is shown in Figure 2.4. The main steps of the proposed procedure are as follows:

1. The base system conditions, which correspond to the committed load and generation (e.g. bilateral contract, etc.) and a given system configuration, define the “base” power flow conditions, which are modelled as the already committed transmission usage, i.e. SETC.
2. The load and generation increase patterns determine the power increase above SETC, and are defined by potential transactions obtained from bid matching, i.e. matching selling bids with buying bids and forecasted loads.
3. The SATC computation is the core part of the TOF analysis, and it is performed by a CPF method, taking into account thermal limits, voltage limits and voltage stability limits, in the “system domain”. Thus, the SATC is calculated from the load and generation patterns and “base” system conditions, and it basically consists of determining the maximum power transfer, i.e. STTC, for the power system, considering all credible contingencies.
4. If potential transactions are within the calculated SATC, they are considered as feasible transactions and can be accepted; otherwise, they are infeasible and

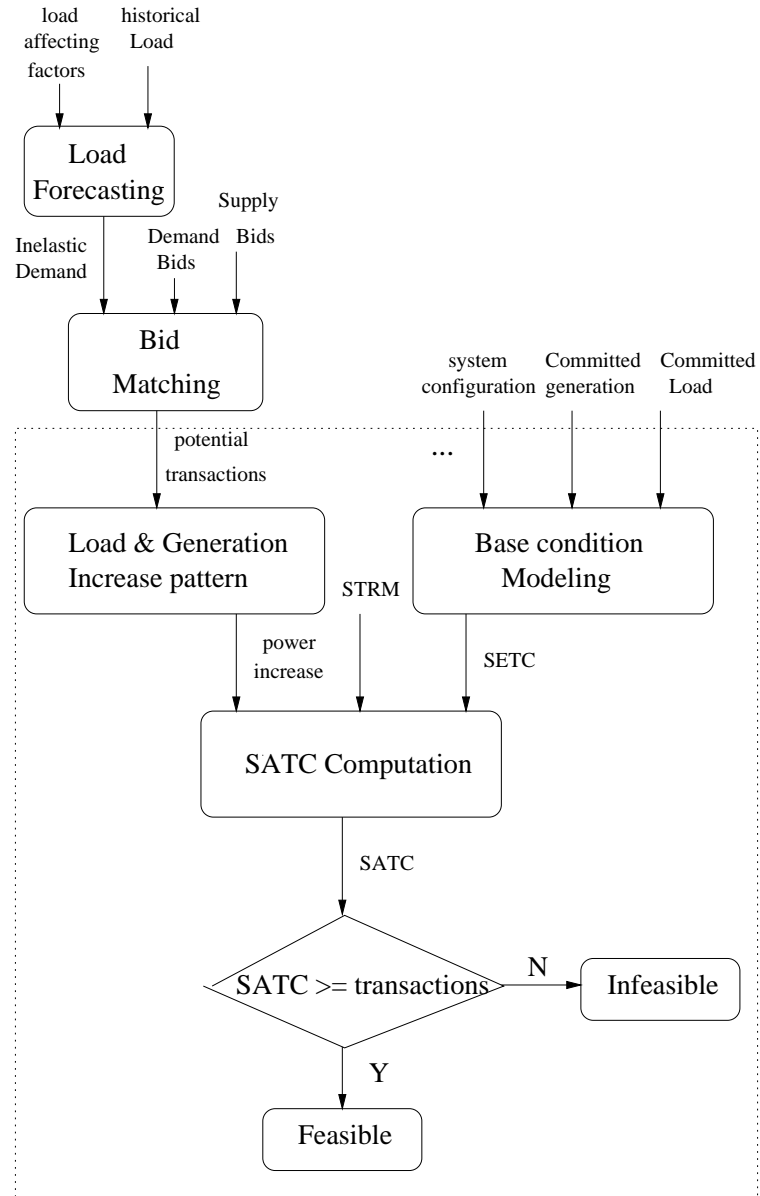


Figure 2.4: TOF analysis procedure.

hence need to be adjusted. Techniques for properly adjusting these proposed transactions are presented in Chapter 3.

The proposed TOF analysis procedure is suitable for efficient real-time market operation, which requires fast and accurate calculations.

2.5 Transaction Impact (TI) on SATC

Because of the physical characteristics of the transmission networks, each transaction has an impact on the voltages and power flows of the whole transmission networks, thus affecting transmission system security, represented here by the SATC.

Transactions in electricity markets can be treated as power injections and extractions from various buses. If only real power transactions are considered, a transaction can be expressed as P_{Si} or P_{Di} , for power supply or power demand at bus i , respectively. The transaction impact on SATC can then be analyzed by determining how the SATC is affected by transaction changes, i.e. changes in P_{Si} and P_{Di} , through the computation of the first order sensitivities at a given operating point from equation (2.19), where STRM is usually assumed to be a fixed value. Thus,

$$\begin{aligned}\frac{dSATC}{dP_{Si}} &\approx \frac{dL}{dP_{Si}} \\ \frac{dSATC}{dP_{Di}} &\approx \frac{dL}{dP_{Di}}\end{aligned}\tag{2.21}$$

As discussed in Section 2.2, assume that the system can be represented using the set of equations

$$F(z, \lambda, p) = 0\tag{2.22}$$

where $z \in \Re^N$ represents the vector of state and algebraic system variables. $\lambda \in \Re$ is the loading parameter used to model load changes in the system, since the load powers are modeled as

$$P_L = P_{L_0} + \lambda P_D \quad (2.23)$$

with P_{L_0} representing the load power levels at the “base” loading conditions; all loads are assumed to have constant power factors. The parameters $p \in \Re^m$ correspond to “controllable” system parameters, such as potential power transactions, P_S and P_D .

In this analysis, generator powers are modeled as

$$P_G = P_{G_0} + (\lambda + k_G)P_S \quad (2.24)$$

where P_{G_0} represents the base generation conditions, and k_G is a variable used to represent a distributed slack bus for the purpose of distribution of losses.

At a system operating point (z_0, λ_0, p_0) , if there is a small transaction change, the system is likely to move to another stable equilibrium point $(z_0 + \Delta z, \lambda_0 + \Delta \lambda, p_0 + \Delta p)$, where

$$F(z_0 + \Delta z, \lambda_0 + \Delta \lambda, p_0 + \Delta p) = 0 \quad (2.25)$$

Using Taylor series expansion on (2.25), and neglecting higher order terms to simplify the problem, it follows that

$$F(z_0, \lambda_0, p_0) + D_z F|_0 \Delta z + D_\lambda F|_0 \Delta \lambda + D_p F|_0 \Delta p = 0 \quad (2.26)$$

where $D_z F|_0$, $D_\lambda F|_0$ and $D_p F|_0$ are the Jacobians of F with respect to z , λ and p respectively, at the equilibrium point (z_0, λ_0, p_0) . Hence, (2.26) can be reduced to

$$D_z F|_0 \Delta z + D_\lambda F|_0 \Delta \lambda + D_p F|_0 \Delta p = 0 \quad (2.27)$$

$$\implies \begin{bmatrix} D_z F|_0 & D_\lambda F|_0 & D_p F|_0 \end{bmatrix} \begin{bmatrix} \Delta z \\ \Delta \lambda \\ \Delta p \end{bmatrix} = 0 \quad (2.28)$$

since $F(z_0, \lambda_0, p_0) = 0$.

The voltage stability limits for the system represented by equations (2.22) are basically associated with SNB and LIB of the corresponding set of nonlinear equations [57]. For the proposed transaction impact analysis, thermal and voltage limits can be treated mathematically in a similar way as LIB, although the system does not present stability problem when these limits are reached.

Saddle-Node Bifurcation

As a SNB can be directly associated with voltage collapse, as discussed in Section 2.2, if the operating point (z_c, λ_c, p_c) corresponds to a SNB point, transaction changes at this point can then be analyzed using (2.27) as follows:

$$\omega^T D_z F|_c \Delta z + \omega^T D_\lambda F|_c \Delta \lambda + \omega^T D_p F|_c \Delta p = 0 \quad (2.29)$$

where ω is the left eigenvector corresponding to the zero eigenvalue of Jacobian $D_z F$ evaluated at the SNB point. Since $\omega^T D_z F|_c = 0$, (2.29) can be reduced to [72]

$$\frac{d\lambda}{dp} \approx \frac{\Delta \lambda}{\Delta p} = -\frac{\omega^T D_p F|_c}{\omega^T D_\lambda F|_c} \quad (2.30)$$

As discussed in Section 2.3,

$$L = \lambda_c \cdot \sum_i P_{Di} \quad (2.31)$$

then, the transaction impact on SATC can be studied using

$$\begin{aligned} \frac{dL}{dp} &= \left. \frac{d\lambda}{dp} \right|_c \cdot \sum_i P_{Di} \approx \frac{\Delta\lambda}{\Delta p} \cdot \sum_i P_{Di} \\ \Rightarrow \quad \frac{dL}{dp} &\approx -\frac{\omega^T D_p F|_c}{\omega^T D_\lambda F|_c} \cdot \sum_i P_{Di} \end{aligned} \quad (2.32)$$

Limits

The value of SATC can also be affected by voltage/thermal limits or LIB. As opposed to a SNB, $D_z F$ is not singular at a LIB; hence, equation (2.30) does not apply at this point.

In general, a system that reaches a limit can be characterized by two different set of nonlinear equations at the limit condition, i.e.

$$\begin{aligned} F_1(z_c, \lambda_c, p_c) &= 0 \\ F_2(z_c, \lambda_c, p_c) &= 0 \end{aligned} \quad (2.33)$$

where, the first set of equations $F_1(\cdot)$ corresponds to the “original” system, whereas $F_2(\cdot)$ corresponds to a modified set of equations where a given limit is active. Assuming that for a small transaction change Δp , one has

$$\begin{aligned} D_z F_1|_c \Delta z + D_\lambda F_1|_c \Delta \lambda + D_p F_1|_c \Delta p &= 0 \\ D_z F_2|_c \Delta z + D_\lambda F_2|_c \Delta \lambda + D_p F_2|_c \Delta p &= 0 \end{aligned} \quad (2.34)$$

Eliminating Δz from (2.34) leads to

$$\begin{aligned} \left. \frac{d\lambda}{dp} \right|_c &\approx \frac{\Delta\lambda}{\Delta p} = \frac{\mu^T (D_z F_2|_c D_z F_1^{-1}|_c D_p F_1|_c - D_p F_2|_c)}{\mu^T \mu} \\ \Rightarrow \quad \frac{dL}{dp} &\approx \frac{\mu^T (D_z F_2|_c D_z F_1^{-1}|_c D_p F_1|_c - D_p F_2|_c)}{\mu^T \mu} \cdot \sum_i P_{Di} \end{aligned} \quad (2.35)$$

where

$$\mu = D_\lambda F_2|_c - D_z F_2|_c D_z F_1^{-1}|_c D_\lambda F_1|_c$$

Observe that the sensitivity formula (2.35) applies to any limit condition, independent of whether it corresponds to a LIB or a voltage/thermal limit.

Equations (2.32) and (2.35) are used here to determine transaction impact on SATC, which is used for rescheduling transactions when transmission congestion occurs, and is also used to distribute total security costs among transactions [32, 33].

2.6 Case Studies

A six-bus test system, as shown in Figure 2.5, is used here to illustrate the proposed TOF and TI analysis procedures. It has 3 generation companies (GENCOs) that provide supply bids, and 3 energy service companies (ESCOs) that may provide demand bids. The system and market data can be found in Appendix B.

2.6.1 Case 1: With Demand-side Bidding

The “standard” high-low method is employed for bid matching, as shown in Figure 2.6. Thus, the potential transactions in this case are: GENCO 2 sells 25 MW, GENCO 3 sells 20 MW, ESCO 1 buys 25 MW, ESCO 2 buys 10 MW, and ESCO 3 buys 10 MW. The uniform market clearing price is \$9.5/MWh, i.e. the market is cleared at point A. These potential transactions define the load and generation increase “direction” for the SATC computation, as shown in Table 2.1.

UWPFLOW [93], which is a robust CPF program, is then used to compute the SATC, which corresponds to the minimum loading margin obtained from bus

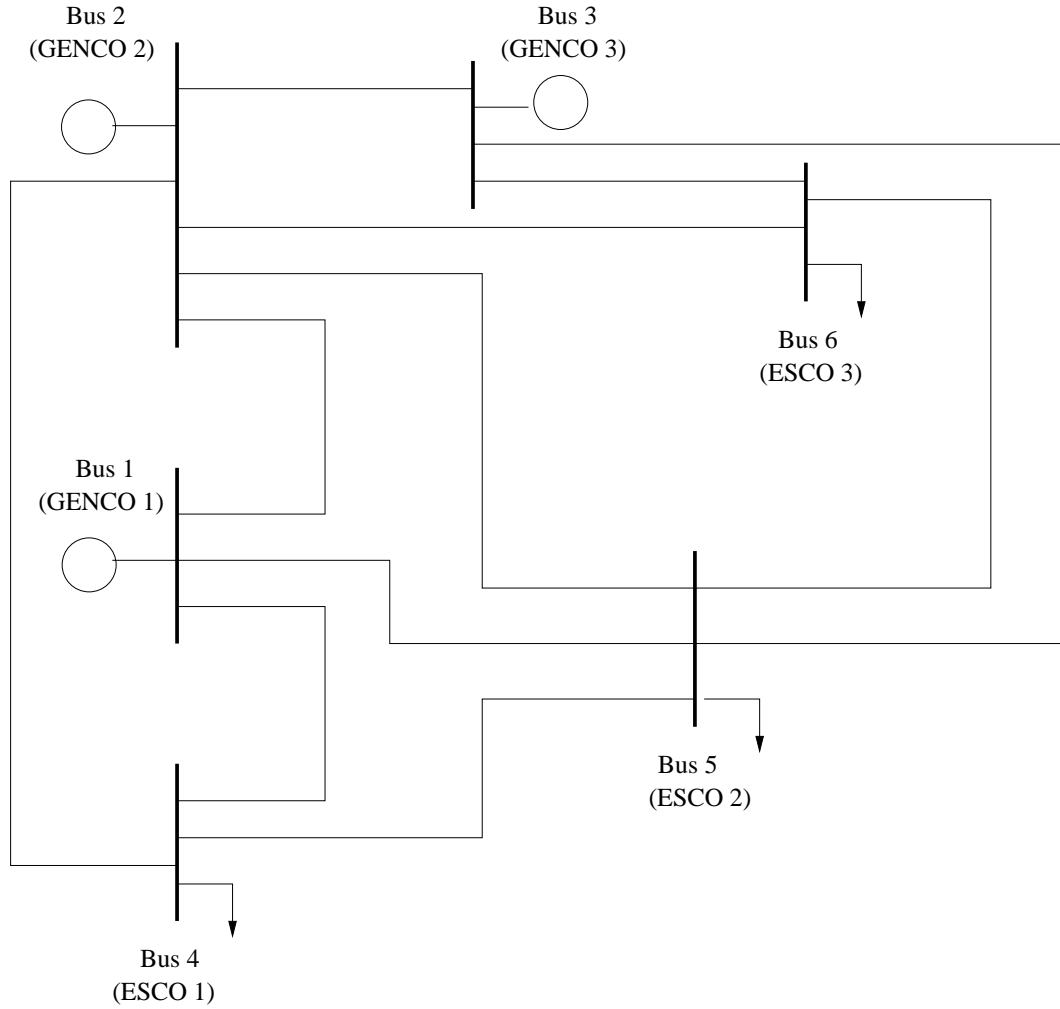


Figure 2.5: Six-bus test system.

voltage, thermal and voltage stability limits. The loading margin results for normal conditions and for the three most significant contingencies are shown in Table 2.2. In this case, the outage of line 2-4 is the most critical contingency. Hence, the SATC value is 38.231 MW, which is less than the total amount of potential transactions, i.e. 45 MW (see Figure 2.6). Therefore, transactions are not feasible in this case, and hence must be rescheduled, as discussed in the next chapters.

In this case, the TI analysis technique described in Section 2.5, generates the

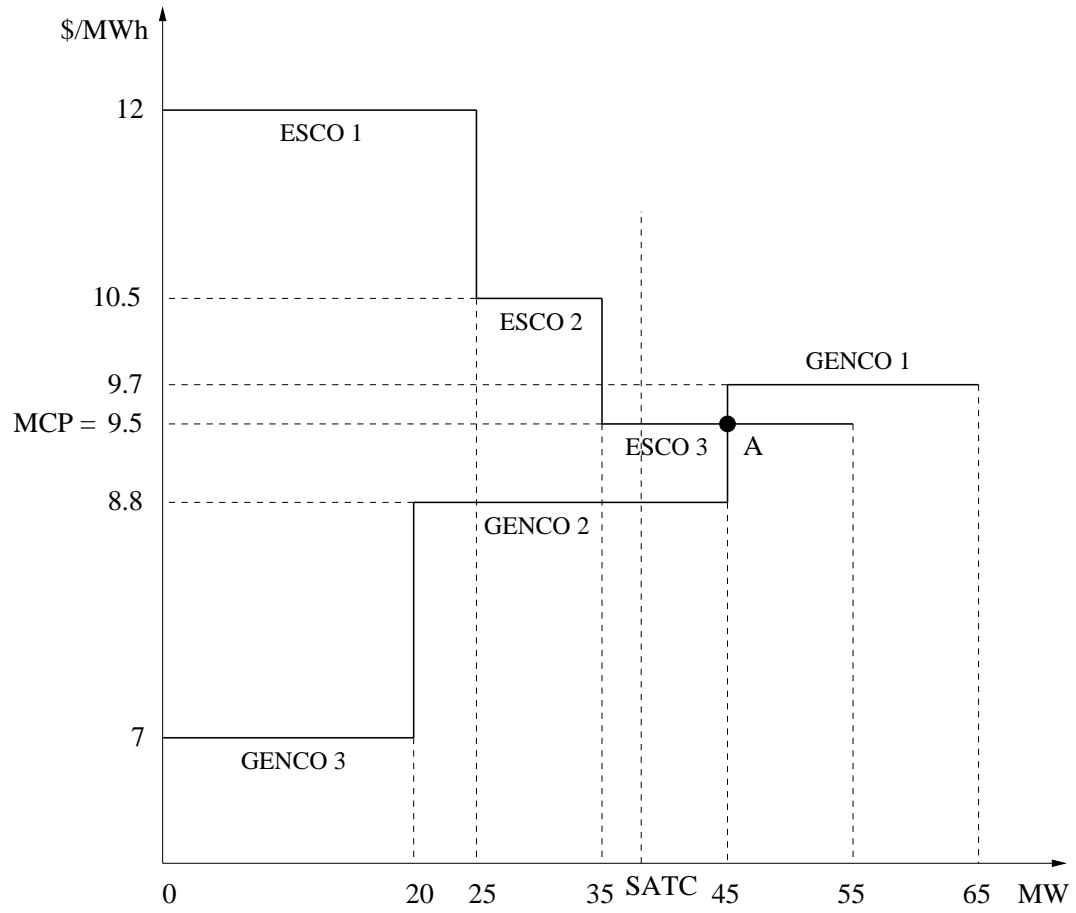


Figure 2.6: High-low bid matching with demand-side bidding, six-bus system.

Table 2.1: Load and generation increase direction with demand-side bidding, six-bus system

Bus (i)	ΔP_g (MW)	ΔP_l (MW)	ΔQ_l (MVar)
1	0	0	0
2	25	0	0
3	20	0	0
4	0	25	16.7
5	0	10	7
6	0	10	6.67

Table 2.2: Loading margin results with demand-side bidding, six-bus system

System Condition	Normal condition (MW)	Line 1-4 out (MW)	Line 2-4 out (MW)	Line 3-6 out (MW)
Loading Margin	175.595	104.729	38.231	59.895

values at the initial point as shown in (2.36).

$$\begin{bmatrix} d\lambda/dP_{S_1}|_c \\ d\lambda/dP_{S_2}|_c \\ d\lambda/dP_{S_3}|_c \\ d\lambda/dP_{D_1}|_c \\ d\lambda/dP_{D_2}|_c \\ d\lambda/dP_{D_3}|_c \end{bmatrix} = \begin{bmatrix} 0.95 \\ -0.03 \\ 0.03 \\ -1.55 \\ -0.49 \\ -0.09 \end{bmatrix} \quad (2.36)$$

These values show that GENCO 1 has the most positive impact on SATC, i.e. increase in GENCO 1 will increase SATC; while GENCO 2 has negative impact on SATC, i.e. increase in GENCO 2 will decrease SATC. All the loads have negative impacts on SATC, and ESCO 1 has the most negative impact on SATC.

2.6.2 Case 2: Inelastic Demand

Assuming that ESCO 1, ESCO 2 and ESCO 3 are inelastic, and determined by a load forecasting procedure to be 25 MW, 10 MW and 20 MW, respectively, the resulting high-low bid matching can be seen on Figure 2.7. The potential transactions are then: GENCO 1 sells 10 MW, GENCO 2 sells 25 MW and GENCO 3 sells 20 MW to satisfy the total load demand of 55 MW. The uniform market clearing price in this case is \$9.7/MWh, i.e. the market is cleared at point B. The

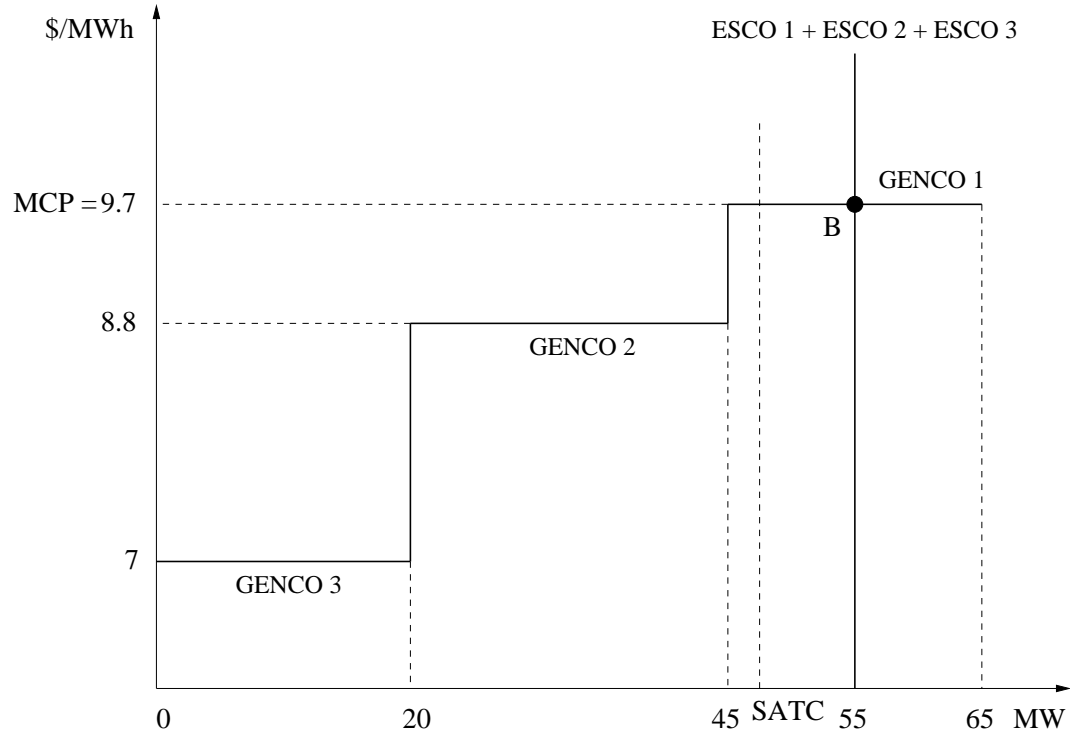


Figure 2.7: High-low bid matching for inelastic demand, six-bus system.

load and generation increase “direction” is then the one shown in Table 2.3. In this case, the loading margin results for normal conditions and for the three most significant contingencies are shown in Table 2.4; the resulting SATC is then 44.74 MW, which is also less than the total amount of potential transactions, i.e. 55 MW, and hence these transactions are not feasible either and need to be rescheduled.

Using the method described in Section 2.5, the transaction impact at the initial point is computed as shown in (2.37).

Table 2.3: Load and generation increase direction for inelastic demand, six-bus system

Bus (i)	ΔP_g (MW)	ΔP_l (MW)	ΔQ_l (MVar)
1	10	0	0
2	25	0	0
3	20	0	0
4	0	25	16.7
5	0	10	7
6	0	20	13.34

Table 2.4: Loading margin results for inelastic demand, six-bus system

System Condition	Normal condition (MW)	Line 1-4 out (MW)	Line 2-4 out (MW)	Line 3-6 out (MW)
Loading Margin	219.186	118.938	51.044	44.74

$$\begin{bmatrix} d\lambda/dP_{S_1}|_c^{(1)} \\ d\lambda/dP_{S_2}|_c^{(1)} \\ d\lambda/dP_{S_3}|_c^{(1)} \\ d\lambda/dP_{D_1}|_c^{(1)} \\ d\lambda/dP_{D_2}|_c^{(1)} \\ d\lambda/dP_{D_3}|_c^{(1)} \end{bmatrix} = \begin{bmatrix} -0.11 \\ 0.29 \\ -0.31 \\ -0.3 \\ -0.33 \\ -0.83 \end{bmatrix} \quad (2.37)$$

These values show that GENCO 2 has the most positive impact on SATC, and GENCO 3 has the most negative impact on SATC. All the loads have negative impacts, and ESCO 3 has the most negative impact on SATC.

2.7 Summary

A TOF analysis procedure is proposed and tested in this Chapter, based on an adequate computation of SATC, which is a concept proposed in this thesis to accurately evaluate transmission congestion for the purpose of transaction security cost analysis. Transaction impact on SATC is also defined and quantitatively analyzed, considering highly non-linear voltage stability constraints, as well as thermal and voltage limits.

Chapter 3

Transaction Security Cost Analysis by Rescheduling Strategy

Chapter Synopsis

A rescheduling strategy is presented in this Chapter for TSC analysis considering generation redispatch and load curtailment. The analysis procedure is based on the iterative computation of the SATC and transaction impact, considering thermal, voltage and stability limits with N-1 contingency criteria discussed in Chapter 2. Results on three different test systems are also described, demonstrating its effectiveness and applicability for both small and large systems.

3.1 Introduction

The rescheduling technique proposed in this thesis considers both generation redispatch and load curtailment for simple auction electricity markets. It is applied to a

market clearing condition that violates the security constraints, defined in Chapter 2.

The costs resulting from dispatching constrained-on units (non-bidding units are not considered), whose bidding prices are higher than the *MCP*, or curtailing loads to solve the congestion problem, are “distributed” among different participants. The idea here is to redispatch units or curtail load based only on the impact of these units or loads on transmission system congestion, considering that at this point system security takes precedence over economic considerations, especially in view that, in most electricity market designs, bidding results can be rejected based on security criteria. The results of this rescheduling will lead to minimum MW rescheduling, thus resulting in a sub-optimal minimum impact on the desired transactions.

The main improvements of this technique with respect to known methodologies are:

- Thermal, bus voltage and voltage stability limits are all considered to compute an SATC value “on-line”, as opposed to just using much simpler approximate MW flow constraints, which are typically determined through off-line studies for particular system conditions that might not correspond to the actual transactions under consideration.
- The total security costs are distributed among the market participants based on the actual impact that each one of them has on the SATC value.
- Nodal Congestion Prices (NCP), which are proposed here node by node to price the security constraint violations, are calculated using the sensitivities of the SATC with respect to the generator and load bids. Thus, the method

could be considered as a sub-optimal mechanism of determining congestion prices, with the advantage that contingencies can be directly considered in the SATC computations, which so far is not possible to do in OPF-based techniques through the use of LMPs.

3.2 Rescheduling Procedure

The proposed rescheduling technique to determine security costs for different market participants in the case of security constraint violation, i.e. not enough SATC, is summarized in the flow-diagram shown in Figure 3.1. The depicted methodology is based on a series of linearizations; however, the SATC does change nonlinearly as the system parameters change due to the highly nonlinear behavior of the system. The latter is the main reason for applying an iterative process. The proposed procedure can be described in detail as follows:

Initialization

Using a simple auction mechanism, the *MCP* and associated total transaction power level T are determined, together with the load and generator power levels that clear the market, namely, P_D and P_S for all loads and generators, respectively; hence

$$T = \sum_i P_{D_i} \quad (3.1)$$

These values of P_D and P_S are used in the determination of the SATC, as these define the load and generator direction used for the computation of λ_c , defined in (2.22) in UWPFLOW [93]. The iteration counter k is set to 1, and step lengths

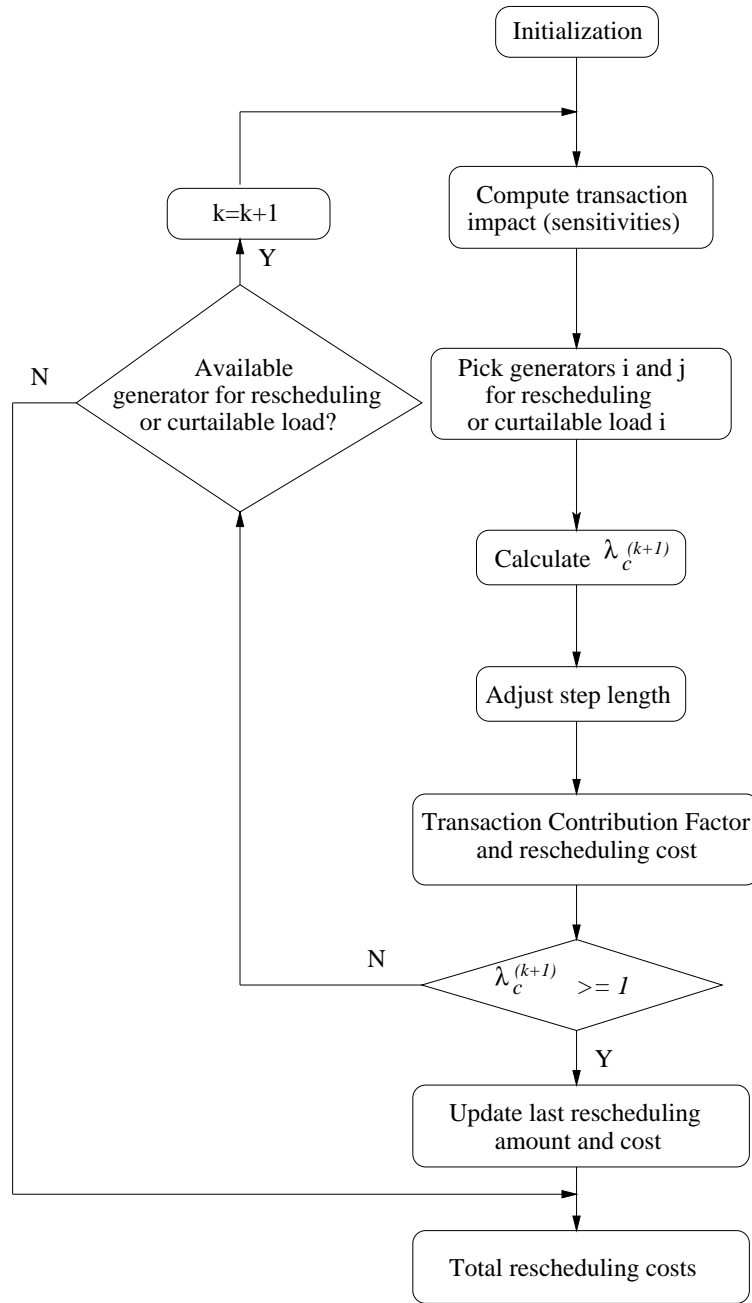


Figure 3.1: Rescheduling procedure.

$\Delta P_S^{(k)}$ and $\Delta P_D^{(k)}$ are chosen to be small values in MW, depending on the required accuracy of the SATC approximations generated in the process.

Transaction Impact and Rescheduling

If the SATC is not enough, i.e. $\lambda_c < 1$, the impact of each possible system transaction is determined using (2.32) or (2.35), depending on the limiting factor that defines the SATC. Thus, the generator i with the most positive impact on the SATC that has not been fully dispatched in the bidding process, and the generator j dispatched in the market clearing process with the most negative or least positive impact on the SATC are chosen for rescheduling. Thus, the corresponding increase and decrease in generation are defined as

$$\Delta P_{S_i}^{(k)} = -\Delta P_{S_j}^{(k)} = \Delta P_S^{(k)}$$

The new value of the SATC is then approximated using

$$\lambda_c^{(k+1)} \approx \lambda_c^{(k)} + \frac{d\lambda}{dP_{S_i}}|_c^{(k)} \Delta P_{S_i}^{(k)} + \frac{d\lambda}{dP_{S_j}}|_c^{(k)} \Delta P_{S_j}^{(k)} \quad (3.2)$$

Here, $d\lambda/dP_{S_i}|_c^{(k)} > d\lambda/dP_{S_j}|_c^{(k)}$, otherwise no SATC improvements can be attained by redispatching generation.

Only if there are no adequate generators available for redispatch, is the load considered for curtailment. This approach is to be expected when the load is inelastic, as these types of loads require that the forecasted load be dispatched, given the high “costs” of load curtailment. In the case of elastic demand, i.e. demand-side bidding or loads with curtailment bids, however, the load could be considered for rescheduling in the same way as the generators, i.e. the load with the most negative impact on the SATC, say i , may be reduced by an amount that

has a “significant” impact on the SATC value, i.e.

$$\Delta P_{D_i}^{(k)} = \Delta P_D^{(k)}$$

and then the corresponding SATC is approximated based on

$$\lambda_c^{(k+1)} \approx \lambda_c^{(k)} - \frac{d\lambda}{dP_{D_i}}|_c^{(k)} \Delta P_{D_i}^{(k)} \quad (3.3)$$

Observe that in the case of demand-side bidding, one may assume that there is no security cost for load curtailment, since the loads are intrinsically running a risk of not being dispatched by participating in the market. However, this means that overall system revenues are lost, as loads that could be served by redispatching available generation would not be dispatched.

When loads are rescheduled, the transaction level T is affected by the load reduction; thus,

$$T^{(k+1)} = T^{(k)} - \Delta P_{D_i}^{(k)}$$

Furthermore, power generation must be reduced in this case to compensate for the reduction in demand. This reduction of excess power generation will depend on the particular market rules. Here, we assume a reduction that considers the original generator’s power bid, the amount to be rescheduled from previous iterations, as well as the transaction level; thus,

$$\Delta P_{S_i}^{(k)} = \Delta P_{D_i}^{(k)} \frac{P_{S_i}^{(0)} - \sum_{j=1}^{k-1} \Delta P_{S_i}^{(j)}}{T^{(k)}}$$

This could be considered a reasonable and fair mechanism to share the load curtailment; however, other mechanisms could be implemented, such as rescheduling the load reduction among the participating generators based on their SATC sensitivities.

Since the whole process is based on a linearization, one cannot make large changes in generation or load, otherwise this might have a large effect on the actual SATC value, which changes nonlinearly as the parameters change, hence the need for an iterative process. The amount of generation chosen for redispatch $\Delta P_S^{(k)}$ or load chosen for curtailment $\Delta P_D^{(k)}$ may be readjusted when determining the actual value of $\lambda_c^{(k+1)}$ using the full nonlinear system.

System losses are considered in the loading margin computation, but not in the pricing. They can be assigned without affecting the rescheduling procedure to: a “slack bus”; distributed among the participants according to their power bids (“distributed slack bus”), as it has been assumed in this thesis; or by any other methodologies.

Rescheduling Adjustment

The step changes in generation or load, i.e. $\Delta P_S^{(k)}$ or $\Delta P_D^{(k)}$, are adjusted by computing the actual value of $\lambda_c^{(k+1)}$ and comparing it to the approximated value computed using (3.2) or (3.3). If the difference is greater than a chosen tolerance, the previous step and this one are repeated with smaller changes in the generation or load until a desired tolerance is met.

Rescheduling Cost Analysis

The total generator redispatch cost of the k^{th} iteration is defined as

$$SC_k = (C_{S_i} - MCP) \Delta P_{S_i}^{(k)} \quad (3.4)$$

where i is the previously chosen generator with a bid C_{S_i} . In the case of non-curtailable loads or inelastic loads, one can assume that there is a bid or a high

cost associated with curtailing the load that should be considered as part of the cost of keeping the system secure; thus, one would have in this case that

$$SC_k = A_{D_i} \Delta P_{D_i}^{(k)} \quad (3.5)$$

where A_{D_i} is the cost of curtailing the load at the chosen bus i , which could be negotiated or “imposed”, making the load elastic. Observe that the full SC_k amount in this case should be given back to the curtailed load to compensate it for the “forced” reduction in demand.

We assume that the security cost incurred by potential transactions will not be distributed among already existing transactions, i.e. those transactions that define the base system conditions, or SETC. This way, preference is given to already committed transactions that previously cleared the market. Under this assumption, the transaction rescheduling costs for the given iteration k are determined based on a Transaction Contribution Factor (TCF) as defined by

$$TCF_i^{(k)} = \frac{d\lambda/dp_i|_c^{(k)} p_i^{(k)}}{\sum_j d\lambda/dp_j|_c^{(k)} p_j^{(k)}} \quad (3.6)$$

where i stands for the bus number, and $p_i^{(k)}$ corresponds to the value of the corresponding parameter, i.e. the value of $P_{S_i}^{(k)}$ or $P_{D_i}^{(k)}$. Only buses with negative impact on the SATC, i.e. buses with $d\lambda/dp_i|_c^{(k)} < 0$, are considered in this computation; buses with positive impact are given a zero TCF value, so that market participants that do not create the security problem are not charged for the cost of keeping the system secure. The parameter values $p_i^{(k)}$ are included in this “normalization” process to account for the “size” of the corresponding transactions in the security cost. Thus, at each iteration, the TSC at each bus i is determined as

$$TSC_i^{(k)} = TCF_i^{(k)} \cdot SC_k \quad (3.7)$$

Convergence Check and Final Rescheduling Adjustment

If the SATC requirements are met, i.e. if $\lambda_c^{(k+1)} \geq 1$, then the iterative process stops, say at $k = m$. At this point, the final generator or load reschedules are adjusted based on (3.2) or (3.3), respectively, so that the SATC and final transaction level $T^{(m)}$ are the same, i.e. $\lambda_c^{(m+1)} \approx 1$. Thus, for generation redispatch,

$$\Delta P_{S_i}^{(m)} = -\Delta P_{S_j}^{(m)} = \frac{1 - \lambda_c^{(m)}}{d\lambda/dP_{S_i}|_c^{(m)} - d\lambda/dP_{S_j}|_c^{(m)}}$$

and for load curtailment

$$\Delta P_{D_i}^{(m)} = \frac{1 - \lambda_c^{(m)}}{d\lambda/dP_{D_i}|_c^{(m)}}$$

Computation of Nodal Congestion Prices (NCP)

The final transaction levels and NCP for each i node are readily determined as follows:

- Generators:

$$\begin{aligned} P_{S_i} &= P_{S_i}^{(0)} + \sum_{k=1}^m \Delta P_{S_i}^{(k)} \\ NCP_{S_i} &= \frac{1}{P_{S_i}} \sum_{k=1}^m TCF_i^{(k)} SC_k \end{aligned} \tag{3.8}$$

- Loads:

$$\begin{aligned} P_{D_i} &= P_{D_i}^{(0)} - \sum_{k=1}^m \Delta P_{D_i}^{(k)} \\ NCP_{D_i} &= \frac{1}{P_{D_i}} \sum_{k=1}^m TCF_i^{(k)} SC_k \end{aligned}$$

It is important to highlight the fact that the proposed technique to compute NCP assumes that all the costs of rescheduling are fully distributed among the market participants, as in [14].

3.3 Case Studies

Three different test systems, namely, a three-area electricity market, a six-bus test system and a 129-bus model of the Italian HV transmission system, are used here to test the proposed rescheduling technique. The three-area electricity market is used to show some of the advantages of the rescheduling technique; the six-bus system is used to illustrate in detail the proposed rescheduling procedure; and the 129-bus Italian system model is used to test the proposed technique in a more realistic environment.

3.3.1 Three-area Electricity Market

The three-area electricity market is depicted in Figure 3.2. Market participants are represented by suppliers G_1 , G_2 and G_3 , and buyers L_2 and L_3 . The system data can be found in Appendix A.

The market participants' price-quantity bids are shown in Table 3.1. High-low bid matching yields an $MCP = \$30/MWh$. The potential transactions are: G_1 sells 150 MW, L_2 buys 50 MW and L_3 buys 100 MW. Thus, the total level of potential transaction is $T = 150$ MW.

From the TOF analysis, the loading margin results under normal and critical contingency conditions are shown in Table 3.2. The most critical contingency, i.e. Line 1-2 outage, determines the $SATC = 101.11$ MW, which is less than the total amount of potential transactions T ; hence, market rescheduling is needed for secure system operation.

The generation redispatching results are depicted in Figure 3.3. The solid-line curve shows the results obtained from the proposed rescheduling method. The

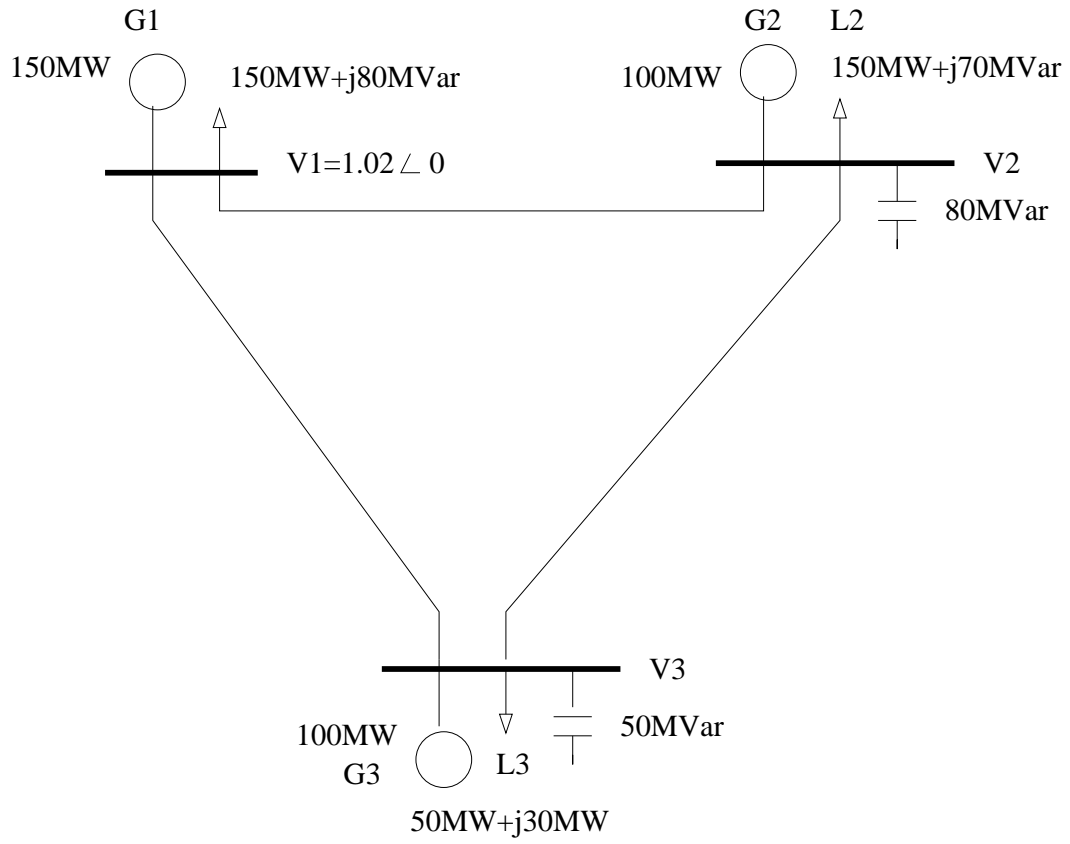


Figure 3.2: Three-area electricity market.

Table 3.1: Price-quantity bids, three-area electricity market

Participants	Quantity (MW)	Bid price (\$/MWh)
G_1	150	25
G_2	100	33
G_3	100	32
L_2	100	30
L_3	100	35

Table 3.2: Loading margin results, three-area electricity market

System Condition	Normal condition (MW)	Line 1-2 out (MW)	Line 1-3 out (MW)	Line 2-3 out (MW)
Loading Margin	177.41	101.11	117.41	261.15

power at G_2 is first chosen for increase, as it has the largest positive impact. When generation on G_2 is increased, the power at G_1 , which has the least impact, must be decreased, to keep the total generation unchanged. After using up all the available power at G_2 (point A in Figure 3.3), power at G_3 is then increased to facilitate all transactions. The total amount of generation redispatching is 105 MW. In this case, the total security cost is $SC = \$310/h$, which can then be distributed among the participants based on the NCP technique proposed, or any other methodology.

If the cheapest available generator G_3 is chosen for redispatching, one obtains the dashed-line curve in Figure 3.3. In this figure, point B represents the point at which G_3 reaches its maximum power bid, and where G_2 is chosen for redispatching. The total rescheduling amount is 150 MW and the total rescheduling cost is $\$350/h$; however, the system is not yet secure, as $\lambda_c < 1$, and thus load curtailment is needed, resulting in higher security cost. This particular example clearly shows the advantages of the proposed method, not only from the security cost and rescheduling point of view, but also from the perspective of possible cost reduction.

For load curtailment, assume that the available amount of curtailable load is $\Delta P_{L2}^m = 50$ MW and $\Delta P_{L3}^m = 100$ MW. L_2 has the biggest impact on SATC, and

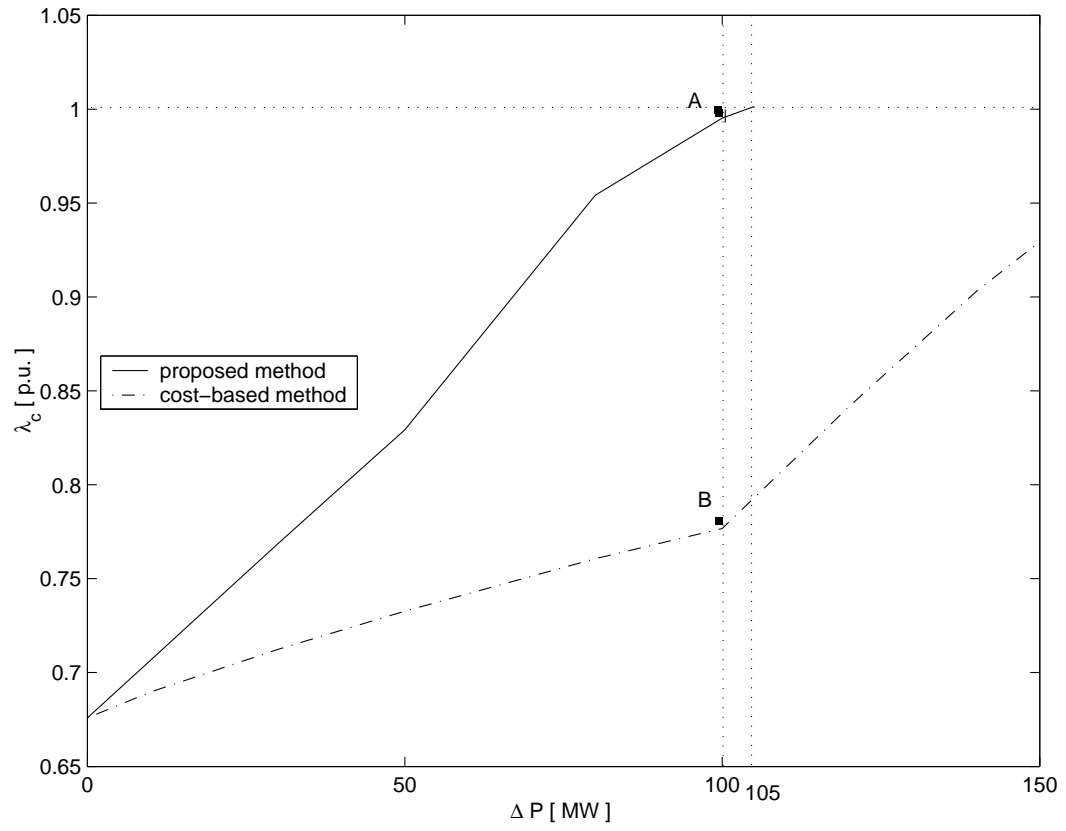


Figure 3.3: Generation redispatching results, three-area electricity market.

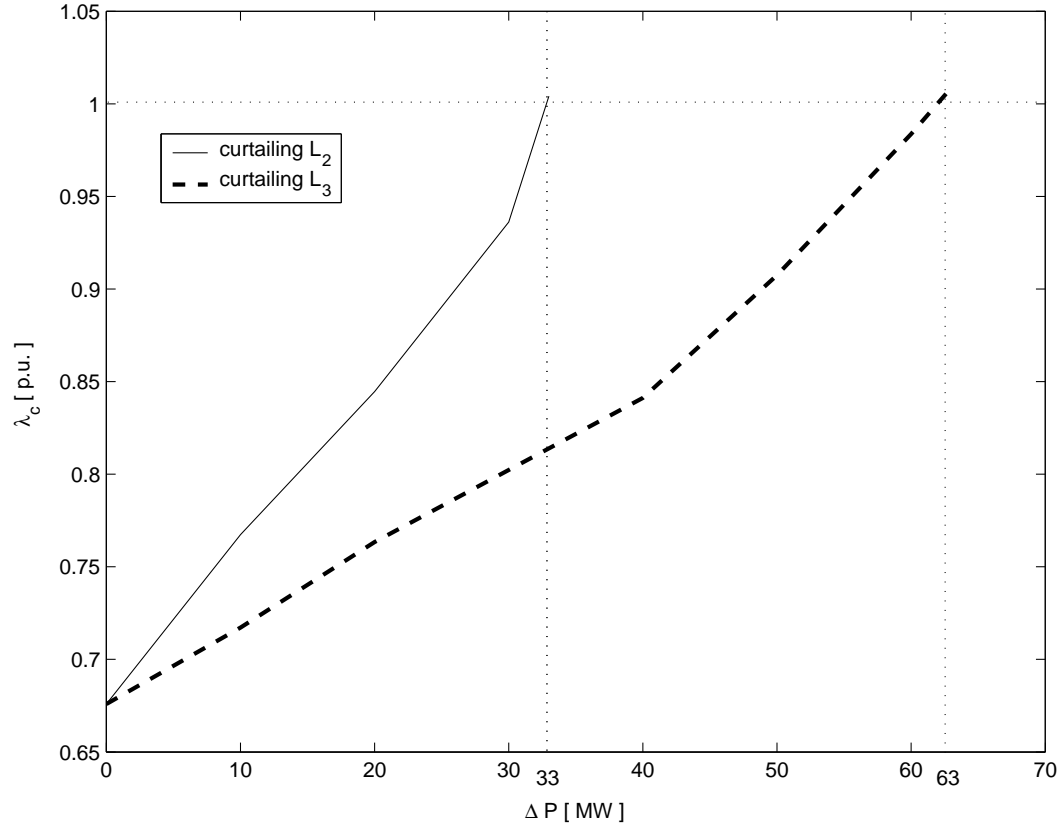


Figure 3.4: Load curtailment results, three-area electricity market.

hence should be adjusted first. The rescheduling results are illustrated by the solid-line curve in Figure 3.4. In this case, the total curtailed load is 33 MW ($T = 117$ MW). If L_3 is used instead, the curtailment process is depicted by the dashed-line curve in Figure 3.4, resulting in a total curtailed load of 63 MW ($T = 87$ MW). This is clearly a worse market condition than that are obtained using the proposed method.

3.3.2 Six-bus System

The six-bus system used in Chapter 2 and depicted in Figure 2.5 is also used here to illustrate the proposed rescheduling procedure for both demand-side bidding and inelastic demand.

Demand-side Bidding

For the case of demand-side bidding, as shown in Section 2.6.1, the SATC is 38.23 MW, corresponding to a minimum bus voltage limit for the worst contingency (Line 2-4 out). Since $\text{SATC} < T$, where $T = 45\text{MW}$, the rescheduling technique is needed to make the transaction feasible. Since GENCO 1 has the most positive impact (0.95 in (2.36) for the initial case), and GENCO 2 has the least impact (-0.03 in (2.36)), the generation of GENCO 1 is increased while at the same time the generation of GENCO 2 is decreased in the same amount to keep power balance; the step length is set in this case to 5 MW. This results in the rescheduling depicted on Table 3.3. Three iterations of generation redispatch are needed; the rescheduling amount for the last step is reduced to make $\lambda_c = 1$, i.e. just enough to facilitate all transactions. The total rescheduling amount is 13.79 MW, and the total security cost $SC = \$2.758/h$.

The TCFs at each iteration are shown in Table 3.4. The variation on the TCF values are due to the change in transaction impact, illustrating the high nonlinearity of the system. The corresponding NCP results are shown in Table 3.5. Observe that bus 4 has the highest NCP; hence, ESCO 1 needs to pay more for keeping the system secure than other market participants, which is reasonable, since ESCO 1 has the most negative impact on system security.

Table 3.3: Rescheduling results with demand-side bidding, six-bus system

k	$\Delta P_{G_1}^{(k)}$ [MW]	$\Delta P_{G_2}^{(k)}$ [MW]	$\lambda_c^{(k)}$	SC_k [\$/h]
1	5	-5	0.90089	1
2	5	-5	0.95642	1
3	3.79	-3.79	1.0	0.758

Table 3.4: TCFs with demand-side bidding, six-bus system

k	1	2	3
$TCF_1^{(k)}$	0	0	0
$TCF_2^{(k)}$	0.0166	0.0607	0.08
$TCF_3^{(k)}$	0	0.0324	0.0772
$TCF_4^{(k)}$	0.8554	0.8198	0.7767
$TCF_5^{(k)}$	0.1082	0.087	0.0662
$TCF_6^{(k)}$	0.0199	0	0

Table 3.5: NCPs with demand-side bidding, six-bus system

Bus i	Participants	V [p.u.]	NCP [\$/MWh]	P_S or P_D [MW]
1	GENCO 1	1.05	0.0	15.14
2	GENCO 2	1.05	0.0129	11.9
3	GENCO 3	1.05	0.005	21.63
4	ESCO 1	0.966	0.0917	25.00
5	ESCO 2	0.956	0.0246	10.00
6	ESCO 3	0.984	0.002	10.00

Inelastic Demand

Similarly, for inelastic demand, as shown in Section 2.6.2, the SATC is 44.74 MW, corresponding to a minimum bus voltage limit for the worst contingency (Line 3-6 out). Since $SATC < T$, where $T = 55$ MW, rescheduling is also needed to make the transaction feasible. In this case, there is not enough power generation available to solve the congestion problem; hence, load curtailment is considered assuming the curtailment costs or “bids” depicted in Table 3.6. The rescheduling results are shown in Table 3.7 and Table 3.8. The generation of GENCO 1 is chosen for increase, and the generation of GENCO 3 is chosen for decrease based on their impacts. There is no security cost associated with redispatch in this case, based on the definition of SC in (3.4), since the bidding price of GENCO 1 is equal to the MCP. After two iterations of generation redispatch, there is no more available generation for redispatching, since GENCO 1 has reached its maximum bidding amount. However, the SATC is still less than the total transaction level T ,

Table 3.6: Curtailment bids for inelastic demand, six-bus system

Bus i	Participant	A_{D_i} [\$ / MWh]	P_{\max} [MW]
4	ESCO 1	24	25
5	ESCO 2	21	10
6	ESCO 3	19	20

Table 3.7: Generation redispatch results for inelastic demand, six-bus system

k	$\Delta P_{G1(k)}$ (MW)	$\Delta P_{G3(k)}$ (MW)	$\lambda_c^{(k)}$	SC_k (\$ / h)
1	5	-5	0.82307	0
2	5	-5	0.83259	0

i.e. $\lambda_c < 1$; hence, load has to be curtailed in this case, resulting in the rescheduling depicted in Table 3.8. In this case, the load on Bus 6, i.e. ESCO 3, has the most negative impact and hence is considered for curtailment. Because of the high curtailment costs assumed, the associated security cost is higher than that associated with generation redispatch. The associated TCFs and resulting NCPs are shown in Table 3.9 and Table 3.10 respectively; observe the large NCP values due to the relatively large load curtailment costs.

It is important to highlight the fact that not dispatching certain loads is an easy and inexpensive way of handling the security problem in the case of demand-side bidding, since there is “no cost” associated with taking an ESCO out of the auction, fully or partially, based on security concerns. However, this will reduce

Table 3.8: Load curtailment results for inelastic demand, six-bus system

k	$\Delta P_{L6(k)}$ (MW)	$\lambda_c^{(k)}$	SC_k (\$/h)
3	-5	0.95055	95
4	-2	1.0072	38

Table 3.9: TCFs for inelastic demand, six-bus system.

k	1	2	3	4
$TCF_{1,k}$	0.0317	0.0535	0.0894	0.1123
$TCF_{2,k}$	0	0	0	0
$TCF_{3,k}$	0.1787	0.1426	0.1013	0.1217
$TCF_{4,k}$	0.2161	0.2155	0.2161	0.2886
$TCF_{5,k}$	0.0951	0.0951	0.0984	0.1310
$TCF_{6,k}$	0.4784	0.4933	0.4948	0.3463

Table 3.10: NCPs for inelastic demand, six-bus system.

Bus i	Part.	V [p.u.]	NCP [\$/MWh]	P_S or P_D [MW]
1	GENCO 1	1.05	0.6726	18.99
2	GENCO 2	1.05	0.0	23.73
3	GENCO 3	1.05	1.501	9.49
4	ESCO 1	0.9663	1.2597	25.00
5	ESCO 2	0.9555	1.4345	10.00
6	ESCO 3	0.9812	4.6284	13.00

revenue for all market participants, and hence should only be considered in the case of no generation available for redispatching, as previously discussed. If the costs of rescheduling are too high, market participants have always the option of pulling out of the market.

3.3.3 129-bus Model of Italian HV Transmission System

A 129-bus model of the Italian 400 KV transmission used here is shown in Figure 3.5, and the system data and market data can be found in Appendix C. In this model, 32 generators and 82 consumers are assumed to participate in the market auction. All bids are based on prices around 30-40 US \$/MWh, which are the average prices over the last few years in other European countries where electricity markets are currently in operation, and considering the actual operating costs of thermal plants. The total fixed generation P_{G0} and fixed load P_{l0} are assumed to be 17016 MW, which is about 80 % of the average power level for a typical working

day. The power bids are chosen to be about 30 % of the average consumption to force transmission congestion. All system data and most of the security constraints, i.e. voltage limits, generation reactive power limits and transmission line thermal limits, were provided by CESI, the Italian electrical research center.

High-low bid matching yields a $MCP = \$34.4/MWh$, and a total potential transaction level $T = 3822.49MW$. The potential transactions are shown in Tables 3.11 and 3.12. The TOF analysis yields the loading margin results under normal condition and critical contingencies shown in Table 3.13. The outage of the line connecting Baggio (bus 36) to Turbigo (bus 50) is the most critical, and defines the $SATC = 3440.7 MW$, which is less than total transaction level T . Therefore, rescheduling is needed; the results of this process are shown in Table 3.14. The total rescheduling amount is 60.44 MW and the total security cost is \$127.5527/h. The NCPs at some nodes, which represent either generation centers or load centers for each area, are shown in Figure 3.6. In this example, generation redispatch is enough to facilitate all potential transactions. Generator Turbigo (bus 13) has the most negative impact on the SATC, thus it is constrained-off; while generators Tavazzano (bus 12), La Casella (bus 6) and Ostiglia (bus 8) have the most positive impact, so they are constrained-on.

3.4 Summary

A rescheduling technique is proposed, described and tested in this Chapter for TSC analysis in a simple-auction-based electricity market. It is essentially an iterative generation redispatch and load curtailment methodology

This rescheduling technique could be considered as a feasible and better alternative to other methodologies that have been proposed and are currently being

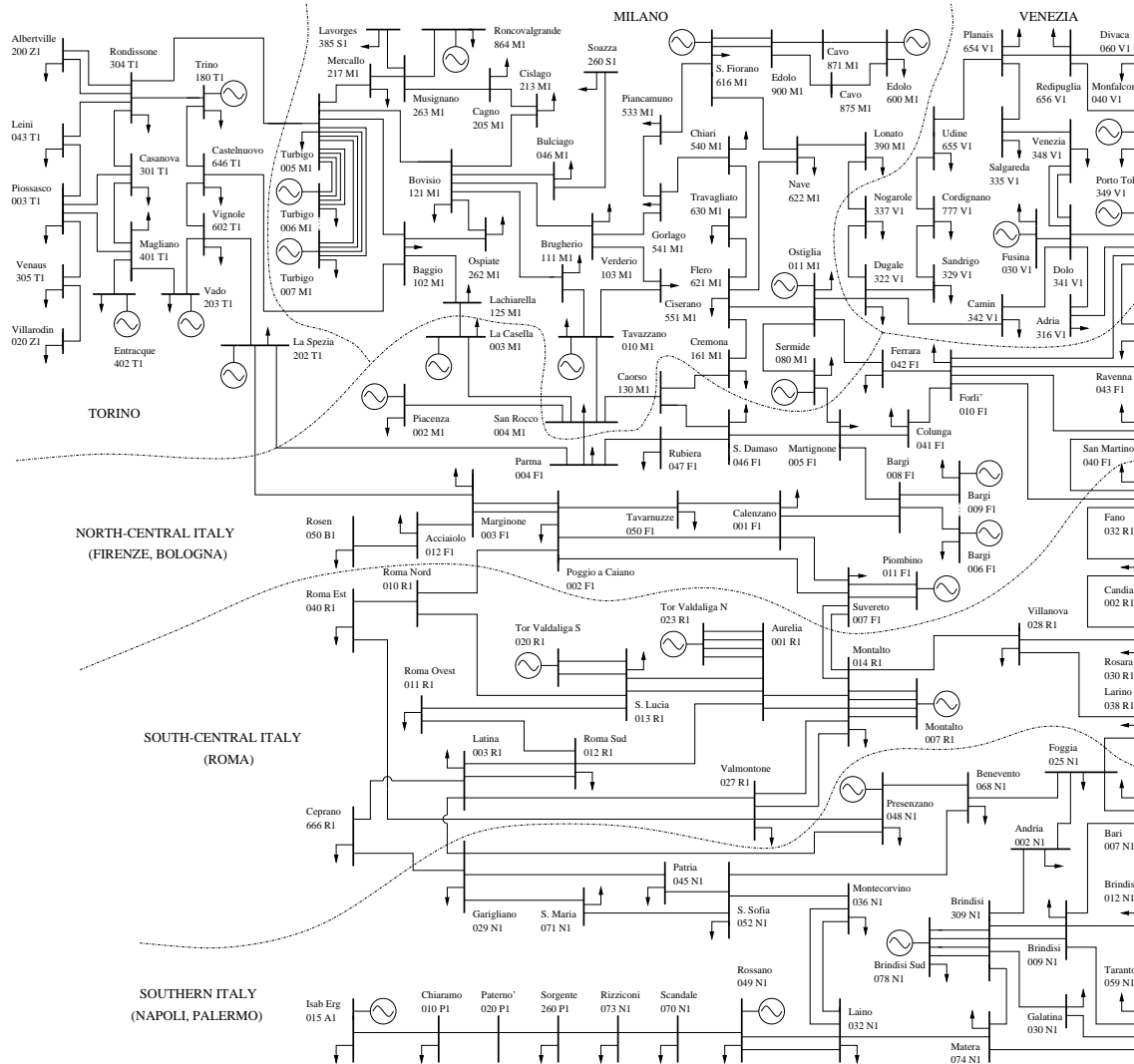


Figure 3.5: 129-bus model of the Italian HV transmission system.

Table 3.11: Generation increase direction, 129-bus Italian system

Bus (i)	1	2	3	4	5	7	9	13
ΔP_g (MW)	251.67	185	116.67	246.67	213.33	93.33	51.67	328.33
Bus (i)	14	15	17	19	20	23	32	34
ΔP_g (MW)	368.33	500	27.33	500	343.33	200	123.61	92.95
Bus (i)	87	95	108	120	129			
ΔP_g (MW)	38.09	37.4	25.85	77.55	1.38			

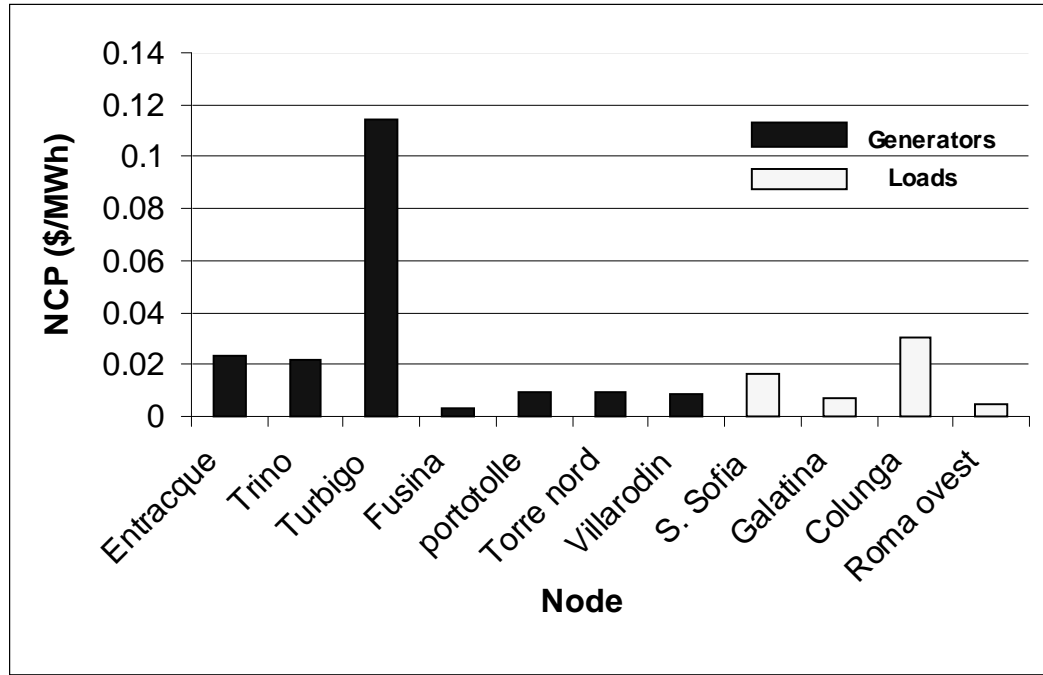


Figure 3.6: Some NCPs by rescheduling technique, 129-bus Italian system.

Table 3.12: Load increase direction, 129-bus Italian system

Bus (i)	26	27	28	29	30	31	35	36
ΔP_l (MW)	79.4	49.8	61.7	72.9	63.1	34.2	44.4	61.7
Bus (i)	37	38	39	41	42	46	48	49
ΔP_l (MW)	77.1	56	46.7	50.6	69.8	30	22.1	69.4
Bus (i)	53	58	59	60	61	62	63	64
ΔP_l (MW)	53.3	73.1	51.9	68.5	95	99.2	104.2	12.5
Bus (i)	65	69	70	71	72	74	76	77
ΔP_l (MW)	60.2	29	117.3	125.4	101.5	40.4	57.1	52.3
Bus (i)	78	79	80	83	85	88	89	90
ΔP_l (MW)	41.3	43.8	29.8	122.5	80	49.8	74.8	23.1
Bus (i)	92	93	94	96	97	98	99	100
ΔP_l (MW)	68.8	46.5	10.4	18.1	59.2	19.2	53.3	52.7
Bus (i)	101	103	104	105	106	107	110	111
ΔP_l (MW)	23.5	54.6	52.9	54.8	45.4	23.1	96.7	86
Bus (i)	112	113	114	115	117	118	119	122
ΔP_l (MW)	20	34.6	87.5	11.5	24	49.6	55.6	33.1
Bus (i)	123	124	125	127	128			
ΔP_l (MW)	21.9	70.6	74.2	43.5	36.7			

Table 3.13: Loading margin results, 129-bus Italian system

System Condition	Normal condition (MW)	Line 36-50 out (MW)	Line 122-121 out (MW)	Line 123-122 out (MW)
Loading Margin	8919.78	3440.70	3894.74	5364.48

Table 3.14: Rescheduling results, 129-bus Italian system

k	Constrained-on Generator	Constrained-off Generator	$\lambda_c^{(k)}$	$\Delta P_s^{(k)}$ [MW]	SC_k [\$ / h]
1	12	13	0.92098	10	4.4
2	6	13	0.93026	10	35.6
3	8	13	0.94864	10	8.0
4	6	13	0.96939	10	35.6
5	8	13	0.97846	10	8.0
6	6	13	0.99908	10	35.6
7	8	13	1.0	0.44	0.3528

used in simple-auction-based electricity markets to handle transmission congestion, as the full nonlinearities of the system as well as certain system stability issues are considered in the pricing process.

The proposed iterative technique could be readily adapted to integrate full dynamic SATC computations, as long as the required SATC values and sensitivities can be determined on-line.

Chapter 4

Transaction Security Cost Analysis by Take-risk Strategy

Chapter Synopsis

A novel take-risk strategy is proposed in this chapter for TSC analysis. It is based on a probabilistic view of SATC, taking a risk of system collapse to facilitate more market transactions. The TSC analysis methodology is proposed based on expected system collapse costs, and tested in three different systems for illustration purposes.

4.1 Introduction

The take-risk technique proposed here also applies to a market clearing condition that violates certain security constraints. It applies to the case where the total amount of potential transactions fall between the SATC and the maximum loading margin of the system.

As mentioned in Chapter 2, the SATC of a system is determined by thermal limits, voltage limits and stability limits, considering possible contingencies; usually an N-1 contingency criterium is used to account for possible contingencies. Since contingencies usually decrease these security limits, the system feasibility region and SATC can be considered to be conservative [51, 52], thus reducing the amount of power that can be delivered. In a competitive market environment, this situation may lead to loss of revenue.

In this thesis, a take-risk strategy is proposed by taking a probabilistic view of the SATC, i.e. one takes a risk by assuming that the contingencies may not actually occur, and thus these conservative security limits are relaxed to facilitate more transactions. A security cost is then associated with this risk based on the costs of system collapse. How much risk can be taken depends on how reliable the system is, and also how big the related security costs are.

4.2 Analysis Procedure

Under the proposed take-risk strategy, one assumes that the system may be loaded beyond its SATC value, which is referred to as $\lambda_{c_{\min}}$, up to the maximum loading value for the system without contingencies, which is referred to as $\lambda_{c_{\max}}$. Hence, if the transaction level T obtained from the solution of high-low bid matching falls between $\lambda_{c_{\min}}$ and $\lambda_{c_{\max}}$, i.e. $\lambda_{c_{\min}} < T < \lambda_{c_{\max}}$, the operator can take a risk of losing the system due to a possible contingency, and hence security costs have to be determined based on the value of T , the probability of the contingency occurring, and the cost of losing the system. As suggested in [52], the total security cost SC is defined as

$$SC = EC = C_{collapse} \cdot \psi \quad (4.1)$$

where EC is the expected system collapse cost; $C_{collapse}$ is the cost of losing the system, which in principle represents a very high value that market participants would realistically not be willing to accept; and ψ represents the probability of system collapse, and thus depends on the values of T , λ_{cmin} , and λ_{cmax} . This equation should reflect the obvious fact that the closer the value of T to λ_{cmax} , the more likely it is for the system to collapse, since the system is more stressed. Thus, the probability of system collapse is expressed as

$$\psi = h(T, \lambda_{cmin}, \lambda_{cmax})$$

where the function h is a probability distribution function, associated with a probability density. The following distribution function is used in this thesis to represent a variety of probability densities:

$$\psi = \begin{cases} 0 & \text{for } T \leq \lambda_{cmin} \\ \left(\frac{T - \lambda_{cmin}}{\lambda_{cmax} - \lambda_{cmin}} \right)^a & \text{for } \lambda_{cmin} < T < \lambda_{cmax} \\ 1 & \text{for } T \geq \lambda_{cmax} \end{cases} \quad (4.2)$$

where $a \geq 0$ is a constant that is used to represent the risk of collapse due to contingencies in the system; the higher this value, the lower is the *assumed* risk of collapse due to a critical contingency for a given transaction level T , i.e. the less likely a contingency is to occur at a given loading level, and hence the lower the security costs. For the six-bus test system at Figure 2.5 and assuming demand-side bidding, Figure 4.1 depicts the value of ψ versus the transaction level T for various values of a , where Figure 4.2 illustrates the probabilistic density associated with ψ .

- When $a = 1$, the probability of system collapse is uniformly distributed on $[\lambda_{cmin}, \lambda_{cmax}]$ (solid-line curves in Figure 4.1 and Figure 4.2).
- When $a = 2$, the probability of system collapse is linearly distributed on $[\lambda_{cmin}, \lambda_{cmax}]$ (dashed-line curves in Figure 4.1 and Figure 4.2).

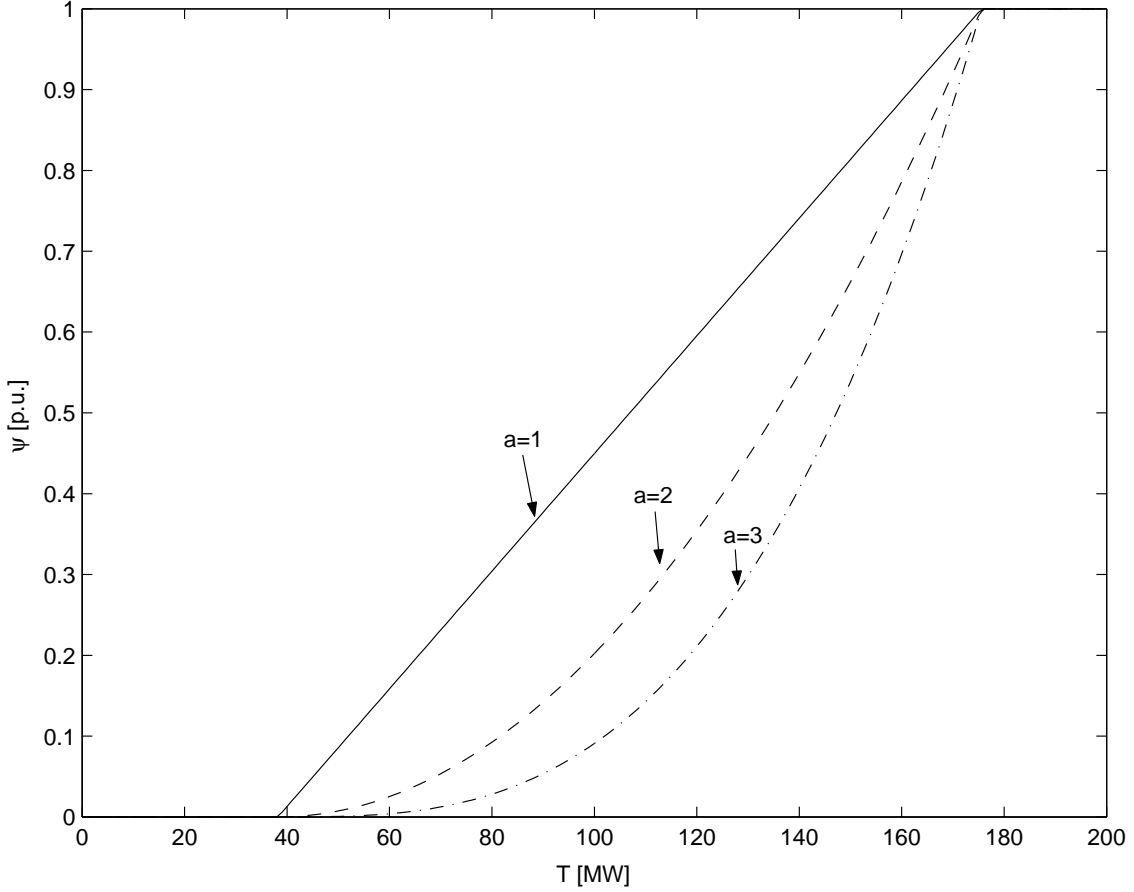


Figure 4.1: Probability distribution of collapse, six-bus test system.

- When $a = 3$, the probability of system collapse is quadratically distributed on $[\lambda_{min}, \lambda_{max}]$ (dot-dashed-line curves in Figure 4.1 and Figure 4.2).

To determine the actual probabilistic distribution function, or risk level a , more detailed probabilistic analysis, such as Monte-Carlo simulations, could be used based on the history of system contingencies. These types of probability-based techniques to determine an actual value for a are complex and time consuming in general, and are not discussed in this thesis (topic for future research). However, system operators, based on the knowledge of their system, should be able to heuris-

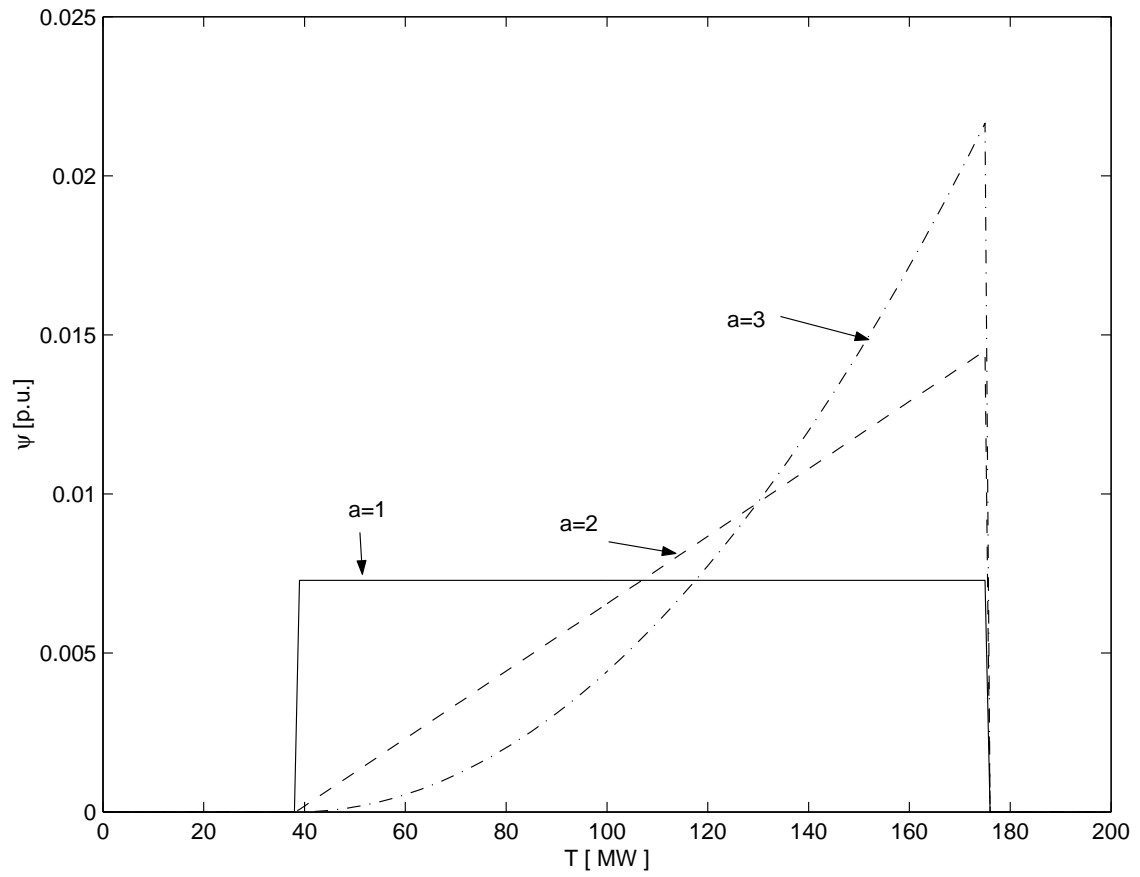


Figure 4.2: Probabilistic density of system collapse, six-bus test system.

tically determine an “adequate” value of a for their particular system and operating conditions by analyzing the results obtained for different values of a . Generally the more robust the system condition, the less likelihood of system collapse, i.e. a large value of a can be used in systems where the history of collapse in the system is low.

The security cost SC is distributed among the transactions that have negative impact on the SATC, in a similar way as previously proposed for the rescheduling technique in Chapter 3. Thus, a TCF is determined for each participant bus i as follows:

$$TCF_i = \frac{d\lambda/dp_i|_c p_i}{\sum_j d\lambda/dp_j|_c p_j}$$

where, as in equation (3.6), p_i represents the transaction value of the corresponding participant, i.e. the value of P_{S_i} or P_{D_i} ; and $d\lambda/dp_i|_c$ represents the impact of the participant i on the SATC, as discussed in Section 2.5. Only participants with $d\lambda/dp_i|_c < 0$ are considered in this computation, whereas participants with positive impact are given a zero TCF_i value, as they do not create a security problem under consideration. Transaction security cost for transaction i can be expressed as

$$TSC_i = TCF_i \cdot SC \quad (4.3)$$

And the Nodal Congestion Prices (NCP) can then be obtained as follows:

$$NCP_i = \begin{cases} TCF_i SC / P_{S_i} & \text{for generators} \\ TCF_i SC / P_{D_i} & \text{for loads} \end{cases} \quad (4.4)$$

Observe that the security costs are fully distributed among the bidding participants only. Other security pricing mechanism could be readily implemented depending on the particular market rules, based on the main idea proposed here.

4.3 Case Studies

Three different test systems are used here to test the proposed take-risk TSC technique. The three-area electricity market is used to illustrate the proposed take-risk strategy, and show how this compares to the rescheduling strategy discussed in Chapter 3; the six-bus system is used to illustrate take-risk procedure in detail; and the 129-bus model of the Italian system is used to show the applicability of the take-risk technique to realistic systems.

4.3.1 Three-area Electricity Market

From the loading margin results obtained by TOF analysis, as shown in Table 3.2, $\lambda_{max} = 177.41$ MW, and $\lambda_{min} = 101.11$ MW. Since the transaction level T is larger than λ_{min} , a take-risk strategy is used here to facilitate all potential transactions.

The security costs under different probability distributions are shown in Table 4.1. It is obvious that the higher the value of a , the lower the assumed probability of system collapse, and thus the lower the total security costs. For robust systems, a higher value of a can be chosen to facilitate more transactions for economic benefit. The TCFs obtained based on a transaction impact analysis are shown in Table 4.2. The final NCPs for the case of $a = 5$ are shown in Table 4.3. Observe that NCPs for L_2 and L_3 are very high, due to the closeness of the total transaction level T to λ_{max} . In this case, participants L_2 and L_3 are more likely to pull out of the market.

The total security costs obtained using this technique for different values of the probability distribution factor a are compared with the results obtained from the rescheduling technique, i.e. generation redispatch and load curtailment, as shown in

Table 4.1: Security costs vs. probability distribution, three-area electricity market

a	ψ	SC [\$/h]
1	0.6408	$3.204 * 10^6$
2	0.4106	$2.053 * 10^6$
3	0.2631	$1.3155 * 10^6$
4	0.1686	$0.843 * 10^6$
5	0.1080	$0.54 * 10^6$

Table 4.2: TCFs, three-area electricity market

Participant(i)	TCF_i
L_1 (1)	0.0
L_2 (2)	0.5187
L_3 (3)	0.4813

Table 4.3: NCPs, three-area electricity market

Participant(i)	NCP_i (\$/MWh)
L_1 (1)	0.0
L_2 (2)	5600
L_3 (3)	2600

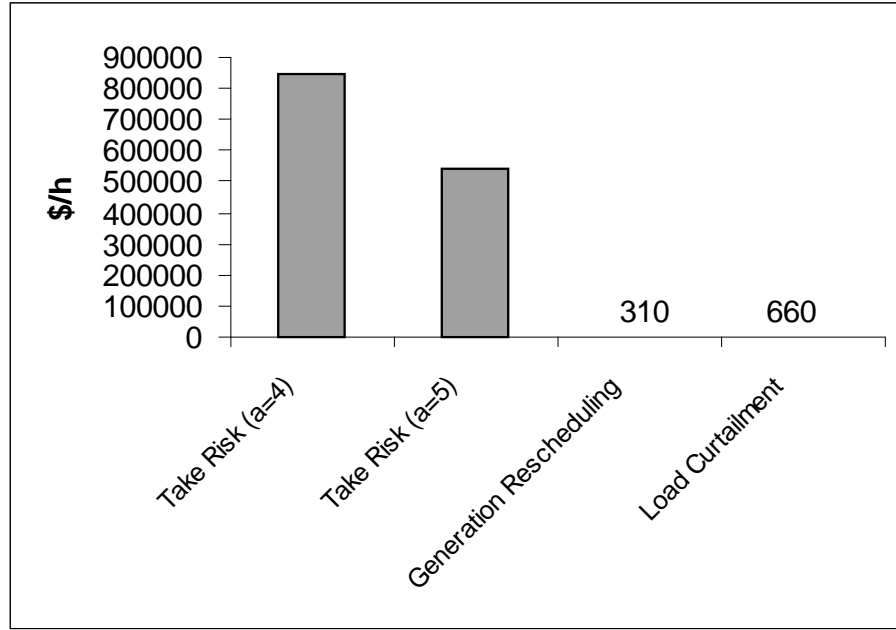


Figure 4.3: Security cost comparison, three-area electricity market

Figure 4.3. Observe that, in general, the total security costs under take-risk strategy are higher than those obtained from the rescheduling technique, especially for low values of a , as system security could be considered to be managed conservatively. If one would like to take a higher risk, i.e. choose a bigger value of a , the total security costs may become comparable with those obtained from the proposed rescheduling technique, as shown in the 6-bus system later. The latter applies to highly reliable systems, in this case, the proposed take-risk strategy becomes a competitive choice with respect to rescheduling to facilitate transactions.

Table 4.4: TCFs with demand-side bidding, six-bus system.

Participant(i)	TCF_i
S_2 (2)	0.0166
S_3 (3)	0
D_1 (4)	0.8554
D_2 (5)	0.1082
D_3 (6)	0.0199

4.3.2 Six-bus System

The six-bus system of Figure 2.5 is used here to illustrate the detailed take-risk procedure. Since the proposed procedure is the same for demand side bidding and inelastic demand, only demand side bidding is used here as an example.

Based on the transaction impact analysis described in Section 2.5, TCFs for the successful market participants are shown in Table 4.4. Based on the assumption that the average direct interruption cost of system load is \$10.00/kWh [46, 52, 94], $C_{collapse}$ is assumed to be $\$3.25 * 10^6/h$ for the total 325 MW system load. The total security costs for different probability distribution functions are shown in Table 4.5; the larger the value of a , the lower the assumed risk of system collapse for a given transaction level, and hence the lower the security costs associated with the transactions.

In this example, if a is chosen to be less than 4, the TSC would be very high due to the high costs and the high assumed risks associated with system collapse, and hence market participants may choose to pull out of the market. One would expect that in competitive electricity markets with reliable transmission systems,

Table 4.5: Security costs vs. probability distribution with demand-side bidding, six-bus system.

a	ψ	SC [\$/h]
1	0.04929	$1.6 * 10^5$
2	$2.43 * 10^{-3}$	7900
3	$1.2 * 10^{-4}$	390
4	$5.9 * 10^{-6}$	19.175
5	$2.91 * 10^{-7}$	0.946

a large value of a would be chosen (e.g. $a = 5$), which would facilitate market transactions. The NCPs for all market participants in this case are shown in Table 4.6 for a risk level $a = 5$. As expected, the cost results are somewhat comparable to those obtained with rescheduling; however, in this case, all the requested load is supplied at certain risk for the system.

4.3.3 129-bus Model of Italian HV Transmission System

The 129-bus Italian system model is used here to show the applicability of the take-risk technique to realistic systems.

From the loading margin results shown in Table 3.13, λ_{cmax} and λ_{cmin} are determined to be 8919.78 MW and 3440.70 MW, respectively. The total system collapse cost is assumed to be \$2.08E8/h, based on the total system load and the assumption of an average direct interruption cost of system load of \$10.00/kWh [46, 52, 94]. The total security costs under different probability distribution are shown in Table 4.7. The resulting NCPs at a risk level $a = 5$ for certain selected load buses, which

Table 4.6: NCPs with demand-side bidding, six-bus system

Bus i	Participants	V [p.u.]	NCP [\$/MWh]	P_S or P_D [MW]
1	GENCO 1	1.05	0.0	0
2	GENCO 2	1.05	0.0006	27.03
3	GENCO 3	1.05	0.0	21.62
4	ESCO 1	0.966	0.0324	25.00
5	ESCO 2	0.956	0.0102	10.00
6	ESCO 3	0.983	0.0019	10.00

correspond to load centers for each area, are shown in Figure 4.4, and the NCP of generator Turbigo is \$0.0078/MWh. Comparing with the results obtained from rescheduling technique, the NCPs are lower for generators and higher for loads.

Table 4.7: Security costs vs. probability distribution, 129-bus Italian system

a	ψ	SC [\$/h]
1	0.06968145	$1.45 * 10^7$
2	$4.856 * 10^{-3}$	$1.012 * 10^6$
3	$3.38 * 10^{-4}$	70504
4	$2.357 * 10^{-5}$	4912.87
5	$1.64 * 10^{-6}$	342.34

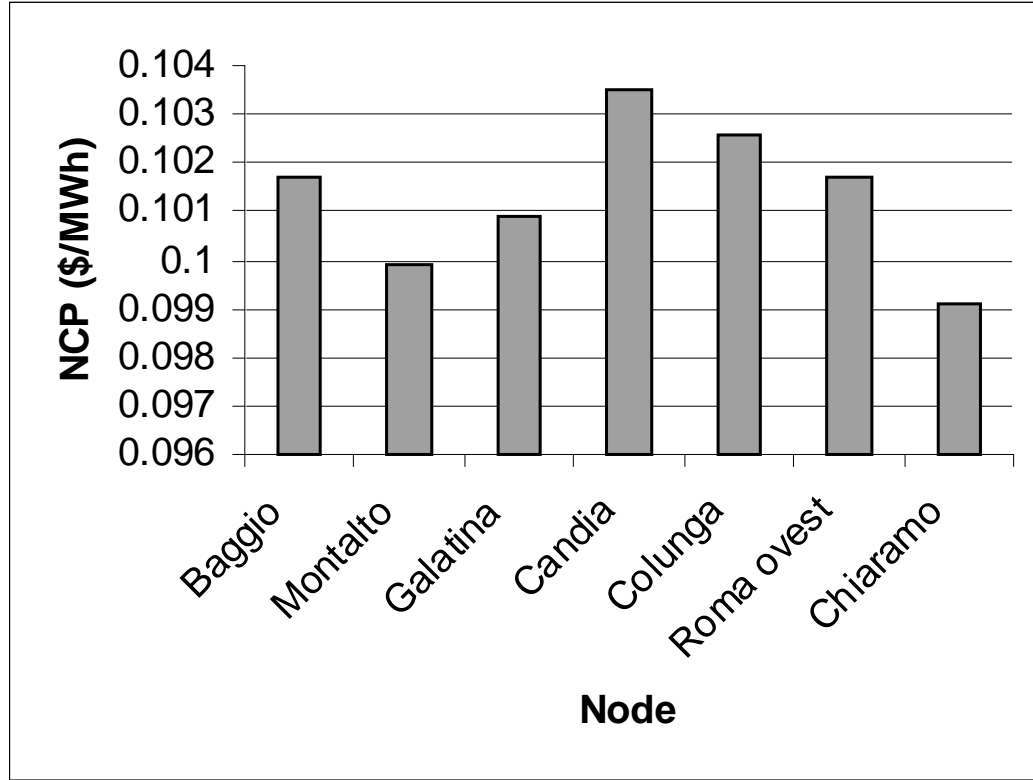


Figure 4.4: Some NCPs by take-risk technique, 129-bus Italian system.

4.4 Summary

A new TSC analysis method based on a take-risk strategy is presented in this Chapter. It is based on a probabilistic point of view of the SATC, to generate proper operating and price signals for the market participants. Test results indicate that the proposed take-risk TSC analysis method can be readily integrated in simple auction market structures. However, a more detailed probabilistic analysis should be used to determine the actual values of the risk level, based on the history of system contingencies. Nevertheless, an operator may be able to use the proposed

probability distribution functions with a risk level consistent with the operational knowledge of the system.

Chapter 5

Short Term Load Forecasting in Electricity Markets

Chapter Synopsis

Short-Term Load Forecasting (STLF) is important for system and market operation. In this thesis, STLF is used to define the direction of load increase for SATC computations and security cost analysis.

In this Chapter, STLF and the related forecasting techniques are first briefly introduced. Load characteristics are then analyzed with the aim of providing accurate and fast forecasting. An ANN-based STLF method considering the price of electricity is then discussed, using the Ontario Hydro system as a case study to evaluate the performance of the proposed technique.

5.1 Introduction

STLF is basically aimed at predicting system load with a leading time of one hour to seven days, which is necessary for adequate scheduling and operation of power systems. STLF traditionally has been an essential component of Energy Management Systems (EMS) [95, 96, 97], as it provides the input data for load flow and contingency analysis.

With the worldwide deregulation of the power industry, load forecasting is becoming even more important, not only for system operators, but also for market operators, transmission owners, and any other market participants, so that adequate energy transactions can be scheduled, and appropriate operational plans and bidding strategies can be established. Thus, load forecasting has also become an important component of energy brokerage systems [26]. In this new context, high forecasting accuracy and speed are required not only for reliable system operation, but also for adequate market operation, as both under-forecasts and over-forecasts would result in increased operational costs and loss of revenue.

Various forecasting techniques have been applied to STLF to improve accuracy and efficiency. In general, STLF techniques can be classified as either traditional or modern [98]. Traditional statistical load forecasting techniques, such as regression [99], time series [100], pattern recognition [101], Kalman filters [102], etc. have been used in practice for a long time, showing the forecasting accuracy that is system dependent. These traditional methods can be combined using weighted multi-model forecasting techniques, showing adequate results in practical systems [58]. However, these methods cannot properly represent the complex nonlinear relationships that exist between the load and a series of factors that influence it, which are typically dependent on system changes (e.g. season or time of day).

Modern load forecasting techniques, such as expert systems [103], Artificial Neural Networks (ANN) [95, 104, 105, 106], fuzzy logic [107], wavelets [108], have been developed more recently, showing good results. Among them, ANN methods are particularly attractive, as they have the ability to handle the nonlinear relationships between load and the factors that directly affect it, based only on historical data and without the need for selecting a given model. Different types of ANNs have been applied to STLF; for example, multi-layer feed-forward with one hidden layer [104], recurrent [106], and functional links [105].

To achieve high forecasting accuracy and speed, which are the two most important requirements of STLF, it is important to analyze the load characteristics and identify the main factors affecting the load. In electricity markets, in addition to the traditional load affecting factors such as season, day type and weather, electricity price, which is voluntary and may have a complicated relationship with system load, is also becoming an important factor influencing the load.

In this thesis, the effect of pricing on the STLF is examined, using the Ontario system as the test case, showing that better results are obtained when price is considered in the forecasting method. The more common multi-layer feed-forward ANN is used for the analysis.

5.2 Load Characteristics

Traditionally, system load at any given time is assumed to be a combination of four separate components, i.e.

$$L = L_n + L_w + L_s + L_r \quad (5.1)$$

where

L stands for the total system load;

L_n represents the “normal” part of the load, which is a set of standardized load shapes for each “type” of day that has been identified as occurring throughout the year;

L_w corresponds to the weather-sensitive part of the load, which is tightly coupled to the season of the year;

L_s stands for the special event part of the load, which is the occurrence of an unusual or special event leading to a significant deviation from the typical load behavior;

L_r corresponds to a random part of the load, which is an “unexplained” component of the load usually represented as zero mean white noise.

In competitive electricity markets, system load may also be significantly affected by prices. Since electricity must be produced and consumed instantaneously, and there are only limited transfer capabilities of transmission systems [5], electricity prices vary depending on place and time, presenting relatively high variations as compared to other commodities. Consumers, especially price-elastic consumers, tend to adjust their consumption behavior according to the price information to achieve maximum benefits. Hence, price should be factored in the relationship between system load and its influencing factors, i.e.

$$L = f(\text{day,weather,special,price,random}) \quad (5.2)$$

where $f(\cdot)$ is a highly nonlinear function that is difficult to represent explicitly. Thus forecasting the system load accurately with traditional statistical methods would be a rather complex problem; this is why ANN-based techniques are used here for STLF.

5.3 An ANN-based STLF

ANN-based methods are a good choice to study the STLF problem, as these techniques are characterized by not requiring explicit models to represent the complex relationship between the load and the factors that determine it.

5.3.1 Forecasting Model

Neuron model

ANNs are made up of a number of simple and highly interconnected Processing Elements (PE), called neurons, as depicted in Fig. 5.1 [109]. Its mathematical model is expressed as

$$O_j = f_j \sum_k (w_{jk} X_k) \quad (5.3)$$

where

O_j is the output of a neuron;

f_j is a transfer function, which is differentiable and non-decreasing, usually represented using a sigmoid function, such as a logistic sigmoid, a tangent sigmoid, etc.;

w_{jk} is an adjustable weight that represents the connection strength;

X_k is the input of a neuron.

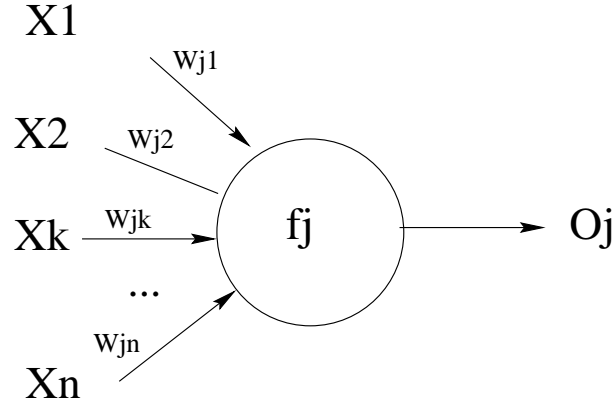


Figure 5.1: Mathematical model of an ANN neuron.

Network Architecture

The three-layer fully connected feed-forward neural network depicted in Figure 5.2 is used here; it includes an input layer, one hidden layer and an output layer [110]. Signal propagation is allowed only from the input layer to the hidden layer and from the hidden layer to the output layer. The input variables come from historical data corresponding to the factors that affect the load, whereas the outputs are the desired forecasting results, which in this case are $m = 24$, i.e. one for each hour of the day.

The number of inputs, the number of hidden nodes, transfer functions, scaling schemes, and training methods affect the forecasting performance and hence need to be chosen carefully.

Training

ANN training basically consists on determining the network parameters, such as weights and others, that allow achieving the desired objective based on the available training sets. Usually, multi-layer feed-forward neural networks are trained in a

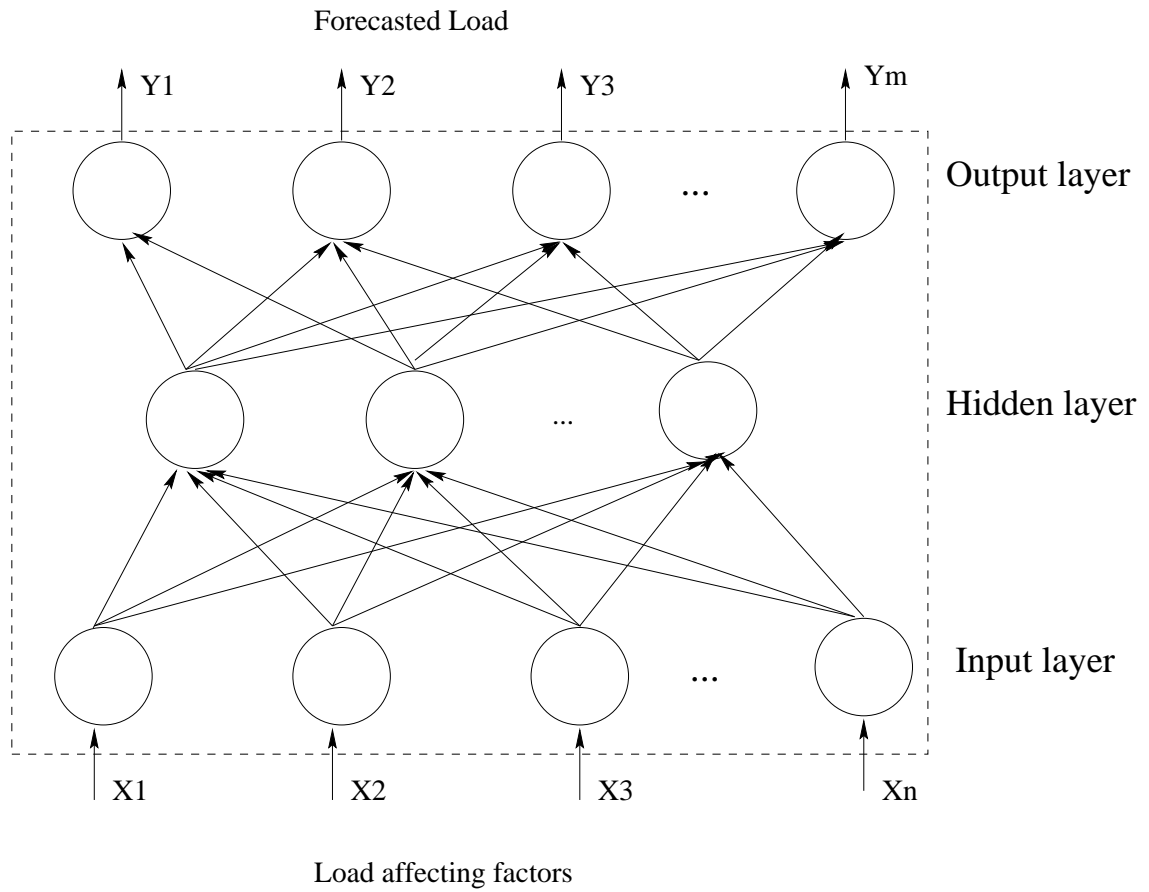


Figure 5.2: Schematic of the three layer feed-forward ANN for STLF.

supervised manner. Back-propagation is used as the training method here [109], which is an iterative procedure that has three steps during each iteration:

1. Forward: The outputs are calculated for given inputs.
2. Backward: The errors at the output layer are propagated backwards toward the input layer, with the partial derivatives of the performance with respect to the weights and biases calculated in each layer.
3. Weight adjustment: A multivariate nonlinear numeric optimization algorithm finds the weights that minimize the error based on the gradient.

Training stops when the performance has been minimized to the goal, or the performance gradient falls below a minimum gradient, or the maximum number of epochs is reached, or the maximum amount of time has been exceeded.

The error function used in the back-propagation training process is the sum-squared error, i.e.

$$E = \frac{1}{2} \sum_p \sum_j (t_{pj} - O_{pj})^2 \quad (5.4)$$

where t_{pj} and O_{pj} are the target output and the actual output j for input pattern p , respectively.

The learning function used in the training process is a gradient descent with momentum weight/bias function, which allows to calculate the weight change for a given neuron. It is expressed as

$$dW = m_c * dW_{prev} + (1 - m_c) * l_r * gW \quad (5.5)$$

where dW_{prev} is the previous weight change, gW is the weight gradient with respect to the performance, l_r is the learning rate, and m_c is the momentum. Different values for the learning rate and momentum affect the convergence properties.

5.3.2 Forecasting Procedure

The STLF procedure for the chosen ANN model is shown in Figure 5.3, and consists of the following steps:

1. Input Variable Selection: Input variables such as load, day type, temperature and spot prices of the previous day, and day type, temperature and spot prices of the forecasting day are initially chosen.
2. Data Pre-processing: Improperly recorded data and observation errors are inevitable. Hence, bad and abnormal data are identified and discarded or adjusted using a statistical method to avoid contamination of the model [97].
3. Scaling: Since the variables have very different ranges, the direct use of network data may cause convergence problems. Two scaling schemes are used and compared. In the first scheme, all input X_i and output O_i variables are scaled to be in the $[0, 1]$ range; hence, the input and output variables are scaled as follows:

$$\begin{aligned} X_i^{(k)'} &= X_i^{(k)} / \max(X_i^{(k)}) \\ O_i^{(k)'} &= O_i^{(k)} / \max(O_i^{(k)}) \end{aligned} \quad (5.6)$$

where k is the index of input X and output O vectors/patterns.

In the second scheme, the input and output variables are scaled to be in the $[-c, c]$ range, where c is a positive number. The inputs and outputs in this case are scaled as follows:

$$\begin{aligned} X_i^{(k)'} &= (X_i^{(k)} - \tilde{X}_i) / S_i \\ O_i^{(k)'} &= (O_i^{(k)} - \tilde{O}_i) / SO_i \end{aligned} \quad (5.7)$$

where S_i and SO_i are the estimates of the standard deviation of input and output i , respectively, and \tilde{X}_i and \tilde{O}_i are the average values of the corresponding input and output. The error function has different minimum values for the two different scaling schemes.

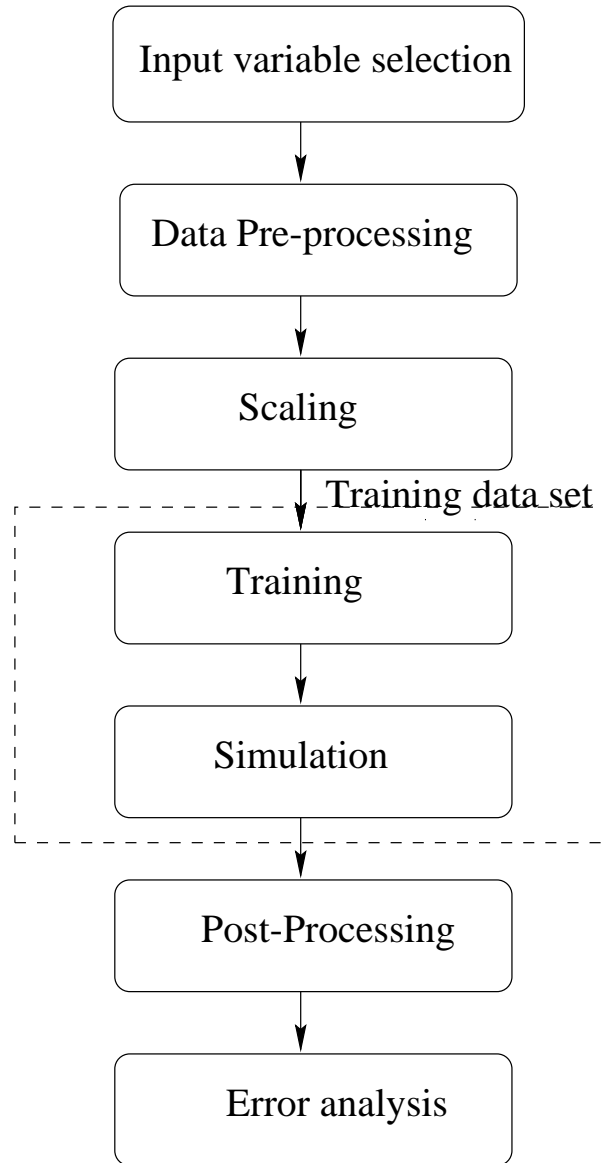


Figure 5.3: ANN-based demand forecasting procedure.

4. Training: Each layer's weights and biases are initialized when the neural network is set up. The network adjusts the connection strength among the internal network nodes until the proper transformation that links past inputs and outputs from the training cases is learned. Data windows are used for training and moved one day ahead.
5. Simulation: Using the trained neural network, the forecasting output is simulated using the input patterns.
6. Post-Processing: The neural network output need de-scaling to generate the desired forecasted loads. If necessary, special events can be considered at this stage.
7. Error Analysis: As characteristics of load vary, error observations are important for the forecasting process. Hence, the following Mean Absolute Percentage Error (MAPE) ε and Root Mean Square Error (RMSE) σ are used here for after-the-fact error analysis:

$$\varepsilon = \frac{1}{N} \sum_{i=1}^N \frac{|X_t - X_f|}{X_t} * 100 \quad (5.8)$$

$$\sigma = \sqrt{\frac{1}{N} \sum_{i=1}^N (X_t - X_f)^2} \quad (5.9)$$

where X_t is the actual load and X_f is the forecasted load.

5.4 Case Study

The historical data of Ontario system load for May 1999 was used for testing the proposed ANN-based STLF. Due to the demerger of Ontario Hydro in early 1999,

Ontario electricity prices may be assumed to have had no major impact on the load of interest. However, due to the large power exchange between Pennsylvania-New Jersey-Maryland (PJM) and Ontario, and the fact that PJM has operated a large energy spot market for a while, one may reasonably assume that these prices may have had a significant impact on the Ontario power exchange, and thus affect the overall Ontario system load for the period of interest. Thus, PJM electricity spot price data for the corresponding time period is used here as the price input for the forecasting process.

A neural network with 100 inputs, 48 hidden nodes, and 24 outputs, with the second scaling scheme previously described, is used here. A tangent sigmoid function was chosen as the transfer function for the hidden layer, and a linear function for the output layer. This particular ANN was chosen based on several tests with different number of inputs, hidden nodes, transfer functions and scaling schemes.

The training performance for $l_r = m_c = 0.6$ is shown in Figure 5.4. The fast convergence without oscillation is due to the relative large values of l_r and m_c , which were chosen based on multiple tests carried out with different values of these two parameters.

The Ontario system loads in May 1999 are used for the training process. The STLF results for Monday May 24, 1999, Thursday May 27, 1999 and Saturday May 29, 1999 are depicted in Figures 5.5, 5.6 and 5.7; observe the satisfactory forecasted results for these days (part of the training set). The adequate performance of the proposed STLF is also illustrated in the absolute percentage error plot for each hour on each day of May 1999 shown in Figure 5.8; the MAPE is 0.0048 (0.48%) and the maximum absolute error is 0.03 (3%).

If price effects are not considered, the number of iterations required to achieve

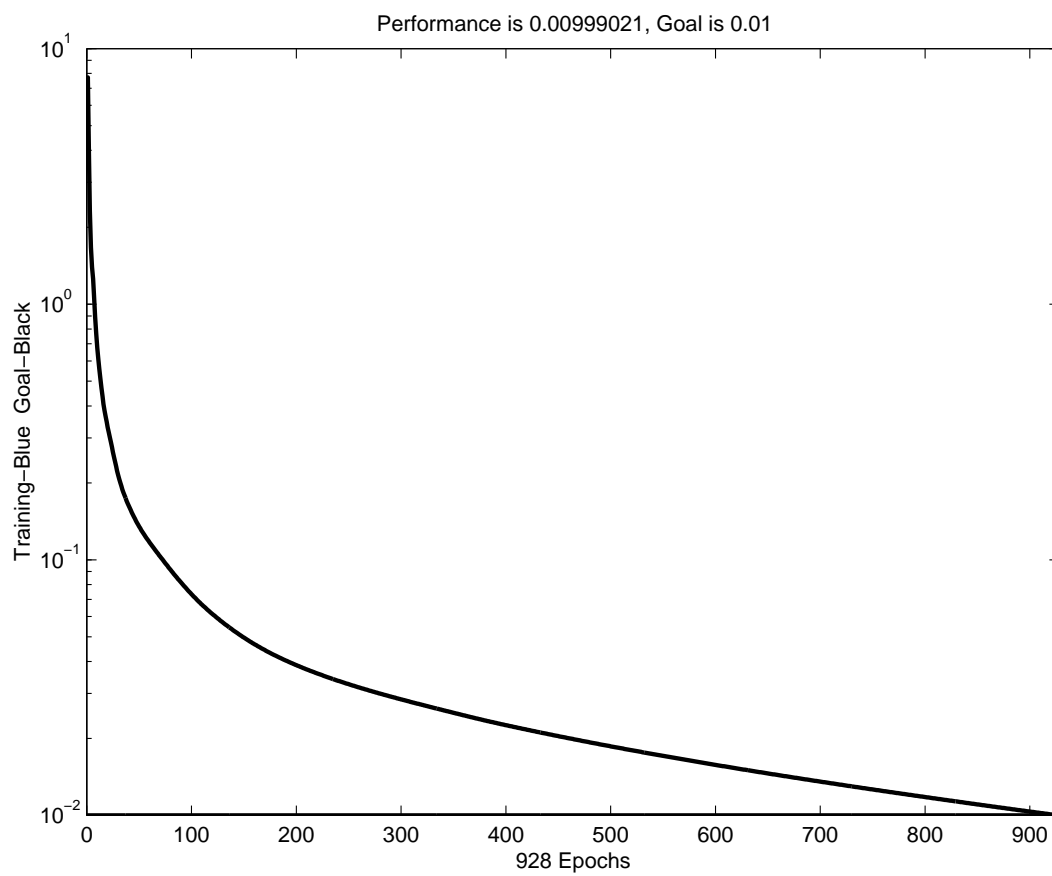


Figure 5.4: Training performance of the chosen ANN.

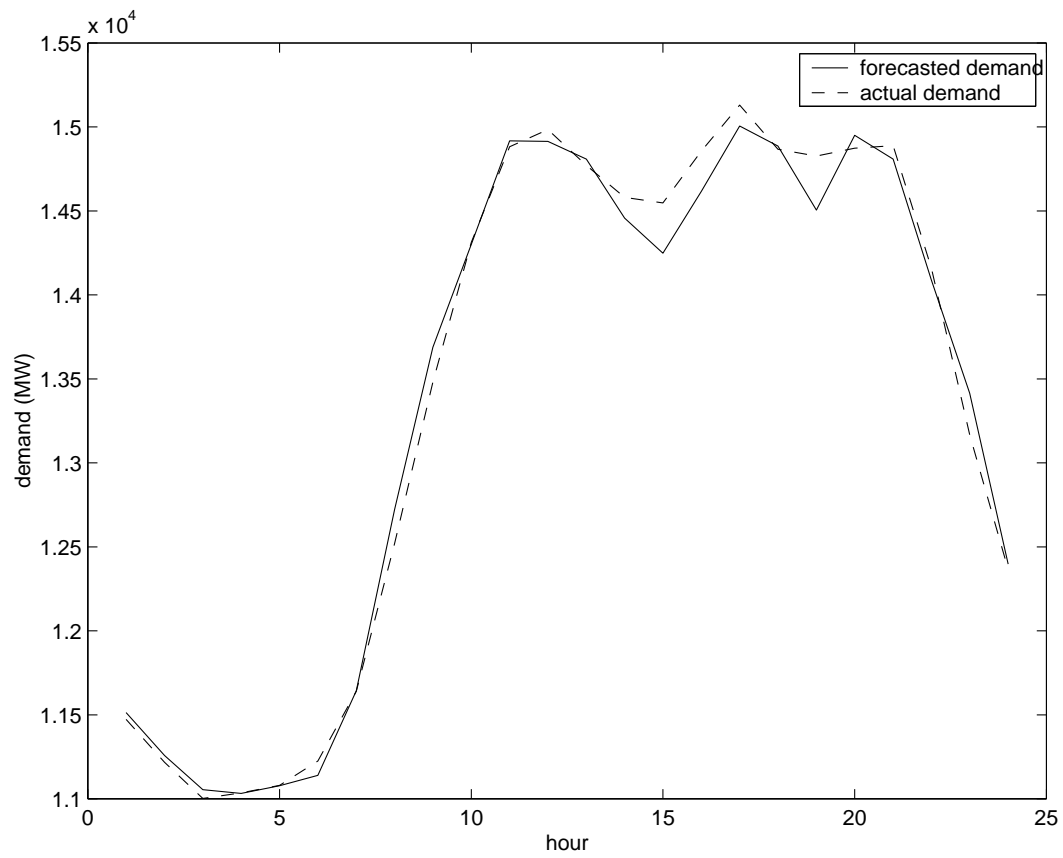


Figure 5.5: Forecasting results for Monday May 24, 1999.

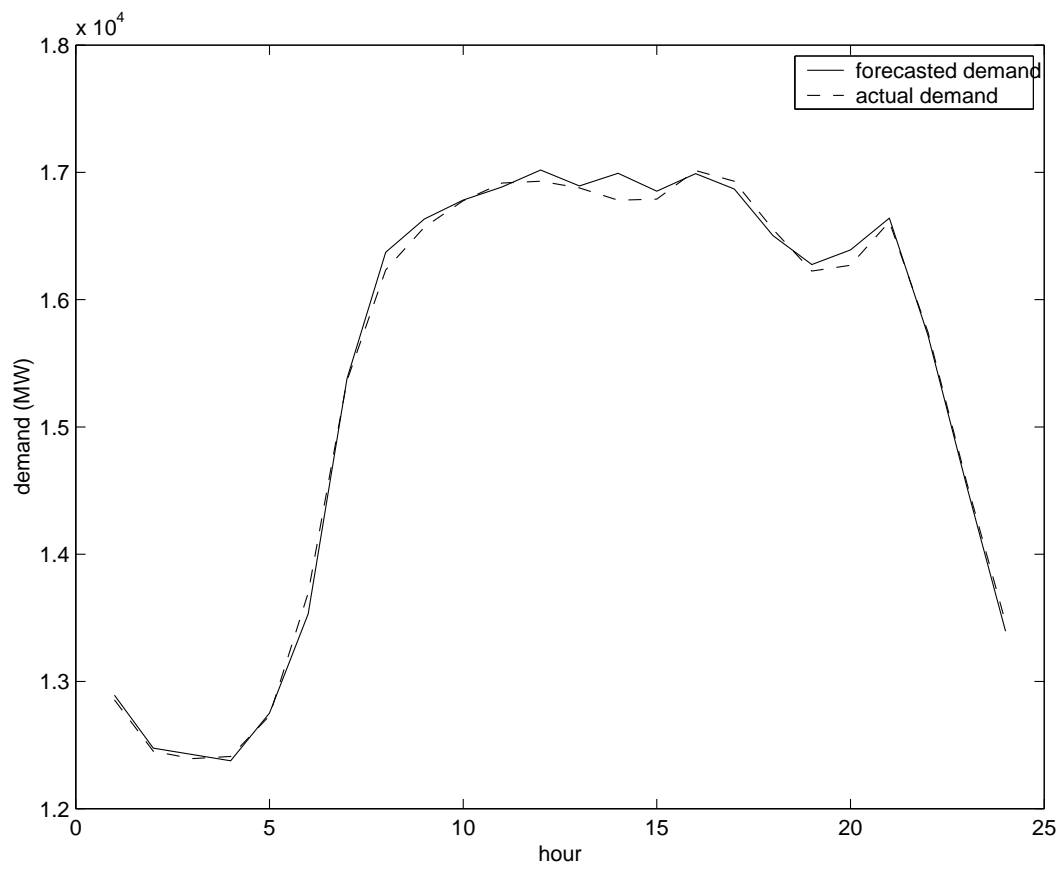


Figure 5.6: Forecasting results for Thursday May 27, 1999.

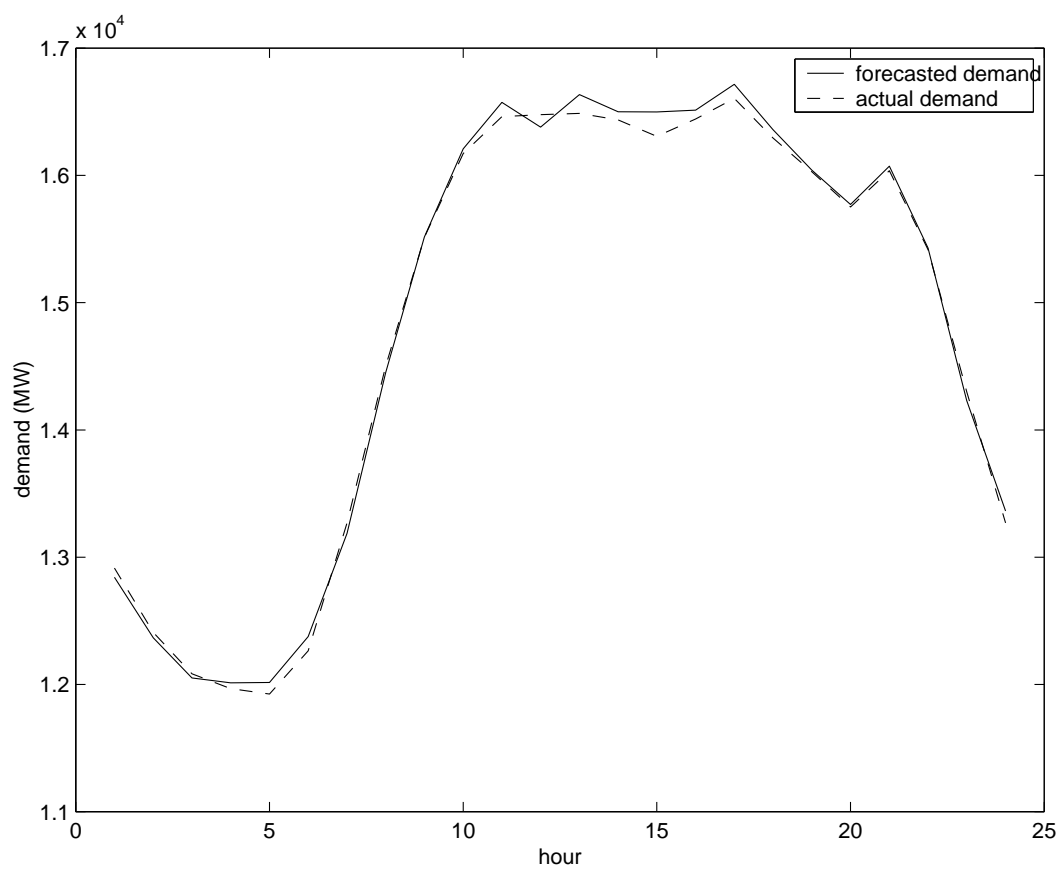


Figure 5.7: Forecasting results for Saturday May 29, 1999.

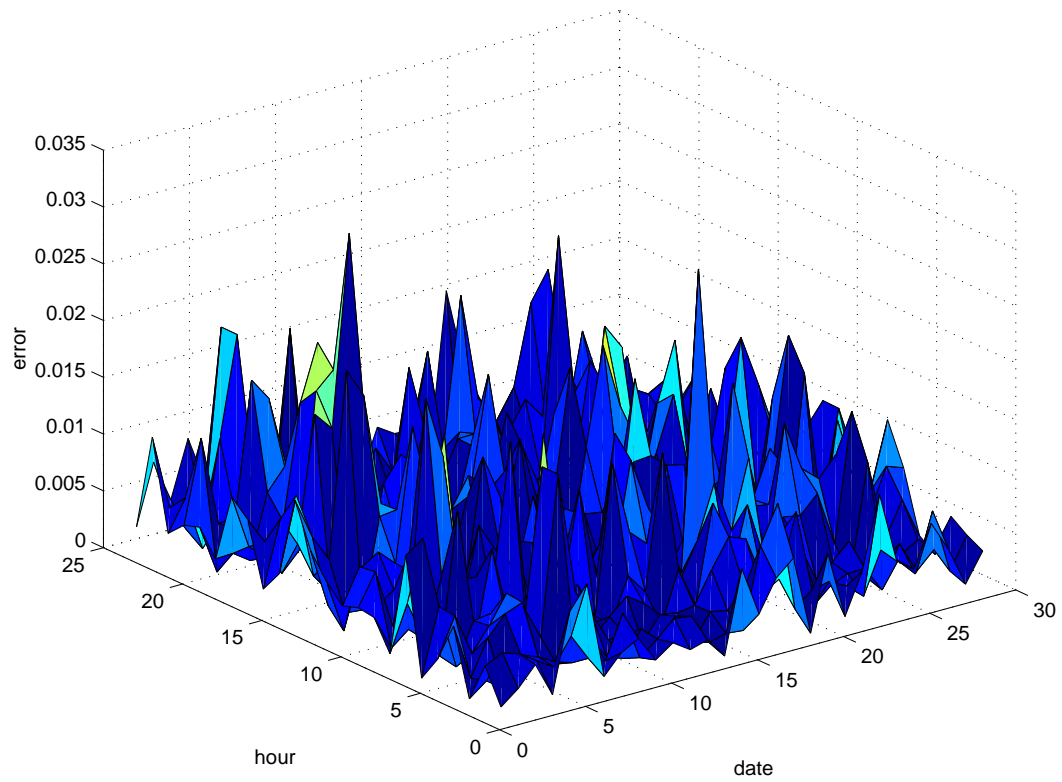


Figure 5.8: Absolute percentage errors for the May 1999 load data set.

Table 5.1: Comparison of the number of iterations

l_r, m_c	without price	with price
$l_r=0.6$ $m_c=0.4$	1790	1079
$l_r=0.6$ $m_c=0.5$	2278	1065
$l_r=0.6$ $m_c=0.6$	1711	927
$l_r=0.6$ $m_c=0.7$	4170	1131

the same forecasting accuracy practically doubled, as shown in Table 5.1. If the ANN parameters obtained from the training process in both cases, i.e. with and without price consideration, are used for future STLF, better forecasting results, such as higher forecasting accuracy, can be obtained by including price factor, as shown in Figure 5.9. In other words, the PJM energy spot market prices do have an influence on the Ontario system load, and hence better overall STLF performance can be achieved when the price effect is considered.

5.5 Summary

An ANN-based STLF method that uses a three layer feed-forward neural network and a back-propagation training method is presented here, including electricity prices as one of the main factors affecting the load in deregulated markets. The

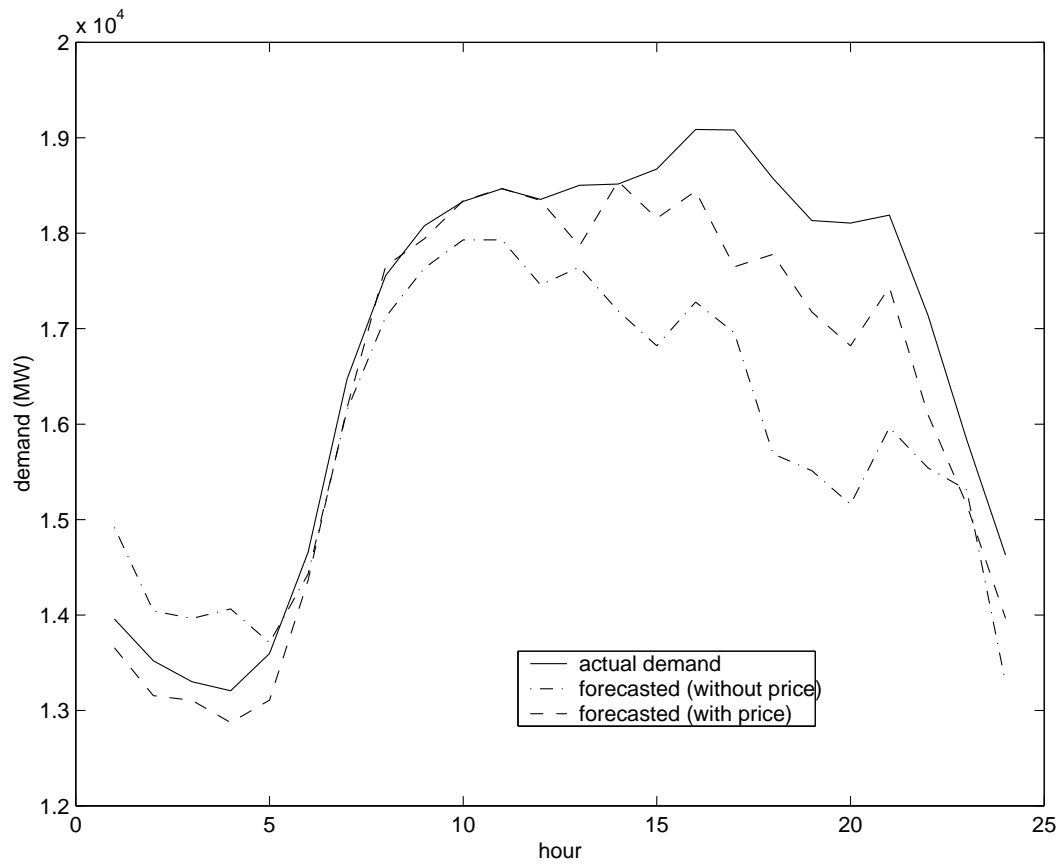


Figure 5.9: Comparison of the forecasting results for June 1, 1999. This data is not used for the ANN training.

load-price relationship is highly nonlinear and difficult to model directly; hence, by using a neural network, it is shown here that it is possible to readily account for the impact of price on system load, without the need for determining an actual nonlinear function to represent this relationship. The historical load data for the Ontario system as well as the prices from the neighbouring electricity market were used in the case study for testing, demonstrating that price factor does have an impact on the STLF performance.

Chapter 6

Web-based Implementation

Chapter Synopsis

The implementation of the TSC analysis discussed throughout this thesis using web-based computing techniques for easy accessibility and maintenance, as well as flexibility is presented here.

In this chapter, web-based computing techniques and their applications to electricity markets are briefly reviewed. The requirement analysis, design and prototype implementation of the TSC and STLF computation modules are presented in detail, together with a brief discussion of their applicability to competitive electricity markets.

6.1 Introduction

With the evolution and widespread deployment of the World Wide Web, accelerated by the rapid adoption of web browsers, web-based computing has gained popularity and importance in many different areas. Web technologies enable communication

between dissimilar computers over a large geographical region via Intranet or Internet. The web is not only a medium to conveniently access information on the network, but also provides a general distributed computing environment as an application platform. Distributed applications can be implemented on it to exploit cheap but powerful network of machines.

Web-based computing, based on the Internet Protocol, distributed processing and web browsers, permits data sharing and computing over a large range of heterogeneous hardware and software platforms, and also provides the possibility of the execution of a number of operations simultaneously, based on client/server paradigms and concurrent programming. Web-based computing can be performed at much lower costs and with expectable computational speed-up for some coarse-grained applications using distributed computing techniques, as compared to the traditional stand-alone solutions [111]. It is platform independent, highly available and expandable, and relatively easy to maintain and update. However, the efficiency is highly influenced by the network reliability and communication speeds; fast and reliable networks are needed. Furthermore, security is another important issue that has to be considered for web-based applications.

In the deregulation era, system data and market data are becoming increasingly distributed, together with more stringent and complex operational and control requirements. Higher computational and communication requirements are needed to allow for feasible and profitable energy transactions among different market participants [112]. Web-based applications have been introduced for a variety of challenges in electricity markets [26, 113, 114, 115, 116, 117]. Most efforts use web techniques for information access and exchange. With the help of high performance CPU and fast network communications, more sophisticated applications have also been built on the web, using it as a widely distributed platform to share data and resources

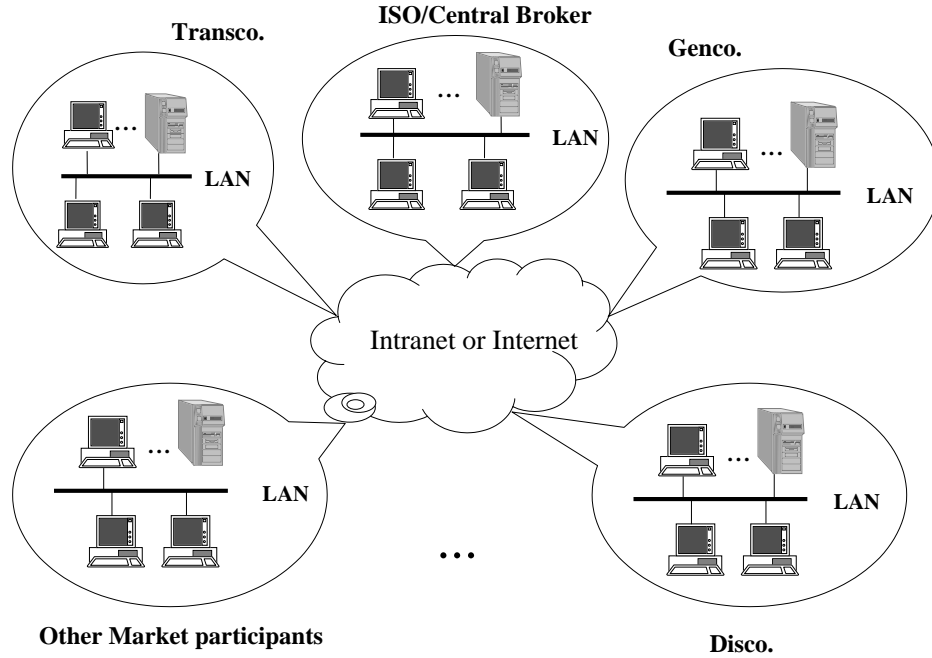


Figure 6.1: Web-based distributed computational network.

for parallel computing application [111]. Nevertheless, using web-based computing to implement electricity market decision support system is still a challenge [61, 114, 116, 118].

A possible interconnected computational network in electricity markets is shown in Figure 6.1. The network is composed of different LANs according to market participants. By using web-based computing, the analysis modules can be distributed widely and easily accessed by all the participants.

As discussed in Chapters 3 and 4, the TSC analysis is not only used by ISOs for the transaction coordination and other market operation purposes, but can also

be used by other market participants, who are geographically widely distributed and have different software and hardware platforms, to make competitive decisions, such as OASIS in US, which is a web-based information board where ATC values are posted so that all transmission users can access for transactions. Besides wide accessibility and platform independency, there is no configuration cost to use web browsers as GUIs. Hence, web-based computing is used in the thesis for the implementation of the proposed TSC analysis. Furthermore, researchers around the world can also access to the main results of this thesis. For STLF, distributed computing was used to improve computational efficiency.

6.2 Web-based TSC Analysis

6.2.1 Requirements

Based on the bid matching results and forecasted loads, TOF, TI and TSC are analyzed to generate incentive price signals, i.e. NCPs, for market participants. Figure 6.2 summarizes the data flow of the TSC analysis procedure; and the data dependence between the nine function modules that make the complete application, is shown in Figure 6.3. These modules are:

1. Bid matching module, which provides the MCP and potential transactions to module 3, based on market information such as supply and demand bids, and forecasted load (module 2), using a high-low bid matching method.
2. Load Forecasting module, which provides forecasted load information to module 1, based on historical load and other affecting factors, and using the ANN-based STLF method described in Chapter 5.

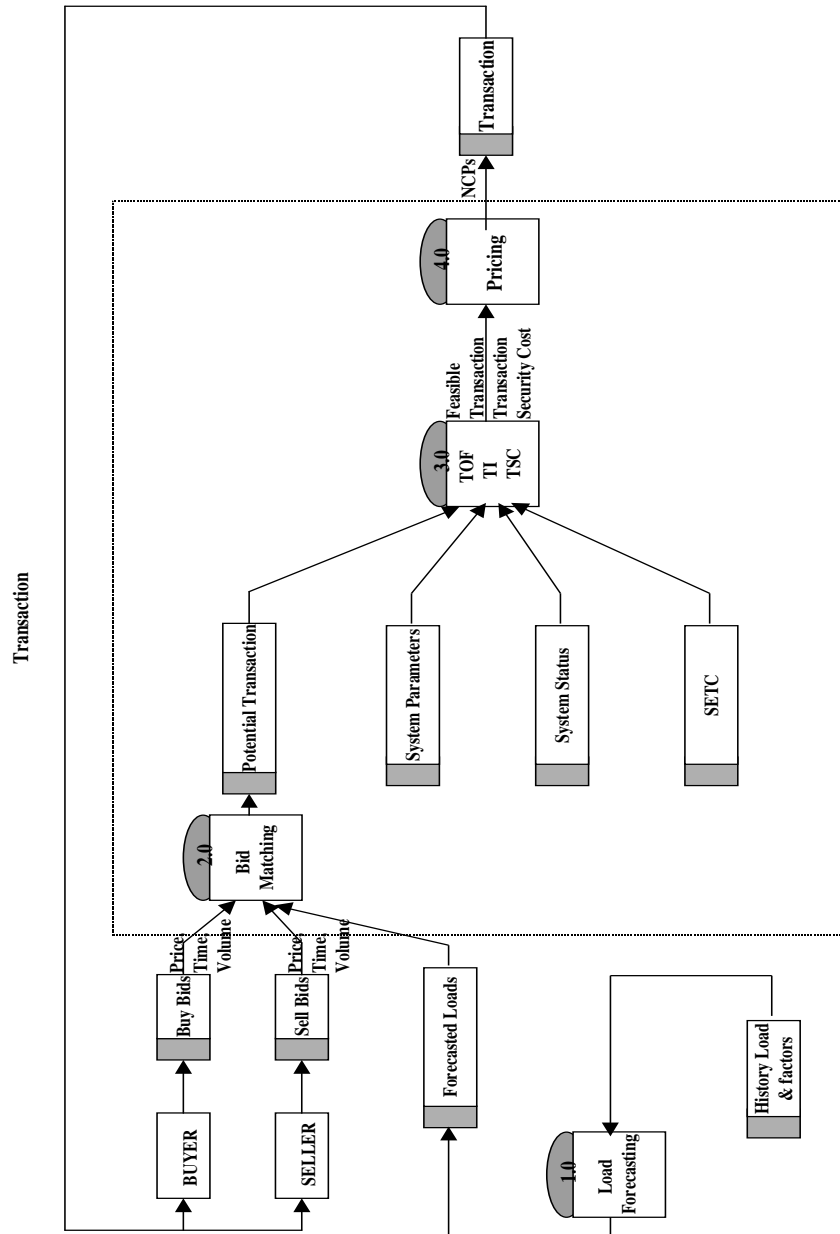


Figure 6.2: Level-0 data flow diagram of the TSC analysis.

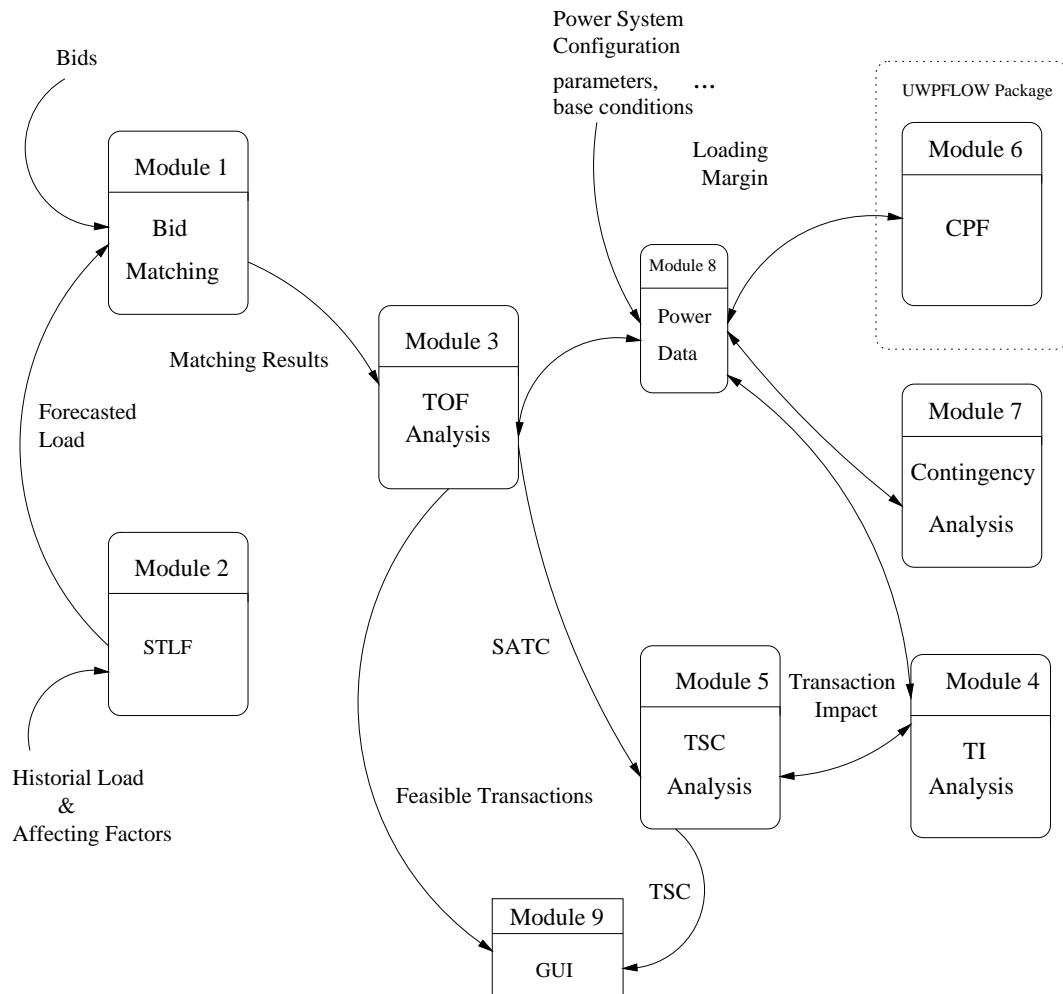


Figure 6.3: Data dependence between the web-based TSC modules.

3. TOF analysis module, which generates and sends “realistic” load and generation patterns, SATC values and feasible transactions to modules 5, 8 and 9, based on bid matching results and loading margin computation, using the methods described in Section 2.4.
4. TI analysis module, which provides transaction impact information to modules 5 and 8, based on SATC values and system data.
5. TSC analysis module, which calculates and provides the transaction security cost results to module 9, based on the SATC and transaction impact information provided by modules 3 and 4, using the analysis methods described in Chapters 3 and 4.
6. CPF module, which takes care of the power flow analysis tasks and loading margin computation, and then delivers the results to module 8, based on power system data, generation and loading patterns, and contingencies using the CPF method described in Section 2.2.2.
7. Contingency analysis module, which analyzes the critical contingencies for module 8, based on power system data and the power flow results produced by module 6.
8. Power data module, which is a data interface module that provides the power system data to modules 3, 4, 5, 6 and 7, based on power system configuration, parameters, SETC, and load and generation patterns.
9. GUI module, which provides the user interface.

The complexity of the data flow would make it costly to implement a solution from scratch. Some existing resources, such as UWPFLOW [93], a robust imple-

mentation of the CPF method, can be readily integrated into the TSC analysis procedure (module 6).

6.2.2 Architecture

The web-based application is designed using three-tier client/server architecture, as shown in Figure 6.4. The application logic is separated from the Graphic User Interface (GUI) and the backend database, so that changing any one of the layers can be done without the need to change other layers. Java is chosen as the program language and software platform [119], so that the application can run on any hardware and software platform, on the presence of Java Virtual Machine (JVM); servlets are used for implementing secure, protocol- independent and platform-independent server side web-enabled computation modules; and JDBC, which is cross-platform and non-database product specific, is used for accessing and manipulating relational database. A more detailed review of these supporting web technologies can be found in [61].

The top layer is the presentation layer, which is located on the client machine. Data is presented by a thin client solution, using a web browser and the HTML standard file format. It is the GUI of the application. The parameters of the application are controlled by the client side using HTML forms. The user sets the parameters and then activates the process on the server side via the network. What the client sees is an abstract operation request which takes input and output parameters. Since web browsers are available for almost all platforms, using them as GUI eliminates the need for designing different application interfaces across different platforms, and also allows to adequately present the application to the user without too much coding efforts.

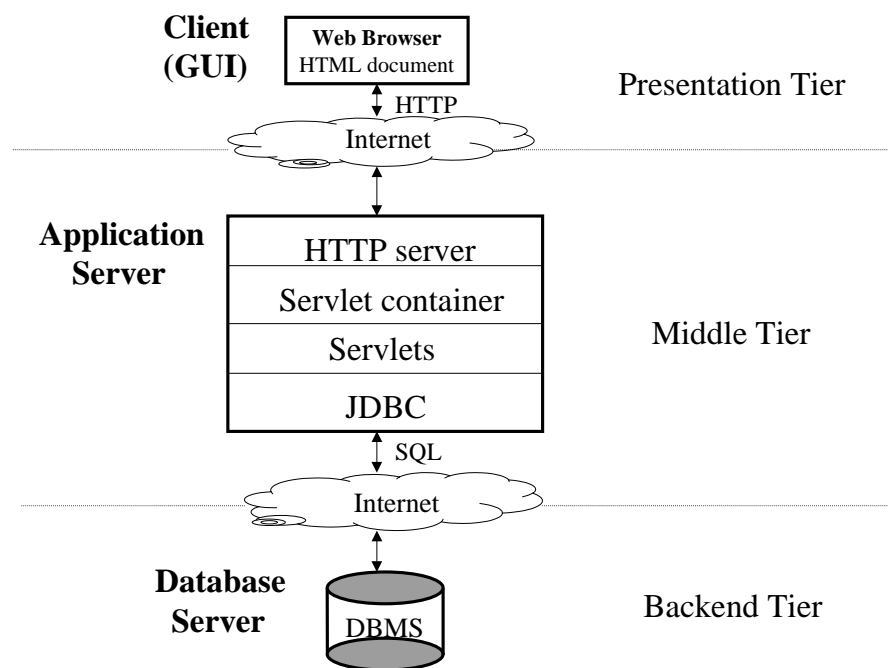


Figure 6.4: Three-tier client/server architecture.

The middle layer is the application server, which implements the application logic to process data requests. An HTTP web server is running on the machine to receive HTTP request from clients, and send HTTP response back to clients. A Servlet container and Servlet API must be installed to allow the Servlets to run. JDBC API and a JDBC driver associated with the database should be installed to communicate with DBMS by SQL statements. The main control logic is encapsulated on the server side through Java Servlets, which represent different modules of the application. Using modular design enables modifications and enhanced features to be added easily to the system to properly respond to specific user requirements.

The backend layer is the Database Server, which uses a typical relational database that stores and manipulates the data at the backend. The connectivity to the database from the middle layer is through the JDBC drivers, this allows the application logic to be written with little dependency on the type of database use.

The way the system works is as follows: The user fills in a HTML form and clicks the Submit button, which posts the request to a Java Servlet. The Servlet reads the input parameters and performs the business logic, and the same time uses JDBC to communicate with a database to obtain necessary data; a response is then generated and given back to client for display, depending on the user inputs.

6.2.3 Implementation

The prototype of the web-based application was implemented on Sun machines, using Sun Solaris 2.8 operating system. A Sun Enterprise 450 machine is used in the middle tier as application server and web server, whereas a Sun Ultra 10 machine is used in the backend tier as database server. The client can be any machine that has a web browser installed with an access to the Internet. The prototype was

tested using a PC running Windows 2000 with either Internet Explorer or Netscape browser as a client.

In the middle tier, an Apache HTTP Server 1.3 is installed as the web server. *Java*TM Web Services Developer Pack 1-0-01 is installed for the support of the Java Servlet API. Java JDK-1.3.1 is installed as the Java runtime environment. MySQL Connector/J 2.0.14 is used as the JDBC Driver to access MySQL relational database. MySQL 3.23.52 resides on the backend tier.

Six main modules, implemented as six Servlets, run on the application server:

1. **basecon**: Receives base system conditions from the client and calculates the base power flow.
2. **bidMatching**: Receives supply and demand bids from the client and performs high-low bid matching.
3. **atc**: Calculates SATC using the method described in Section 2.3.
4. **impact**: Computes the impact of potential transactions on the SATC using the method described in Section 2.5.
5. **rescheduling**: Analyzes the transaction security costs by means of the rescheduling technique described in Chapter 3.
6. **takerisk**: Analyzes the transaction security costs by means of the take-risk technique described in Chapter 4.

The pseudocode of Servlets **basecon** and **atc** are shown in Figure 6.5 and Figure 6.6 for illustration purposes.

UWPFLOW, the computing engine for power flow and loading margin calculations, is treated as legacy software and was not changed, thus avoiding extra

```
Public class basecon extends HTTPServlet
{
    ...
    Public void doPost(HttpServletRequest request,
                        HttpServletResponse response)
                        throws ServletException, IOException
    {
        PrintWriter out=response.getWriter( );
        response.setContentType("text/html");
        ...

        //parse the parameters of HTML form and
        //save the uploaded file

        //encapsulate UWPFLOW to generate base
        //power flow using Java Runtime.exec( )

        //Database Interface: update tables

        //generate response web page
    }
}
```

Figure 6.5: Pseudocode of `basecon` servlet.

```
Public class atc extends HTTPServlet
{
    ...
    Public void doPost(HttpServletRequest request,
                        HttpServletResponse response)
                        throws ServletException, IOException
    {
        PrintWriter out=response.getWriter( );
        response.setContentType("text/html");
        ...

        //Database Interface: retrieve data from tables

        //use UWPFLOW to calculate loading margins
        //under normal condition and N-1 contingencies

        //Database Interface: update tables

        //generate response web page
    }
}
```

Figure 6.6: Pseudocode of `atc` servlet.

programming costs and errors; this way, the engine used for SATC calculations can be readily changed to any other application designed for these purposes. This package is thus encapsulated in Servlets `basecon`, `atc`, `impact` and `rescheduling`, using `Java Runtime.exec`, which creates a native process and returns an instance of a subclass of `Process` that can be used to control the process and obtain information about it, as shown in Figures 6.5 and 6.6.

A database interface is included in each module to retrieve and update information from the database. Its main code is shown in Figure 6.7.

Parts of the input and output GUIs are depicted in Figures 6.8, 6.9, 6.10 and 6.11 for the six-bus example described in Sections 2.6 (Figure 6.9), 3.3.2 (Figure 6.10) and 4.3.2 (Figure 6.11). Figure 6.8 shows the first input GUI of the application. There are several input forms presented to clients to provide the server with all the required data. The application can be accessed at the website <http://www.power.uwaterloo.ca/~hchen/webTSC/webTSCNew.html>.

Three different systems, namely, the three-area electricity market, six-bus test system and the 129-bus Italian system model, have been tested, obtaining the results described in detail in Chapters 2, 3 and 4.

6.3 Implementation of the STLF Module

Traditionally, STLF is mainly performed at the system control centre. Hence, complete and accurate system information is usually difficult to obtain. To speed up the forecasting process and generate more accurate forecasting results, especially in large systems, parallelism can be introduced using the natural system division by districts to carry out the necessary computations. Therefore, STLF can be


```
//loading driver
try{
    class.forName("org.gjt.mm.mysql.Driver");
}catch(ClassNotFoundException e){
    System.err.print("ClassNotFoundException:");
    System.err.println(e.getMessage( ));
}

try{
    //making the connection
    Connection con=DriverManager.getConnection(
        Dburl, "login", "password");

    //creating JDBC statements
    Statement stmt=con.createStatement( );

    //create or update database
    stmt.executeUpdate("....");

    //retrieve information from database
    ResultSet rs=stmt.executeQuery("...");
    //retrieve values from ResultSet
    while(rs.next( )){
        float p=rs.getFloat("Pg");
        ...
    }
}catch(SQLException e){
    System.err.println("SQLException:" + e.getMessage( ));
}
```

Figure 6.7: Database interface.

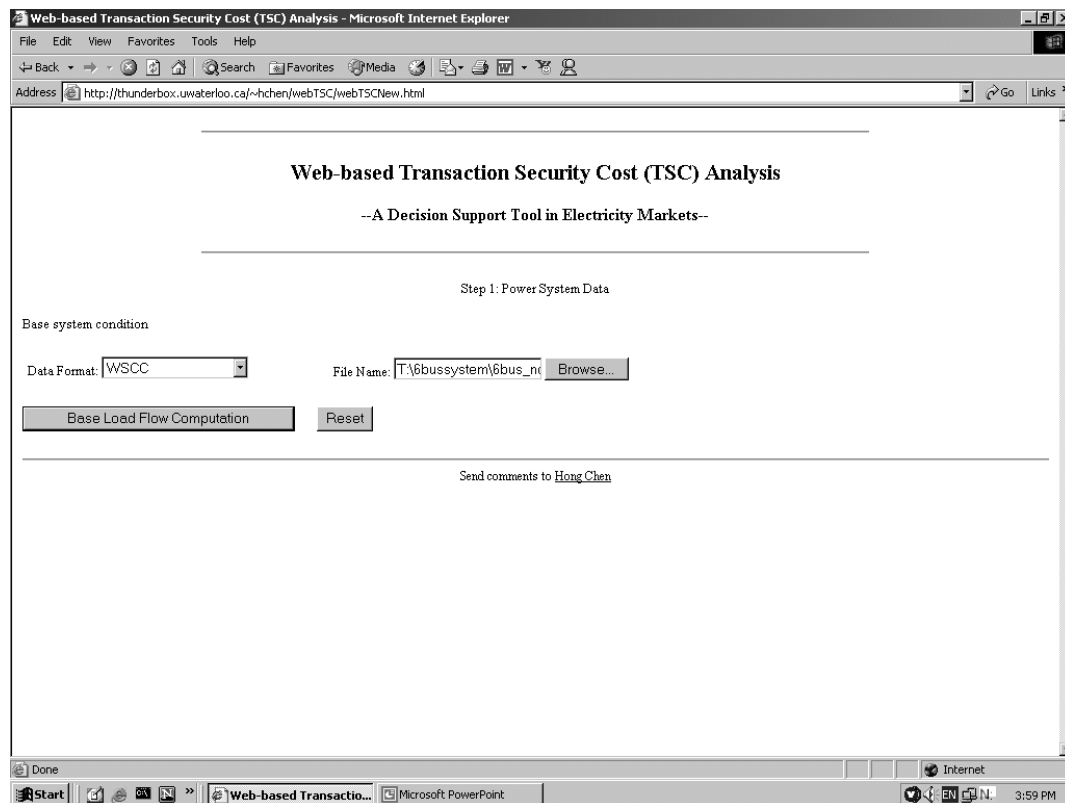


Figure 6.8: Part of the input GUI.

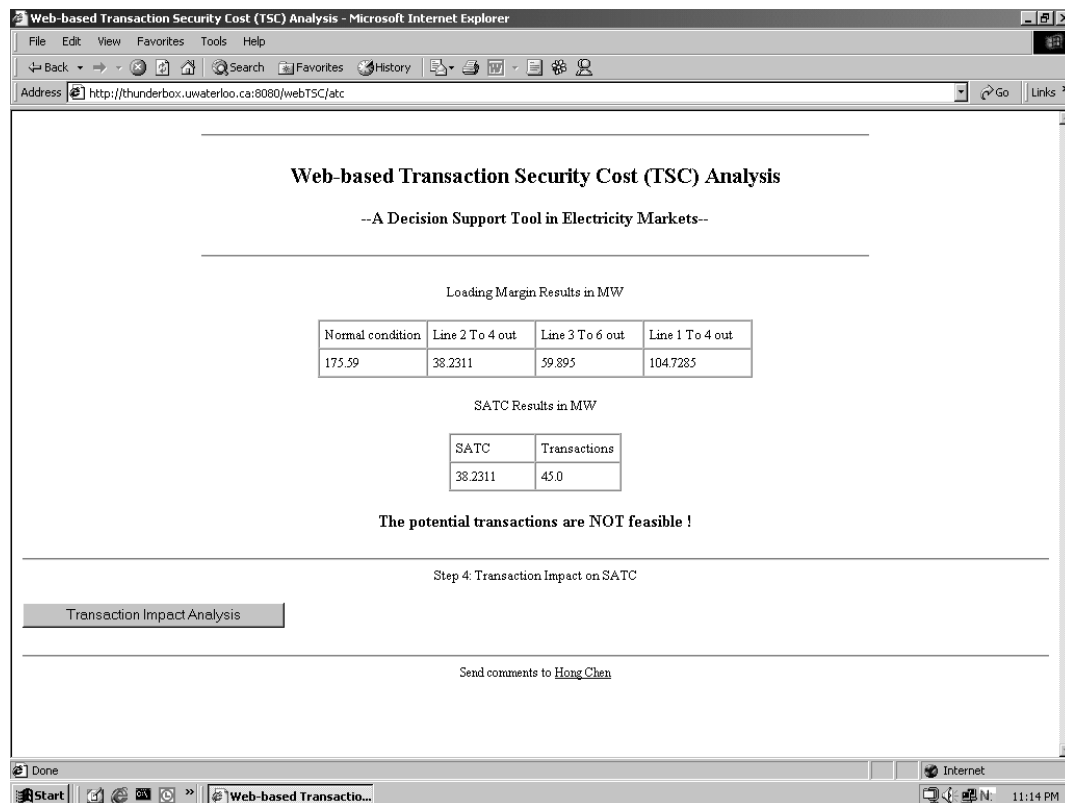


Figure 6.9: SATC results.

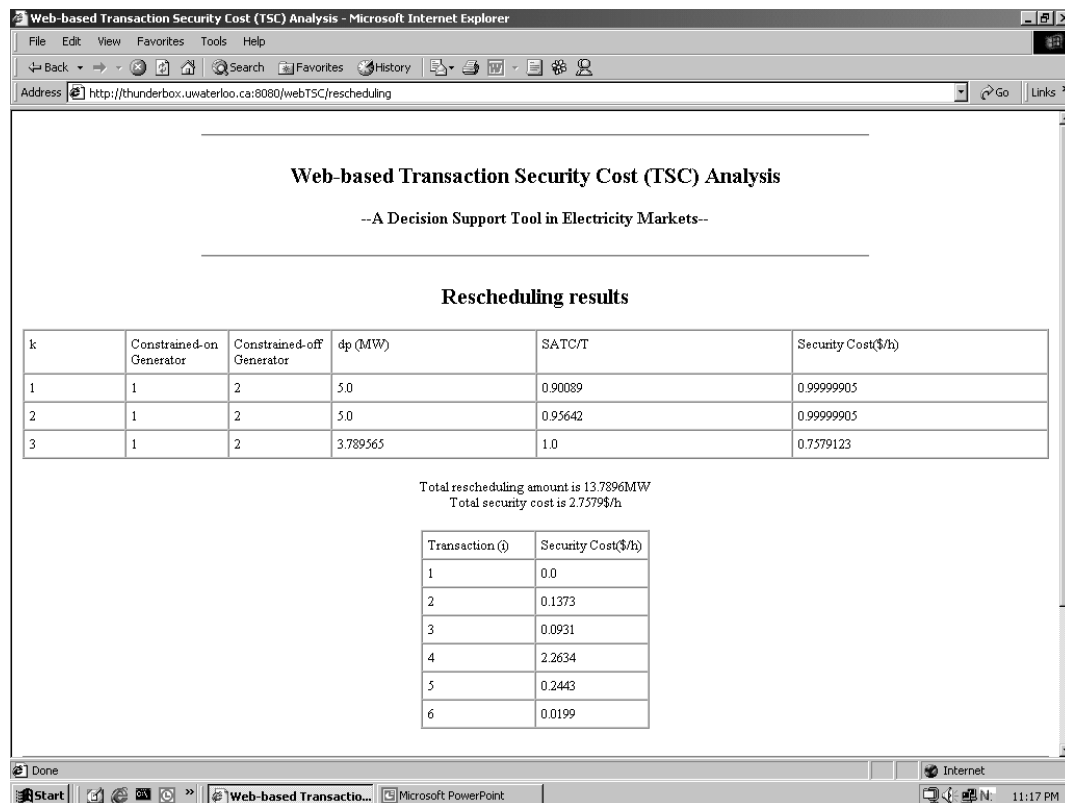


Figure 6.10: Rescheduling results.

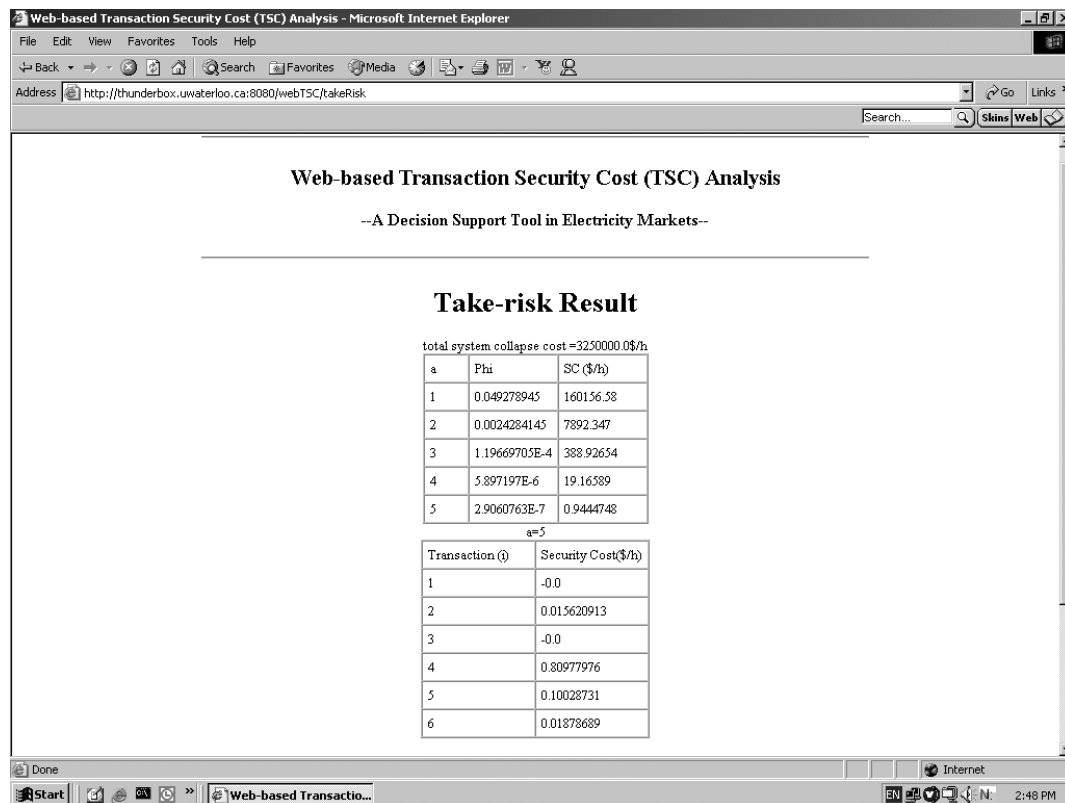


Figure 6.11: Take-risk results.

performed using distributed processing by forecasting the total system load based on distributed district load forecasts. Any forecasting method can be used, such as time series, linear regression, expert systems, ANN, etc.

6.3.1 Architecture

Here, a distributed STLF is configured as a master/slave concurrent program, using the familiar client/server paradigm. The block diagram of the architecture is depicted in Figure 6.12. The master and the slaves reside in different virtual machines, and these machines are connected through an Intranet or the Internet. The STLF is decomposed based on districts. The master is located at the system control centre and the slaves are located at the district centers. The forecasting entity for each district is encapsulated in a slave process, and each slave works on its own local data obtained from district SCADA and other historical data resources.

The master invokes the slaves to do district-wise STLF simultaneously. Multithreading is used to allow concurrency in execution. Each child thread on the master invokes a slave machine to perform district load forecasting, as shown in Figure 6.12. In order to keep the system consistency, the slaves are synchronized with the master. Message passing is used for the master and the slaves to share data and also to maintain synchronization between them.

6.3.2 Implementation

Java was chosen as the implementation platform and language, which is suitable for large, geographically distributed, dissimilar, loosely interconnected computational systems. Remote interfaces and remote objects were created on each slave, as

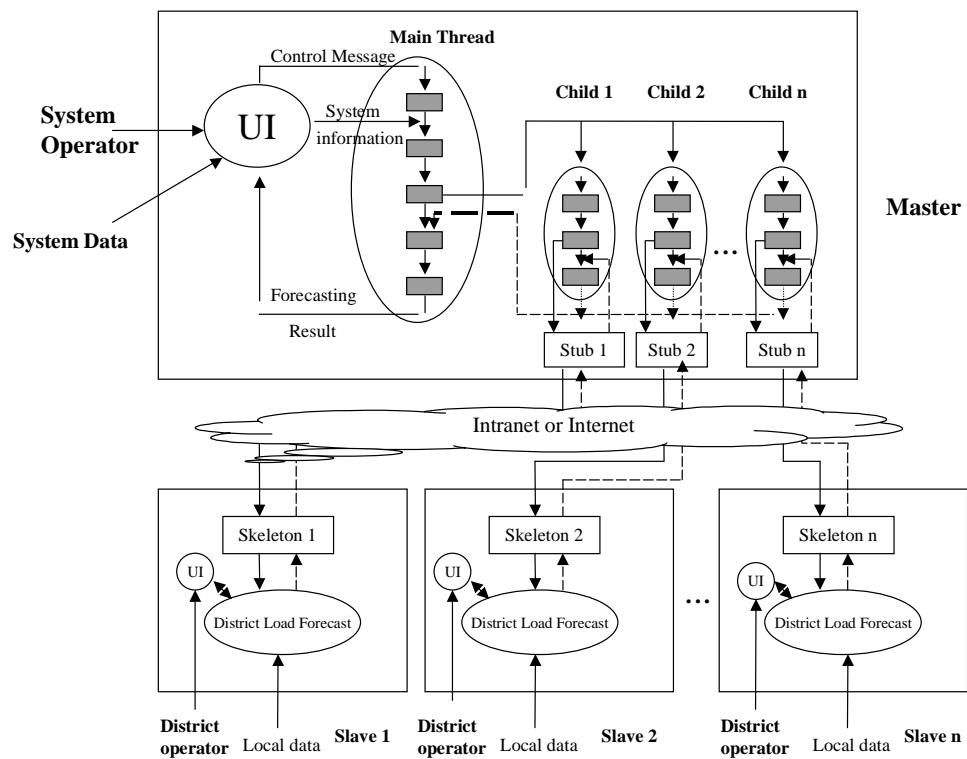


Figure 6.12: Distributed STL architecture.

Remote Interface

```
Public interface Forecast extends Remote{
    ForeDay executeForecast (Control c)
        throws RemoteException;
}

public interface Control extends Serializable {
    //interface of control function
}
```

Remote Object

```
Public class DistrictForecast extends UnicastRemoteObject
implements Forecast{
    ...
    public ForeDay executeForecast(Control c){
        //district load forecasting
    }
    public static void main(String[] args){
        ...
        //bind a name
    }
}
```

Figure 6.13: Remote interface and remote object.

shown in Figure 6.13. The Java Remote Method Invocation (RMI) was used as the mechanism by which the master and the slaves communicate and pass information back and forth.

The distributed STL_F was tested on a LAN network of up to 6 SUN 170-Ultra Sparcs workstations, one working as the master and the others as the slaves. Performance was tested by varying the number of slaves. The resulting execution times are listed in Table 6.1 for the load data from a utility in China. Observe that the use of increasing number of slaves does not lead to a significant increase

Table 6.1: Execution times

Number of slaves	Execution time (ms)
2	335
3	339
4	353
5	359

in the execution time, i.e. just a small amount of Inter-Process Communication (IPC) time is required. Compared to the sequential implementation, i.e. the same calculations performed on one machine, speedup can be expected using this parallel implementation. It is a typical coarse-grained parallel application, and hence very suitable for a distributed implementation.

Compared to centralized STLF [58], the distributed STLF should yield higher forecasting accuracy, as district historical data used is typically more complete and up-to-date than centralized data.

6.4 Summary

A web-based prototype of the proposed TSC analysis is designed and implemented based on a three-tier client/server architecture and using up-to-date web technologies, so that it can be easily and effectively accessed by market/system operators, as well as any other market participant. In addition, the STLF function model is configured and implemented as a distributed master/slave concurrent program to achieve higher forecasting accuracy without the increase of execution time.

The implemented prototypes demonstrate the feasibility of integrating complex power system and market computation tasks in an open platform, like the web, using available existing resources and software to avoid extra development costs. It is user friendly, and the client end is free of any configuration, installation or update operations. It also shows the possibility of decomposing computational intensive power system applications using parallel and distributed computing techniques on the web for better performance, such as higher accuracy and increased computational speed.

Chapter 7

Conclusions

7.1 Summary

Based on simple auction market model, this thesis presents an efficient and transparent approach for transaction security cost analysis to quantify the correlation between market operation and power system operation, which is a challenging and demanding issue in electricity markets. Two different strategies, i.e. rescheduling and take-risk, are proposed and discussed in detail based on adequate SATC and transaction impact computations, considering thermal and voltage limits, as well as voltage stability criteria. To facilitate the access of all market participants to the proposed techniques, a web-based prototype is implemented, including an ANN-based STLF module. Several sample systems are used to test and demonstrate the advantages of the proposed techniques.

To evaluate transmission congestion, the basic ATC concept is extend to the more generic SATC concept, which is computed for the whole system instead of a given interchange path, considering thermal limits, voltage limits and voltage

stability limits and using an N-1 contingency criteria. The CPF method is used for the SATC computation. A TOF analysis procedure is proposed based on the SATC computations to determine the feasibility of potential transactions. TI is defined and determined to find the most effective rescheduling direction, as well as to distribute total security cost among transactions.

From a deterministic point of view, the rescheduling procedure consists of an analysis of transaction security costs associated with a generation redispatch and/or load curtailment procedure, based on an iterative computation of SATC and TI, with the goal of minimizing the amount of rescheduling. This technique can be considered as an efficient and transparent method for congestion management and pricing, which takes account of the non-linearity of the system and some stability issues. From a probabilistic point of view, the proposed take-risk technique determines the transaction security costs based on the idea of taking a less conservative approach to consider operating risks to facilitate transactions. A novel pricing method based on the actual impact of transactions is proposed to generate price signals that ensure system security. The results of several case studies on various test systems show the effectiveness and applicability of the proposed techniques.

To provide a proper load prediction for the proposed TSC analysis, an ANN-based STLF method considering the effect of price on the load is presented. Using practical market data, load forecasting results could be improved by also considering price factors. A distributed implementation of STLF is described, based on a master/slave parallel architecture to achieve higher forecasting accuracy without increase in execution time.

The proposed TSC analysis methods are implemented in a web-based prototype using a three-tier client/server architecture for wide accessibility, easy maintenance and flexibility.

7.2 Contributions

The main contributions of this work can be summarized as follows:

- TSC is quantified considering nonlinear voltage stability limits, as well as thermal and voltage limits, based on adequate SATC and transaction impact computations, to address the correlation between market operation and power system operation. It can be used as an efficient and transparent method for congestion management and pricing.
- A rescheduling technique is developed to determine TSC using an iterative procedure for generation redispatching and/or load curtailment. It is considered as a sub-optimal method to minimize the amount of rescheduling.
- A take-risk technique is proposed for TSC calculation based on the idea of taking a less conservative approach to system operation to facilitate market transactions.
- The effect of price in STLF is studied with an ANN-based method to identify the nonlinear relationship between electricity price and system load, in order to improve load forecasting accuracy and to provide realistic load increase direction for the above analysis.
- The distributed, web-based techniques are introduced into electricity market analysis, to utilize existing resources for wide accessibility, easy maintenance, improved performance and flexibility.

Most of the material presented in this thesis has been published in [32, 33, 61, 111, 120, 121, 122, 123].

7.3 Future Work

The following are a few research ideas resulting from the work presented in this thesis that need to be explored further:

- System dynamics, such as transient stability, are desired to be considered in the SATC and its sensitivity computation, to better evaluate transmission congestion and analyze transaction impact.
- It will be an interesting challenge to determine the actual probabilistic distribution functions of a system, based on the history of system contingencies, using detailed probabilistic studies.
- It is valuable to enhance the proposed technique in the practical market operation with different market structures, comparing to other security pricing techniques.
- The current web-based implementation is a research prototype. The computation speed can be improved in the future, as well as the considerations of secure system access and data access.

This work is established upon advanced voltage stability theory and web-based computing techniques. It addresses the power system security concerns in the electricity market operation, which is a widely acknowledged demanding challenge for the successful competitive power industry. Practical market/system data has been applied to show the achievements of this work, as well as its wide applicability.

Bibliography

- [1] M. D. Ilic and S. Liu, *Hierachical Power Systems Control: Its value in a challenging Industry*. Springer-Verlag London Limited, London, UK, 1996.
- [2] M. D. Ilic, F. D. Galiana, and L. H. Fink, *Power Systems restructuring: engineering and economics*. Kluwer Academic Publishers, Boston, U.S.A., 1998.
- [3] S. V. Vadari and J. D. Hammerly, “New Faces and Functions in a Competitive Market,” *IEEE Computer Applications in Power*, vol. 10, no. 1, January 1997, pp. 47–52.
- [4] M. Madrigal, *Optimization Models and Techniques for Implementation and Pricing of Electricity Markets*. Ph.D. thesis, Canada, 2000.
- [5] F. C. Schweppe, M. C. Caramanis, R. D. Tabors, and R. E. Bohn, *Spot Pricing of Electricity*. Kluwer Academic Publishers, USA, 1988.
- [6] H. Rudnick and J. Zolezzi, “Electric Sector Deregulation and Restructuring in Latin America: Lessons to be Learnt and Possible Ways to Forward,” *IEE Proceedings on Generation, Transmission and Distribution*, vol. 148, no. 2, March 2001, pp. 180–184.

- [7] D. Watts and R. Ariztia. “The Electricity Crises of California, Brazil and Chile: Lessons to the Chilean Market”. In *Proceeding of Power Engineering 2002 Large Engineering Systems Conference, LESCOPE 02*, pp. 7–12, 2002.
- [8] National Grid. Website: <http://www.nationalgrid.com/uk/>.
- [9] Power Pool of Alberta. Website: <http://www.powerpool.ab.ca/>.
- [10] “PJM Manuals,” technical report, PJM Interconnection, Website: <http://www.pjm.com>, 2002.
- [11] J. J. Gonzalez and P. Basagoiti. “Spanish Power Exchange Market and Information System Design concepts, and Operating Experience”. In *Proceeding of Power Industry Computer Application (PICA) conference*, pp. 245–252, Santa Clara, CA, May 1999.
- [12] California ISO. Website: <http://www.caiso.com>.
- [13] “Marketplace Overview,” technical report, New York ISO, Website: <http://www.nyiso.com>, 2002.
- [14] “Market Rules and Procedures,” technical report, ISO New England, Website: <http://www.iso-ne.com>, 2002.
- [15] “Market Rule,” technical report, Independent Electricity Market Operator, Website: <http://www.theIMO.com>, 2002.
- [16] F. A. Rahimi and A. Vojdani, “Meet the Emerging Transmission Market Segments,” *IEEE Computer Applications in Power*, vol. 12, no. 1, January 1999, pp. 26–32.

- [17] L. S. Hyman, "Transmission, Congestion, Pricing, and Incentives," *IEEE Power Engineer Review*, vol. 19, no. 8, August 1999, pp. 4–10.
- [18] R. D. Christie, B. F. Wollenberg, and I. Wangensteen, "Transmission Management in the Deregulated Environment," *Proceedings of the IEEE*, vol. 88, no. 2, February 2000, pp. 170–195.
- [19] "Market Surveillance Panel Monitoring Report on the IMO-Administered Electricity Markets for the First Four Months, May to August 2002," technical report, Independent Electricity Market Operator, Website:<http://www.theimo.com>, October 2002.
- [20] G. B. Sheble, *Computational Auction Mechanisms for Restructured Power Industry Operation*. Kluwer Academic Publishers, USA, 1999.
- [21] M. Madrigal and V. H. Quintana. "Using Optimization Models and Techniques to Implement Electricity Auctions". In *Proceedings of IEEE-PES 2000 Winter Meeting*, Singapore, January 2000.
- [22] M. Madrigal and V. H. Quintana. "Degeneracy and Duality Gap on Optimization-Based Electricity Auctions". In *Proceeding of International Conference on Electric Utility Deregulation and Restructuring and Power Technologies*, pp. 332–337, London, April 2000.
- [23] T. Alvey, D. Goodwin, X. Ma, D. Streiffert, and D. Sun, "A Security-constrained Bid-clearing System for the New Zealand Wholesale Electricity Market," *IEEE Transactions on Power Systems*, vol. 13, no. 2, May 1998, pp. 340–346.

- [24] A. L. Motto, F. D. Galiana, and A. J. Conejo, "Network-Constrained Multi-period Auction for a Pool-Based Electricity Market," *IEEE Transactions on Power Systems*, vol. 17, no. 3, August 2002, pp. 646–653.
- [25] S. Dekrajangpetch, G. B. Sheble, and A. J. Conejo, "Auction Implementation Problems Using LaGrangian Relaxation," *IEEE Transactions on Power Systems*, vol. 14, no. 1, February 1999, pp. 82–88.
- [26] I. Slutsker, K. Nodehi, S. Mokhtari, K. Burns, D. Szymanski, and P. Clapp, "Market Participants Gain Energy Trading Tools," *IEEE Computer Applications in Power*, vol. 11, no. 2, April 1998, pp. 47–52.
- [27] K. W. Doty and P. L. McEntire, "An Analysis of Electric Power Brokerage Systems," *IEEE Transactions on Power Apparatus and Systems*, vol. 101, no. 2, February 1982, pp. 389–396.
- [28] G. Fahd and D. A. Richards, "The Implementation of an Energy Brokerage System Using Linear Programming," *IEEE Transactions on Power Systems*, vol. 7, no. 1, February 1992, pp. 90–96.
- [29] G. Fahd and G. B. Sheble, "Optimal Power Flow Emulation of Interchange Brokerage Systems Using Linear Programming," *IEEE Transactions on Power Systems*, vol. 7, no. 4, May 1992, pp. 497–504.
- [30] D. Chattopadhyay, "An Energy Brokerage System with Emission Trading and Allocation of Cost Savings," *IEEE Transactions on Power Systems*, vol. 10, no. 4, November 1995, pp. 1939–1945.
- [31] H. Singh, S. Hao, and A. Papalexopoulos, "Transmission Congestion Management in Competitive Electricity Markets," *IEEE Transaction on Power Systems*, vol. 13, no. 2, May 1998, pp. 672–680.

- [32] C. A. Cañizares, H. Chen, and W. Rosehart. “Pricing System Security in Electricity Markets”. In *Proceedings of Bulk Power Systems Dynamics and Control-V*, Onomichi, August 2001.
- [33] H. Chen, C. A. Cañizares, and A. Singh. “Transaction Security Cost Analysis by Take-risk Strategy”. In *Proceedings of 14th Power Systems Computation Conference*, Spain, June 2002.
- [34] R. D. Tabors, “Transmission System Management and Pricing: New Paradigms and International Comparisons,” *IEEE Transactions on Power Systems*, vol. 9, no. 1, February 1994, pp. 206–215.
- [35] G. Hamoud and I. Bradley. “Assessment of Transmission Congestion Cost and Locational Marginal Pricing in a Competitive Electricity Market”. In *Proceedings of IEEE-PES 2001 Summer Meeting*, Vancouver, July 2001.
- [36] N. S. Rau, “Transmission Loss and Congestion Cost Allocation - An Approach Based on Responsibility,” *IEEE Transactions on Power Systems*, vol. 15, no. 4, December 2000, pp. 1401–1409.
- [37] E. Bompard, E. Carpaneto, G. Chicco, and G. Gross. “The Role of Load Demand Elasticity in Congestion Management and Pricing”. In *Proceedings of IEEE-PES 2000 Summer Meeting*, Seattle, July 2000.
- [38] M. E. Baran, V. Banunarayanan, and K. E. Garren, “Equitable Allocation of Congestion Relief Cost to Transactions ,” *IEEE Transactions on Power Systems*, vol. 15, no. 2, May 2000, pp. 579–585.
- [39] X. Wang, Y. H. Song, and Q. Lu. “Primal-Dual Interior Point Linear Programming Optimal Power Flow for Real-time Congestion Management ”. In *Proceedings of IEEE-PES 2000 Winter Meeting*, Singapore, January 2000.

- [40] A. K. David, "Dispatch Methodologies for Open Access Transmission Systems," *IEEE Transactions on Power Systems*, vol. 13, no. 1, February 1998, pp. 46–53.
- [41] J. Yu and J. Galvin. "Zonal Congestion Management and Settlement". In *Proceedings of IEEE-PES 2001 Summer Meeting*, Vancouver, July 2001.
- [42] NERC, *Transmission Transfer Capability*. NERC, USA, May 1995.
- [43] S. N. Singh and A. K. David. "Dynamic Security Constrained Congestion Management in Competitive Electricity Markets". In *Proceedings of IEEE-PES 2000 Winter Meeting*, Singapore, January 2000.
- [44] C. D. Vournas. "Interruptible Load as a Competitor to Local Generation for Preserving Voltage Security. In *Proceedings of IEEE-PES 2000 Winter Meeting*, Singapore, January 2000.
- [45] L. Willis, J. Finney, and G. Ramon, "Computing the Cost of Unbundled Services," *IEEE Computer Applications in Power*, vol. 9, no. 4, October 1996, pp. 16–21.
- [46] G. Strbac, S. Ahmed, D. Kirschen, and R. Allan, "A Method for Computing the Value of Corrective Security," *IEEE Transactions Power Systems*, vol. 13, no. 3, August 1998, pp. 1096–1102.
- [47] O. Moya, "Model for Security of Service Costing in Electric Transmission Systems," *IEE Proc.—Generation, Transmission, and Distribution*, vol. 144, no. 6, November 1997, pp. 521–524.
- [48] A. Jayantilal and G. Strbac, "Load Control Services in the Management of

- Power System Security Costs,” *IEE Proc.—Generation, Transmission and Distribution*, vol. 146, no. 3, May 1999, pp. 269–275.
- [49] T. J. Overbye, D. R. Hale, T. Leckey, and J. D. Weber, “Assessment of Transmission Constraint Costs: Northeast U.S. Case Study,” *IEEE Winter Meeting*, January 2000.
- [50] B. Corniere, L. Martin, S. Vitet, N. Hadjsaid, and A. G. Phadke. “Assessment of the Congestion Cost and the Risk of Curtailment Associated with Available Transfer Capability (ATC)”. In *Proceedings of IEEE-PES 2000 Winter Meeting*, Singapore, January 2000.
- [51] R. J. Kaye, F. F. Wu, and P. Varaiya, “Pricing for System Security,” *IEEE Transactions on Power Systems*, vol. 10, no. 2, May 1995, pp. 575–583.
- [52] F. Alvarado, Y. Hu, D. Ray, R. Stevenson, and E. Cashman, “Engineering Foundations for the Determination of Security Costs,” *IEEE Transactions on Power Systems*, vol. 6, no. 3, August 1991, pp. 1175–1182.
- [53] R. Rajaraman, J. V. Sarlashkar, and F. L. Alvarado, “The Effect of Demand Elasticity on Security Prices for the Poolco and Multi-Lateral Contract Models,” *IEEE Transactions on Power Systems*, vol. 12, no. 3, August 1997, pp. 1177–1184.
- [54] K. Xie, Y. H. Song, J. Stonham, E. Yu, and G. Liu, “Decomposition Model and Interior Point Methods for Optimal Spot Pricing of Electricity in Deregulation Environments,” *IEEE Transactions Power Systems*, vol. 15, no. 1, February 2000, pp. 39–50.
- [55] D. Gan and Q. Chen. “Locational Marginal Pricing-New England Perspective

- ". In *Proceedings of IEEE-PES 2001 Winter Meeting*, Columbus, January 2001.
- [56] L. Chen, H. Suzuki, T. Wachi, and Y. Shimura. "Decomposition of Nodal Price for Electric Power System" . In *Proceedings of IEEE-PES 2000 Summer Meeting*, Seattle, WA, July 2000.
- [57] C. A. Cañizares Editor, "Voltage Stability Assessment, Procedures and Guides," technical report, University of Waterloo, <http://www.power.uwaterloo.ca>, July 2002.
- [58] H. Chen and J. Liu. "A Weighted multi-model Short-term Load Forecasting System". In *Proc. of IEEE International Conference on Power System Technology*, pp. 557–561, New York, August 1998.
- [59] J. Flory and T. Caramanis, "Electricity Transactions in an Open Access Market," *IEEE Power Engineering Review*, vol. 16, no. 1, January 1996, pp. 15–18.
- [60] D. T. Y. Cheng, "Economic Analysis of the Electricity Market in England and Wales," *IEEE Power Engineering Review*, vol. 19, no. 4, April 1999, pp. 57–59.
- [61] H. Chen, C. A. Canizares, and A. Singh. "Web-based Transaction Operational Feasibility Analysis in Electricity Markets". In *Proceeding of IEEE/PES 2002 Summer Meeting*, July 2002.
- [62] NERC, *Available Transfer Capability Definitions and Determination*. NERC, USA, 1996.

- [63] F. L. Alvarado, R. J. Camfield, and R. Rajaraman. “ Open transmission access: an efficient minimal role for the ISO ”. In *Proceedings of the Thirtieth Hawaii International Conference on System Sciences*, pp. 571–580, Hawaii, 1997.
- [64] R. S. Fang and A. K. David, “Transmission Congestion Management in an Electricity Market,” *IEEE Transactions on Power Systems*, vol. 14, no. 3, August 1999, pp. 877–883.
- [65] “Open Access Same-Time Information System and Standards of Conduct, Order No.889,” technical report, FERC, 1996.
- [66] W. Y. Ng, “Generalized Generation Distribution Factors for Power System Security Evaluation,” *IEEE Transactions On Power Application Systems*, vol. 100, no. 3, August 1981, pp. 1001–1005.
- [67] C. Kirby and M. A. Rahman. “Generator Contribution Coefficients for Pricing Transmission Services ”. In *Proceeding of IEEE/PES 2000 Winter Meeting*, January 2000.
- [68] J. Yang and M. D. Anderson. “ Tracing the Flow of Power in Transmission Networks for Use-of-Transmission-System Charges and Congestion Management ”. In *Proceeding of IEEE/PES 1998 Winter Meeting*, pp. 399–405, January 1998.
- [69] J. G. Vlachogiannis, “Accurate Model for Contribution of Generation to Transmission System Effect on Charges and Congestion Management,” *IEE Proc.-Gener, Transm. Distrib*, vol. 147, no. 6, November 2000, pp. 342–348.

- [70] M. E. Baran, V. Banunarayanan, and K. E. Garren, "A Transaction Assessment Method for Allocation of Transmission Services," *IEEE Transactions on Power Systems*, vol. 14, no. 3, August 1999, pp. 920–928.
- [71] K. R. W. Bell and D. S. Kirschen, "Improved Sensitivities in MW Dispatch for Control of Voltage," *IEEE Transactions on Power Systems*, vol. 15, no. 3, August 2000, pp. 1034–1040.
- [72] S. Greene, I. Dobson, and F. L. Alvarado, "Sensitivity of the Loading Margin to Voltage Collapse with Respect to Arbitrary Parameters," *IEEE Transactions on Power Systems*, vol. 12, no. 1, February 1997, pp. 262–272.
- [73] S. Greene, I. Dobson, and F. L. Alvarado, "Sensitivity of Transfer Capability Margins with a Fast Formula," Accepted for *IEEE Transaction on Power Systems* subject to mandatory revisions, preprint available at www.pserc.cornell.edu/tcc, December 1999.
- [74] C. A. Cañizares and F. L. Alvarado, "Point of Collapse and Continuation Methods for Large AC/DC Systems," *IEEE Transactions on Power Systems*, vol. 8, no. 1, February 1993, pp. 1–8.
- [75] V. Ajjarapu and C. Christy, "The Continuation Power Flow: A Tool for Steady State Voltage Stability Analysis," *IEEE Transactions on Power Systems*, vol. 7, no. 1, February 1992, pp. 416–423.
- [76] C. A. Cañizares, A. C. Z. Souza, and V. H. Quintana, "Comparison of Performance Indices for Detection of Proximity to Voltage Collapse," *IEEE Transactions On Power Systems*, vol. 11, no. 3, August 1996, pp. 1441–1450.
- [77] S. X. Guo and J. A. Momoh. "The Homotopy Continuation Method to Approach Voltage Collapse of Electric Power Systems". In *1993 IEEE Interna-*

- tional Symposium on Circuits and Systems*, volume 4, pp. 2644–2647, may 1993.
- [78] C. A. Cañizares, F. L. Alvarado, C. L. DeMarco, I. Dobson, and W. F. Long, “Point of Collapse Methods Applied to AC/DC Power Systems,” *IEEE Transactions on Power Systems*, vol. 7, no. 2, May 1992, pp. 673–683.
- [79] C. A. Cañizares, “Conditions for Saddle-node Bifurcations in ac/dc Power Systems,” *Int. J of Electric Power and Energy Systems*, vol. 17, no. 1, February 1995, pp. 61–68.
- [80] C. A. Cañizares, “On Bifurcations, Voltage Collapse and Load Modelling,” *IEEE Transactions on Power Systems*, vol. 10, no. 1, February 1995, pp. 512–522.
- [81] C. A. Cañizares, “Calculating Optimal System Parameters to Maximize the Distance to Saddle-node Bifurcations,” *IEEE Transactions on Circuits and Systems I: Fundamental Theory and Applications*, vol. 45, no. 3, March 1998, pp. 225–237.
- [82] I. Dobson, “Observations on the Geometry of Saddle Node Bifurcation and Voltage Collapse in Electrical Power Systems,” *IEEE Transactions on Circuits and Systems*, vol. 39, no. 3, March 1992, pp. 240–243.
- [83] I. Dobson and L. Lu, “Voltage Collapse Precipitated by the Immediate Change in Stability When Generator Reactive Power Limits are Encountered ,” *IEEE Transactions on Circuits and Systems*, vol. 39, no. 9, September 1992, pp. 762–766.
- [84] P. Kundur, *Power System Stability and Control*. McGraw-Hill, Inc., California, USA, 1994.

- [85] A. A. Fouad, V. Vittal, and T. K. Oh, "Critical Energy for Direct Transient Stability Assessment of Multi-machine Power System," *IEEE Transactions on Power Application System*, vol. 103, no. 8, 1984, pp. 2199–2206.
- [86] A. A. Fouad and V. Vittal, "Direct Transient Stability Analysis Using Energy Functions Application to Large Power Networks," *IEEE Transactions on Power System*, vol. 2, no. 1, 1987, pp. 37–44.
- [87] H. Chiang, F. F. Wu, and P. P. Varaiya, "Foundation of the Potential Energy Boundary Surface Method for Power System Transient Stability Analysis ," *IEEE Transactions on CAS*, vol. 35, no. 6, 1988, pp. 712–728.
- [88] G. A. Maria, C. Tang, and J. Kim, "Hybrid Transient Stability Analysis ," *IEEE Transactions on Power Systems*, vol. 5, no. 2, May 1990, pp. 384–393.
- [89] H. Chen, J. Xu, and Y. Shan. " A Hybrid Method for Transient Stability Analysis ". In *Proceeding of IFAC/CIGRE Symposium on Control of Power Systems and Power Plants (CPSPP)*, Beijing, China, August 1997.
- [90] G. C. Ejebe, J. G. Waight, J. G. Frame, X. Wang, and W. F. Tinney, "Available Transfer Capability Calculations," *IEEE Transactions on Power Systems*, vol. 13, no. 4, November 1998, pp. 1521–1527.
- [91] C. A. Cañizares, A. Berizzi, and P. Marannino, "Using FACTS Controllers to Maximize Available Transfer Capability," *Proceeding of Bulk Power Systems Dynamics and Control-IV Restructuring*, vol. 1, August 1998, pp. 633–641.
- [92] J. Tong, "Real Time Transfer Limit Calculation," *Proc. IEEE-PES Summer Meeting*, vol. 2, July 2000, pp. 1297–1302.

- [93] C. A. Cañizares, *UWPFLOW*. University of Waterloo, <http://www.power.uwaterloo.ca>, November 1999.
- [94] R. Billinton and R. Ghajar. “Evaluation of the Marginal Outage Costs of Generating Systems for the Purposes of Spot Pricing ”. In *Proceeding of IEEE/PES 1993 Winter Meeting*, january 1993.
- [95] A. D. Papalexopoulos, S. Hao, and T. M. Peng, “An Implementation of a Neural Network Based Load Forecasting Model for the EMS,” *IEEE Transactions on Power Systems*, vol. 9, no. 4, November 1994, pp. 1956–1962.
- [96] H. Chen, “A Practical On-line Predicting System for Short-Term Load,” *East China Electric Power*, vol. 24, no. 3, March 1996.
- [97] H. Chen, “An Implementation of Power System Short-Term Load Forecasting,” *Power System Automation*, December 1997.
- [98] I. Moghram and S. Rahman, “Analysis and Evaluation of Five Short-Term Load Forecasting Techniques,” *IEEE Transactions on Power Systems*, vol. 4, no. 4, October 1989, pp. 1484–1491.
- [99] A. D. Papalexopoulos and T. C. Hesterberg, “A Regression-Based Approach to Short-Term System Load Forecasting,” *IEEE Transactions on Power Systems*, vol. 5, no. 4, November 1990, pp. 1535–1547.
- [100] M. T. Hagan and S. M. Behr, “The Time Series Approach to Short-Term Load Forecasting,” *IEEE Transactions on Power Systems*, vol. 2, no. 3, August 1987, pp. 785–791.
- [101] A. S. Dhdashti, J. R. Tudor, and M. C. Smith, “Forecasting of Hourly Load

- by Pattern Recognition: A Deterministic Approach,” *IEEE Transactions on Power Apparatus and Systems*, vol. 101, no. 9, September 1982, pp. 00–11.
- [102] J. Toyada, M. Chen, and Y. Inoue, “An Application of State Estimation to Short-Term Load Forecasting, I and II,” *IEEE Transactions on Power Apparatus and Systems*, vol. 89, September 1970, pp. 1678–1688.
- [103] S. Rahman and R. Bhatnagar, “An Expert System Based Algorithm for Short-Term Load Forecast,” *IEEE Transactions on Power Systems*, vol. 3, no. 2, May 1988, pp. 392–399.
- [104] C. N. Lu, H. T. Wu, and S. Vemuri, “Neural Network Based Short Term Load Forecasting,” *IEEE Transactions on Power Systems*, vol. 8, no. 1, February 1993, pp. 337–342.
- [105] P. K. Dash, H. P. Satpathy, A. C. Liew, and S. Rahman, “A Real-time Short-Term Load Forecasting System Using Functional Link Network,” *IEEE Transactions on Power Systems*, vol. 12, no. 2, May 1997, pp. 675–680.
- [106] J. Vermaak, “Recurrent Neural Networks for Short-Term Load Forecasting,” *IEEE Transactions on Power Systems*, vol. 13, no. 1, February 1998, pp. 126–132.
- [107] S. E. Papadakis, “A Novel Approach to Short-Term Load Forecasting Using Fuzzy Neural Network,” *IEEE Tran. on Power Systems*, vol. 13, no. 2, May 1998, pp. 480–492.
- [108] T. Zheng, A. A. Girgis, and E. B. Makram, ““A Hybrid Wavelet-Kalman Filter Method for Load Forecasting”,” *Electric Power Systems Research*, vol. 54, no. 1, April 2000, pp. 11–17.

- [109] C. Lau, *Neural Networks Theoretical Foundations and Analysis*. IEEE Press, 1992.
- [110] R. J. Schalkoff, *Artificial Neural Networks*. The McGRAW-HILL Companies, Inc., 1997.
- [111] H. Chen, C. A. Cañizares, and A. Singh, “Web-based Computing for Power System Applications,” *The proceedings of the Thirty-first Annual North American Power Symposium*, October 1999, pp. 302–306.
- [112] W. H. Dunn Jr., M. A. Rossi, and B. Avramovic, “Impact of Market Restructuring on Power Systems Operation,” *IEEE Computer Applications in Power*, vol. 8, no. 1, January 1995, pp. 42–47.
- [113] F. Shahzad and A. Z. Khan, “An Application of Java for Power System Stability,” *IEEE Power Engineering Review*, vol. 18, no. 4, April 1998, pp. 45–46.
- [114] Q. Zhao, G. Huang, X. Luo, and X. Wu, “A Software Architecture Style for Deregulated Power Markets,” *Proceeding of IEEE Power Engineering Society Winter Meeting*, January 2001, pp. 1497–1502.
- [115] B. Qiu and H. B. Gooi, “Web-based SCADA Display Systems (WSDS) for Access via Internet,” *IEEE Transactions On Power Systems*, vol. 15, no. 2, May 2000, pp. 681–686.
- [116] H. Suzuki M. Marmioli, “Web-based Framework for Electricity Market,” *International Conference on Electric Utility Deregulation and Restructuring and Power Technologies 2000*, April 2000.

- [117] W. L. Chan, A. T. P. So, and L. L. Lai, "Internet Based Transmission Substation Monitoring," *IEEE Transactions on Power Systems*, vol. 14, no. 1, February 1999, pp. 293–298.
- [118] H. Chen, *Web-based Transaction Security Cost Analysis in Power Brokerage System*. Ph.D. Comprehensive Proposal, Canada, 2000.
- [119] Sun Microsystems, *The Java Tutorial*. Sun Microsystems, <http://www.javasoft.com/docs/books/tutorial>, 1998.
- [120] H. Chen, C. A. Cañizares, and A. Singh. "ANN-based Short-Term Load Forecasting in Electricity Markets". In *Proc. of IEEE Power Engineering Society Winter Meeting*, pp. 411–415, Columbus, January 2001.
- [121] H. Chen, "Transaction Security Cost Analysis based on Voltage Security Criteria," Presented in the Student Poster Session of 2001 IEEE/PES Winter Meeting, January 2001.
- [122] C. A. Cañizares, H. Chen, F. Milano, and A. Singh, "Transmission Congestion Management and Pricing in Simple Auction Electricity Markets," Submitted to *IEEE Transactions on Power Systems*, November 2002.
- [123] H. Chen, C. A. Cañizares, and A. Singh, "Web-based Transaction Security Cost Analysis," To be submitted to *IEEE Transactions on Power Systems*, December 2002.

Appendix A

Three-area Electricity Market

The system data for the 3-area electricity market example is in WSCC format.

```
C*****
C                                     TITLE
C
C
HDG
    UWPFLOW data file, WSCC format
    3-area example : normal state
    October 2000
BAS
C
C*****
C
C                                     AC BUSES
C
C                                     | SHUNT |
C | Ow|Name |kV |Z|PL |QL |MW |Mva|PM |PG |QM |Qm |Vpu
BE 1 AREA 1  138 1  150  80  0  0  0  150  0  01.02
B  1 AREA 2  138 2  150  70  0  80  0  100  0  01.00
B  1 AREA 3  138 3   50  30  0  50  0  100  0  01.00
C
C*****
```

```

C
C
C          AC LINES
C
C          M          CS      N
C |Ow|Name_1 |kV1||Name_2 |kV2||In || R   | X   | G/2 | B/2 |Mil|
L  1 AREA 1   138 AREA 2   1381 15001 .01  0.12
L  1 AREA 1   138 AREA 3   1381 15001 .01  0.12
L  1 AREA 2   138 AREA 3   1381 15001 .01  0.12
C
C*****
C
C          SOLUTION CONTROL CARD
C
C          1          2          3          4          5          6          7          8
C 34567890123456789012345678901234567890123456789012345678901234567890
C          |Max|  |SLACK BUS |
C          |Itr|  |Name   |kV|   |Angle   |
SOL          50  AREA 1   138      0.
END

```


Appendix B

Six-bus Test System

The system data for the 6-bus test system in WSCC format is listed:

```
C*****
C                                     TITLE
C
HDG
    UWPFLOW data file, WSCC format
    6-bus example : normal state
    December 2000
BAS
C
C*****
C
C                                     AC BUSES
C
C                                     | SHUNT |
C | Ow|Name |kV |Z|PL |QL |MW |Mva|PM |PG |QM |Qm |Vpu
BQ 1 GENCO 1 230 1 0 0 0 0 089.87 150 -1501.05
BQ 1 GENCO 2 230 2 0 0 0 0 0 140 150 -1501.05
BQ 1 GENCO 3 230 3 0 0 0 0 0 60 150 -1501.05
B 1 ESCO 1 230 4 90 60 0 0 0 0 0 00.9754
B 1 ESCO 2 230 5 100 70 0 0 0 0 0 00.9677
```

```

B  1 ESCO 3   230 6   90   60   0   0   0   0   0   00.9930
C
C*****
C
C                      AC LINES
C
C                      M          CS      W
C  |Ow|Name_1 |kV1||Name_2 |kV2||In || R   | X   | G/2 | B/2 |Mil|
L  1 GENCO 1   230 GENCO 2   2301 15001 .1   .2   0.0  0.02
L  1 GENCO 1   230 ESCO 1   2301 15001 .05  .2   0.0  0.02
L  1 GENCO 1   230 ESCO 2   2301 15001 .08  .3   0.0  0.03
L  1 GENCO 2   230 GENCO 3   2301 15001 .05  .25  0.0  0.03
L  1 GENCO 2   230 ESCO 1   2301 15001 .05  .1   0.0  0.01
L  1 GENCO 2   230 ESCO 2   2301 15001 .1   .3   0.0  0.02
L  1 GENCO 2   230 ESCO 3   2301 15001 .07  .2   0.0  0.025
L  1 GENCO 3   230 ESCO 2   2301 15001 .12  .26  0.0  0.025
L  1 GENCO 3   230 ESCO 3   2301 15001 .02  .1   0.0  0.01
L  1 ESCO 1   230 ESCO 2   2301 15001 .2   .4   0.0  0.04
L  1 ESCO 2   230 ESCO 3   2301 15001 .1   .3   0.0  0.03
C
C*****
C
C                      SOLUTION CONTROL CARD
C
C                      1          2          3          4          5          6          7          8
C 34567890123456789012345678901234567890123456789012345678901234567890
C                      |Max|  |SLACK BUS |
C                      |Itr|  |Name   |kV|   |Angle   |
SOL                      50  GENCO 1  230       0.
END

```

The price-quantity bids send by market participants are shown in Table B.1.

Table B.1: Price-quantity bids

Participants	Quantity (MW)	Bid price (\$/MWh)
GENCO 1 (S_1)	20	9.7
GENCO 2 (S_2)	25	8.8
GENCO 3 (S_3)	20	7
ESCO 1 (D_1)	25	12
ESCO 2 (D_2)	10	10.5
ESCO 3 (D_3)	20	9.5

Appendix C

129-bus Model of Italian HV Transmission System

The system data for the 129-bus model of the Italian 400 KV transmission system in IEEE format is:

13/09/02 ULYSSES ARCHIVE					100.00 2002 S 129-Bus 167-Line System																			
BUS DATA FOLLOW					129 ITEMS																			
1	Entracque	1	0	2	1.0526	0.000	0.0000	0.0000	517.628	0.000	380.00	1.0526	1311.00	-986.00	0.0000	0.0000	1							
2	La Spezia	1	0	2	1.0405	0.000	144.0000	102.4000	374.381	0.000	380.00	1.0405	1372.00	-1318.00	0.0000	0.0000	2							
3	Trino	1	0	2	1.0433	0.000	0.0000	0.0000	265.608	0.000	380.00	1.0433	490.00	-375.00	0.0000	0.0000	3							
4	Vado	1	0	2	1.0466	0.000	160.0000	56.0000	511.962	0.000	380.00	1.0466	1176.00	-824.00	0.0000	0.0000	4							
5	Edolo c.le	1	0	2	1.0647	0.000	0.0000	0.0000	393.626	0.000	380.00	1.0647	1152.00	-832.00	0.0000	0.0000	5							
6	La Casella	1	0	2	1.0530	0.000	0.0000	0.0000	241.654	0.000	380.00	1.0530	1176.00	-360.00	0.0000	0.0000	6							
7	Roncoval. c	1	0	2	1.0432	0.000	0.0000	0.0000	183.232	0.000	380.00	1.0432	1008.00	-728.00	0.0000	0.0000	7							
8	Ostiglia	1	0	2	1.0802	0.000	-112.8000	9.6000	256.810	0.000	380.00	1.0802	1174.00	-550.00	0.0000	0.0000	8							
9	S. Fiorano	1	0	2	1.0617	0.000	0.0000	0.0000	308.016	0.000	380.00	1.0617	560.00	-404.00	0.0000	0.0000	9							
10	Piacenza	1	0	2	1.0524	0.000	0.0000	0.0000	236.800	0.000	380.00	1.0524	596.00	-360.00	0.0000	0.0000	10							
11	Sermide	1	0	2	1.0847	0.000	0.0000	0.0000	494.438	0.000	380.00	1.0847	1176.00	-360.00	0.0000	0.0000	11							
12	Tavazzano	1	0	2	1.0530	0.000	164.8000	3.2000	879.238	0.000	380.00	1.0530	1176.00	-404.00	0.0000	0.0000	12							
13	Turbigo c.l	1	0	2	1.0462	0.000	0.0000	0.0000	764.045	0.000	380.00	1.0462	1550.00	-692.00	0.0000	0.0000	13							
14	Fusina	1	0	2	1.0813	0.000	0.0000	0.0000	76.820	0.000	380.00	1.0813	879.00	-194.00	0.0000	0.0000	14							
15	Portotolle	1	0	2	1.0889	0.000	7.2000	4.0000	1383.120	0.000	380.00	1.0889	2460.00	-1412.00	0.0000	0.0000	15							
16	Monfalcone	1	0	2	1.0816	0.000	0.0000	0.0000	254.412	0.000	380.00	1.0816	291.00	-18.00	0.0000	0.0000	16							
17	Bargi c.le	1	0	2	1.0471	0.000	0.0000	0.0000	191.998	0.000	380.00	1.0471	294.00	-214.00	0.0000	0.0000	17							
18	Piombino	1	0	2	1.0568	0.000	0.0000	0.0000	838.390	0.000	380.00	1.0568	1176.00	-836.00	0.0000	0.0000	18							
19	Torre nord	1	0	2	1.0553	0.000	0.0000	0.0000	981.600	0.000	380.00	1.0553	2352.00	-1080.00	0.0000	0.0000	19							
20	Montalto c.	1	0	3	1.0589	0.000	0.0000	0.0000	2173.712	0.000	380.00	1.0589	3272.00	-1432.00	0.0000	0.0000	20							

APPENDIX C. 129-BUS MODEL OF ITALIAN HV TRANSMISSION SYSTEM155

21	Torre sud	1	0	2	1.0536	0.000	0.0000	0.0000	387.190	0.000	380.00	1.0536	1048.00	-496.00	0.0000	0.0000	21
22	Brindisi c.	1	0	2	1.0783	0.000	20.8000	16.8000	1640.880	0.000	380.00	1.0783	2352.00	-900.00	0.0000	0.0000	22
23	Presenzano	1	0	2	1.0526	0.000	0.0000	0.0000	471.168	0.000	380.00	1.0526	1080.00	-780.00	0.0000	0.0000	23
24	Rossano	1	0	2	1.0711	0.000	96.8000	33.6000	599.270	0.000	380.00	1.0711	1235.00	-1048.00	0.0000	0.0000	24
25	Isab Erg	1	0	2	1.0367	0.000	0.0000	0.0000	251.973	0.000	380.00	1.0367	556.00	-354.00	0.0000	0.0000	25
26	Casanova	1	0	1	1.0000	0.000	304.8000	58.4000	0.000	0.000	380.00	0.0000	0.00	0.00	0.0000	0.0000	26
27	Castelnuovo	1	0	1	1.0000	0.000	191.2000	52.8000	0.000	0.000	380.00	0.0000	0.00	0.00	0.0000	0.0000	27
28	Hagliano	1	0	1	1.0000	0.000	236.8000	68.0000	0.000	0.000	380.00	0.0000	0.00	0.00	0.0000	0.0000	28
29	Piossasco	1	0	1	1.0000	0.000	280.0000	140.0000	0.000	0.000	380.00	0.0000	0.00	0.00	0.0000	0.0000	29
30	Rondissone	1	0	1	1.0000	0.000	242.4000	72.0000	0.000	0.000	380.00	0.0000	0.00	0.00	0.0000	0.0000	30
31	Leini	1	0	1	1.0000	0.000	131.2000	80.8000	0.000	0.000	380.00	0.0000	0.00	0.00	0.0000	0.0000	31
32	Albertville	1	0	2	1.0420	0.000	0.0000	0.0000	719.200	0.000	380.00	1.0420	9900.00	-9900.00	0.0000	0.0000	32
33	Venaus	1	0	1	1.0000	0.000	65.6000	-12.8000	0.000	0.000	380.00	0.0000	0.00	0.00	0.0000	0.0000	33
34	Villarodin	1	0	2	1.0518	0.000	0.0000	0.0000	540.800	0.000	380.00	1.0518	9900.00	-9900.00	0.0000	0.0000	34
35	Vignole	1	0	1	1.0000	0.000	170.4000	102.4000	0.000	0.000	380.00	0.0000	0.00	0.00	0.0000	0.0000	35
36	Baggio	1	0	1	1.0000	0.000	236.8000	68.8000	0.000	0.000	380.00	0.0000	0.00	0.00	0.0000	0.0000	36
37	Bovisio	1	0	1	1.0000	0.000	296.0000	16.0000	0.000	0.000	380.00	0.0000	0.00	0.00	0.0000	0.0000	37
38	Ospiate	1	0	1	1.0000	0.000	215.2000	68.0000	0.000	0.000	380.00	0.0000	0.00	0.00	0.0000	0.0000	38
39	Lachiarella	1	0	1	1.0000	0.000	179.2000	38.4000	0.000	0.000	380.00	0.0000	0.00	0.00	0.0000	0.0000	39
40	Caorso	1	0	0	1.0000	0.000	0.0000	0.0000	0.000	0.000	380.00	0.0000	0.00	0.00	0.0000	0.0000	40
41	Cremona	1	0	1	1.0000	0.000	194.4000	96.8000	0.000	0.000	380.00	0.0000	0.00	0.00	0.0000	0.0000	41
42	Ciserano	1	0	1	1.0000	0.000	268.0000	23.2000	0.000	0.000	380.00	0.0000	0.00	0.00	0.0000	0.0000	42
43	Edolo	1	0	0	1.0000	0.000	0.0000	0.0000	0.000	0.000	380.00	0.0000	0.00	0.00	0.0000	0.0000	43
44	Cavo 871H1	1	0	0	1.0000	0.000	0.0000	0.0000	0.000	0.000	380.00	0.0000	0.00	0.00	0.0000	0.0000	44
45	Cavo 875H1	1	0	0	1.0000	0.000	0.0000	0.0000	0.000	0.000	380.00	0.0000	0.00	0.00	0.0000	0.0000	45
46	Flero	1	0	1	1.0000	0.000	115.2000	65.6000	0.000	0.000	380.00	0.0000	0.00	0.00	0.0000	0.0000	46
47	Gorlago	1	0	1	1.0000	0.000	129.6000	52.0000	0.000	0.000	380.00	0.0000	0.00	0.00	0.0000	0.0000	47
48	Have	1	0	1	1.0000	0.000	84.8000	44.8000	0.000	0.000	380.00	0.0000	0.00	0.00	0.0000	0.0000	48
49	S. Rocco	1	0	1	1.0000	0.000	266.4000	102.4000	0.000	0.000	380.00	0.0000	0.00	0.00	0.0000	0.0000	49
50	Turbigo	1	0	0	1.0000	0.000	0.0000	0.0000	0.000	0.000	380.00	0.0000	0.00	0.00	0.0000	0.0000	50
51	Verderio	1	0	1	1.0000	0.000	224.0000	26.4000	0.000	0.000	380.00	0.0000	0.00	0.00	0.0000	0.0000	51
52	Dolo	1	0	0	1.0000	0.000	0.0000	0.0000	0.000	0.000	380.00	0.0000	0.00	0.00	0.0000	0.0000	52
53	Dugale	1	0	1	1.0000	0.000	204.8000	62.4000	0.000	0.000	380.00	0.0000	0.00	0.00	0.0000	0.0000	53
54	Planais	1	0	1	1.0000	0.000	96.0000	3.2000	0.000	0.000	380.00	0.0000	0.00	0.00	0.0000	0.0000	54
55	Redipuglia	1	0	1	1.0000	0.000	-1.6000	3.2000	0.000	0.000	380.00	0.0000	0.00	0.00	0.0000	0.0000	55
56	Venezia	1	0	1	1.0000	0.000	196.8000	21.6000	0.000	0.000	380.00	0.0000	0.00	0.00	0.0000	0.0000	56
57	Bargi	1	0	0	1.0000	0.000	0.0000	0.0000	0.000	0.000	380.00	0.0000	0.00	0.00	0.0000	0.0000	57
58	Calenzano	1	0	1	1.0000	0.000	280.8000	70.4000	0.000	0.000	380.00	0.0000	0.00	0.00	0.0000	0.0000	58
59	Forli'	1	0	1	1.0000	0.000	199.2000	74.4000	0.000	0.000	380.00	0.0000	0.00	0.00	0.0000	0.0000	59
60	Harginone	1	0	1	1.0000	0.000	263.2000	75.2000	0.000	0.000	380.00	0.0000	0.00	0.00	0.0000	0.0000	60
61	Hartignone	1	0	1	1.0000	0.000	364.8000	76.8000	0.000	0.000	380.00	0.0000	0.00	0.00	0.0000	0.0000	61
62	Parma	1	0	1	1.0000	0.000	380.8000	76.0000	0.000	0.000	380.00	0.0000	0.00	0.00	0.0000	0.0000	62
63	Poggio a Ca	1	0	1	1.0000	0.000	400.0000	222.4000	0.000	0.000	380.00	0.0000	0.00	0.00	0.0000	0.0000	63
64	Suvereto	1	0	1	1.0000	0.000	48.0000	51.2000	0.000	0.000	380.00	0.0000	0.00	0.00	0.0000	0.0000	64
65	S. Damaso	1	0	1	1.0000	0.000	231.2000	69.6000	0.000	0.000	380.00	0.0000	0.00	0.00	0.0000	0.0000	65
66	Aurelia	1	0	0	1.0000	0.000	0.0000	0.0000	0.000	0.000	380.00	0.0000	0.00	0.00	0.0000	0.0000	66
67	Fano	1	0	1	1.0000	0.000	0.8000	0.0400	0.000	0.000	380.00	0.0000	0.00	0.00	0.0000	0.0000	67
68	Latina	1	0	1	1.0000	0.000	188.0000	87.2000	0.000	0.000	380.00	0.0000	0.00	0.00	0.0000	0.0000	68
69	Montalto	1	0	1	1.0000	0.000	111.2000	19.2000	0.000	0.000	380.00	0.0000	0.00	0.00	0.0000	0.0000	69
70	Roma nord	1	0	1	1.0000	0.000	450.4000	117.6000	0.000	0.000	380.00	0.0000	0.00	0.00	0.0000	0.0000	70
71	Roma sud	1	0	1	1.0000	0.000	481.6000	83.2000	0.000	0.000	380.00	0.0000	0.00	0.00	0.0000	0.0000	71
72	S. Lucia	1	0	1	1.0000	0.000	389.6000	79.2000	0.000	0.000	380.00	0.0000	0.00	0.00	0.0000	0.0000	72
73	Brindisi 30	1	0	0	1.0000	0.000	0.0000	0.0000	0.000	0.000	380.00	0.0000	0.00	0.00	0.0000	0.0000	73
74	Brindisi 00	1	0	1	1.0000	0.000	155.2000	28.8000	0.000	0.000	380.00	0.0000	0.00	0.00	0.0000	0.0000	74

APPENDIX C. 129-BUS MODEL OF ITALIAN HV TRANSMISSION SYSTEM156

75	Brindisi 01	1	0	0	1.0000	0.000	0.0000	0.0000	0.000	0.000	380.00	0.0000	0.00	0.00	0.0000	0.0000	75
76	Valmontone	1	0	1	1.0000	0.000	219.2000	54.4000	0.000	0.000	380.00	0.0000	0.00	0.00	0.0000	0.0000	76
77	Villanova	1	0	1	1.0000	0.000	200.8000	64.0000	0.000	0.000	380.00	0.0000	0.00	0.00	0.0000	0.0000	77
78	Benevento	1	0	1	1.0000	0.000	158.4000	44.0000	0.000	0.000	380.00	0.0000	0.00	0.00	0.0000	0.0000	78
79	Foggia	1	0	1	1.0000	0.000	168.0000	49.6000	0.000	0.000	380.00	0.0000	0.00	0.00	0.0000	0.0000	79
80	Garigliano	1	0	1	1.0000	0.000	114.4000	10.4000	0.000	0.000	380.00	0.0000	0.00	0.00	0.0000	0.0000	80
81	Laino	1	0	1	1.0000	0.000	113.6000	135.2000	0.000	0.000	380.00	0.0000	0.00	0.00	0.0000	0.0000	81
82	Haterra	1	0	0	1.0000	0.000	0.0000	0.0000	0.000	0.000	380.00	0.0000	0.00	0.00	0.0000	0.0000	82
83	Montecorvin	1	0	1	1.0000	0.000	470.4000	187.2000	0.000	0.000	380.00	0.0000	0.00	0.00	0.0000	0.0000	83
84	Rizziconi	1	0	1	1.0000	0.000	224.8000	77.6000	0.000	0.000	380.00	0.0000	0.00	0.00	0.0000	0.0000	84
85	S. Sofia	1	0	1	1.0000	0.000	307.2000	144.0000	0.000	0.000	380.00	0.0000	0.00	0.00	0.0000	0.0000	85
86	Taranto	1	0	1	1.0000	0.000	52.8000	99.2000	0.000	0.000	380.00	0.0000	0.00	0.00	0.0000	0.0000	86
87	Sorgente	1	0	2	1.0114	0.000	0.0000	0.0000	221.600	0.000	380.00	1.0114	400.00	-400.00	0.0000	0.0000	87
88	Galatina	1	0	1	1.0000	0.000	191.2000	20.0000	0.000	0.000	380.00	0.0000	0.00	0.00	0.0000	0.0000	88
89	Bari ovest	1	0	1	1.0000	0.000	287.2000	126.4000	0.000	0.000	380.00	0.0000	0.00	0.00	0.0000	0.0000	89
90	Larino	1	0	1	1.0000	0.000	88.8000	30.4000	0.000	0.000	380.00	0.0000	0.00	0.00	0.0000	0.0000	90
91	Rosara	1	0	1	1.0000	0.000	226.4000	76.8000	0.000	0.000	380.00	0.0000	0.00	0.00	0.0000	0.0000	91
92	Candia	1	0	1	1.0000	0.000	264.0000	70.4000	0.000	0.000	380.00	0.0000	0.00	0.00	0.0000	0.0000	92
93	S. Martino	1	0	1	1.0000	0.000	178.4000	75.2000	0.000	0.000	380.00	0.0000	0.00	0.00	0.0000	0.0000	93
94	Ravenna	1	0	1	1.0000	0.000	40.0000	27.2000	0.000	0.000	380.00	0.0000	0.00	0.00	0.0000	0.0000	94
95	Divaca	1	0	2	1.0778	0.000	0.0000	0.0000	217.600	0.000	380.00	1.0778	9900.00	-9900.00	0.0000	0.0000	95
96	Adria	1	0	1	1.0000	0.000	69.6000	46.4000	0.000	0.000	380.00	0.0000	0.00	0.00	0.0000	0.0000	96
97	Camin	1	0	1	1.0000	0.000	227.2000	106.4000	0.000	0.000	380.00	0.0000	0.00	0.00	0.0000	0.0000	97
98	Salgareda	1	0	1	1.0000	0.000	73.6000	124.8000	0.000	0.000	380.00	0.0000	0.00	0.00	0.0000	0.0000	98
99	Udine ovest	1	0	1	1.0000	0.000	204.8000	19.2000	0.000	0.000	380.00	0.0000	0.00	0.00	0.0000	0.0000	99
100	Lonato	1	0	1	1.0000	0.000	202.4000	111.2000	0.000	0.000	380.00	0.0000	0.00	0.00	0.0000	0.0000	100
101	Nogarole	1	0	1	1.0000	0.000	90.4000	38.4000	0.000	0.000	380.00	0.0000	0.00	0.00	0.0000	0.0000	101
102	Cordignano	1	0	1	1.0000	0.000	96.0000	64.8000	0.000	0.000	380.00	0.0000	0.00	0.00	0.0000	0.0000	102
103	Sandri	1	0	1	1.0000	0.000	209.6000	127.2000	0.000	0.000	380.00	0.0000	0.00	0.00	0.0000	0.0000	103
104	Ferrara	1	0	1	1.0000	0.000	203.2000	107.2000	0.000	0.000	380.00	0.0000	0.00	0.00	0.0000	0.0000	104
105	Colunga	1	0	1	1.0000	0.000	210.4000	79.2000	0.000	0.000	380.00	0.0000	0.00	0.00	0.0000	0.0000	105
106	Tavarnuzze	1	0	1	1.0000	0.000	174.4000	43.2000	0.000	0.000	380.00	0.0000	0.00	0.00	0.0000	0.0000	106
107	Roma est	1	0	1	1.0000	0.000	88.8000	30.4000	0.000	0.000	380.00	0.0000	0.00	0.00	0.0000	0.0000	107
108	Rosen	1	0	2	1.0440	0.000	0.0000	0.0000	150.400	0.000	380.00	1.0440	200.00	-200.00	0.0000	0.0000	108
109	Acciaiolto	1	0	1	1.0000	0.000	91.2000	15.2000	0.000	0.000	380.00	0.0000	0.00	0.00	0.0000	0.0000	109
110	Rubiera	1	0	1	1.0000	0.000	371.2000	72.8000	0.000	0.000	380.00	0.0000	0.00	0.00	0.0000	0.0000	110
111	Roma ovest	1	0	1	1.0000	0.000	330.4000	131.2000	0.000	0.000	380.00	0.0000	0.00	0.00	0.0000	0.0000	111
112	Ceprano	1	0	1	1.0000	0.000	76.8000	47.2000	0.000	0.000	380.00	0.0000	0.00	0.00	0.0000	0.0000	112
113	S. Maria	1	0	1	1.0000	0.000	132.8000	41.6000	0.000	0.000	380.00	0.0000	0.00	0.00	0.0000	0.0000	113
114	Patria	1	0	1	1.0000	0.000	336.0000	161.6000	0.000	0.000	380.00	0.0000	0.00	0.00	0.0000	0.0000	114
115	Scandale	1	0	1	1.0000	0.000	44.0000	8.8000	0.000	0.000	380.00	0.0000	0.00	0.00	0.0000	0.0000	115
116	Paterno'	1	0	0	1.0000	0.000	0.0000	0.0000	0.000	0.000	380.00	0.0000	0.00	0.00	0.0000	0.0000	116
117	Chiarano	1	0	1	1.0000	0.000	92.0000	86.4000	0.000	0.000	380.00	0.0000	0.00	0.00	0.0000	0.0000	117
118	Andria	1	0	1	1.0000	0.000	190.4000	6.4000	0.000	0.000	380.00	0.0000	0.00	0.00	0.0000	0.0000	118
119	Hercallo	1	0	1	1.0000	0.000	213.6000	60.8000	0.000	0.000	380.00	0.0000	0.00	0.00	0.0000	0.0000	119
120	Lavorgne	1	0	2	1.0427	0.000	0.0000	0.0000	451.200	0.000	380.00	1.0427	9900.00	-9900.00	0.0000	0.0000	120
121	Husignano	1	0	0	1.0000	0.000	0.0000	0.0000	0.000	0.000	380.00	0.0000	0.00	0.00	0.0000	0.0000	121
122	Cagno	1	0	1	1.0000	0.000	172.0000	57.6000	0.000	0.000	380.00	0.0000	0.00	0.00	0.0000	0.0000	122
123	Cislago	1	0	1	1.0000	0.000	84.0000	41.6000	0.000	0.000	380.00	0.0000	0.00	0.00	0.0000	0.0000	123
124	Bulciago	1	0	1	1.0000	0.000	271.2000	73.6000	0.000	0.000	380.00	0.0000	0.00	0.00	0.0000	0.0000	124
125	Brugherio	1	0	1	1.0000	0.000	284.8000	96.0000	0.000	0.000	380.00	0.0000	0.00	0.00	0.0000	0.0000	125
126	Piancamuno	1	0	1	1.0000	0.000	108.0000	13.6000	0.000	0.000	380.00	0.0000	0.00	0.00	0.0000	0.0000	126
127	Chiari	1	0	1	1.0000	0.000	167.2000	21.6000	0.000	0.000	380.00	0.0000	0.00	0.00	0.0000	0.0000	127
128	Travagliato	1	0	1	1.0000	0.000	140.8000	21.6000	0.000	0.000	380.00	0.0000	0.00	0.00	0.0000	0.0000	128

APPENDIX C. 129-BUS MODEL OF ITALIAN HV TRANSMISSION SYSTEM157

129	Seazza	1	0	2	1.0381	0.000	0.0000	0.0000	8.000	0.000	380.00	1.0381	9900.00-9900.00	0.0000	0.0000	129
-999																
BRANCH DATA FOLLOW																
167 ITEMS																
26	28	1	1	1	0	0.0006063	0.00890000	0.1791360	1422	0	0	0	0	0.0000	0.000	0.0000
26	29	1	1	1	0	0.0005125	0.00599375	0.0867680	1235	0	0	0	0	0.0000	0.000	0.0000
26	30	1	1	1	0	0.0010625	0.00996250	0.1405280	1086	0	0	0	0	0.0000	0.000	0.0000
27	3	1	1	1	0	0.0007500	0.01098120	0.2183680	1853	0	0	0	0	0.0000	0.000	0.0000
27	35	1	1	1	0	0.0004375	0.00636250	0.1299440	1422	0	0	0	0	0.0000	0.000	0.0000
27	36	1	1	1	0	0.0007062	0.01018750	0.2079200	1422	0	0	0	0	0.0000	0.000	0.0000
28	29	1	1	1	0	0.0007500	0.01098750	0.2184800	1422	0	0	0	0	0.0000	0.000	0.0000
28	4	1	1	1	0	0.0007250	0.01236870	0.1932640	1243	0	0	0	0	0.0000	0.000	0.0000
29	31	1	1	1	0	0.0004281	0.00631563	0.1257600	1253	0	0	0	0	0.0000	0.000	0.0000
29	33	1	1	1	0	0.0004281	0.00631563	0.1257600	1253	0	0	0	0	0.0000	0.000	0.0000
33	34	1	1	1	0	0.0004281	0.00631563	0.1257600	1832	0	0	0	0	0.0000	0.000	0.0000
31	30	1	1	1	0	0.0004281	0.00631563	0.1257600	1422	0	0	0	0	0.0000	0.000	0.0000
30	3	1	1	1	0	0.0002563	0.00368125	0.0731200	1853	0	0	0	0	0.0000	0.000	0.0000
30	32	1	1	1	0	0.0002563	0.00368125	0.0731200	2486	0	0	0	0	0.0000	0.000	0.0000
30	50	1	1	1	0	0.0008625	0.01267500	0.2547200	1422	0	0	0	0	0.0000	0.000	0.0000
2	35	1	1	1	0	0.0019875	0.02380630	0.3072000	957	0	0	0	0	0.0000	0.000	0.0000
2	60	1	1	1	0	0.0010437	0.01488120	0.3016800	1414	0	0	0	0	0.0000	0.000	0.0000
2	62	1	1	1	0	0.0010250	0.01755000	0.2674400	1414	0	0	0	0	0.0000	0.000	0.0000
2	109	1	1	1	0	0.0010250	0.01755000	0.2674400	1414	0	0	0	0	0.0000	0.000	0.0000
109	108	1	1	1	0	0.0003125	0.00453125	0.0928000	1134	0	0	0	0	0.0000	0.000	0.0000
109	60	1	1	1	0	0.0003125	0.00453125	0.0928000	2828	0	0	0	0	0.0000	0.000	0.0000
4	35	1	1	1	0	0.0007688	0.01360000	0.1942400	1243	0	0	0	0	0.0000	0.000	0.0000
36	38	1	1	1	0	0.0001563	0.00226562	0.0464000	1422	0	0	0	0	0.0000	0.000	0.0000
38	37	1	1	1	0	0.0001563	0.00226562	0.0464000	1706	0	0	0	0	0.0000	0.000	0.0000
36	39	1	1	1	0	0.0003625	0.00525625	0.1066000	1422	0	0	0	0	0.0000	0.000	0.0000
39	6	1	1	1	0	0.0003625	0.00525625	0.1066000	1422	0	0	0	0	0.0000	0.000	0.0000
36	50	1	1	1	0	0.0003062	0.00450625	0.1696800	1853	0	0	0	0	0.0000	0.000	0.0000
37	123	1	1	1	0	0.0002708	0.00397708	0.0797333	1853	0	0	0	0	0.0000	0.000	0.0000
123	122	1	1	1	0	0.0002708	0.00397708	0.0797333	1365	0	0	0	0	0.0000	0.000	0.0000
122	121	1	1	1	0	0.0002708	0.00397708	0.0797333	1365	0	0	0	0	0.0000	0.000	0.0000
37	125	1	1	1	0	0.0002563	0.00372187	0.0756000	1422	0	0	0	0	0.0000	0.000	0.0000
125	12	1	1	1	0	0.0002563	0.00372187	0.0756000	1853	0	0	0	0	0.0000	0.000	0.0000
37	50	1	1	1	0	0.0002563	0.00364375	0.0762400	1365	0	0	0	0	0.0000	0.000	0.0000
37	51	1	1	1	0	0.0003563	0.00478125	0.0752800	1389	0	0	0	0	0.0000	0.000	0.0000
37	124	1	1	1	0	0.0003563	0.00478125	0.0752800	941	0	0	0	0	0.0000	0.000	0.0000
124	129	1	1	1	0	0.0003563	0.00478125	0.0752800	957	0	0	0	0	0.0000	0.000	0.0000
40	41	1	1	1	0	0.0004438	0.00659687	0.1279200	1243	0	0	0	0	0.0000	0.000	0.0000
41	46	1	1	1	0	0.0004438	0.00659687	0.1279200	1853	0	0	0	0	0.0000	0.000	0.0000
40	49	1	1	1	0	0.0002625	0.00403125	0.0754400	1243	0	0	0	0	0.0000	0.000	0.0000
40	65	1	1	1	0	0.0014062	0.02061250	0.4132800	1414	0	0	0	0	0.0000	0.000	0.0000
43	9	1	1	1	0	0.0000969	0.00127938	0.1864000	2843	0	0	0	0	0.0000	0.000	0.0000
43	44	1	1	1	0	0.0000484	0.00063969	0.0932000	975	0	0	0	0	0.0000	0.000	0.0000
43	45	1	1	1	0	0.0000484	0.00063969	0.0932000	975	0	0	0	0	0.0000	0.000	0.0000
44	5	1	1	1	0	0.0000484	0.00063969	0.0932000	1422	0	0	0	0	0.0000	0.000	0.0000
45	5	1	1	1	0	0.0000484	0.00063969	0.0932000	1422	0	0	0	0	0.0000	0.000	0.0000
46	128	1	1	1	0	0.0001708	0.00253125	0.0507733	1422	0	0	0	0	0.0000	0.000	0.0000
128	127	1	1	1	0	0.0001708	0.00253125	0.0507733	1422	0	0	0	0	0.0000	0.000	0.0000
127	47	1	1	1	0	0.0001708	0.00253125	0.0507733	1422	0	0	0	0	0.0000	0.000	0.0000
46	48	1	1	1	0	0.0003125	0.00357500	0.0520800	1235	0	0	0	0	0.0000	0.000	0.0000
46	8	1	1	1	0	0.0011000	0.01610620	0.3228800	1422	0	0	0	0	0.0000	0.000	0.0000
47	126	1	1	1	0	0.0002375	0.00360625	0.1786000	1422	0	0	0	0	0.0000	0.000	0.0000

APPENDIX C. 129-BUS MODEL OF ITALIAN HV TRANSMISSION SYSTEM158

126	9	1	1	1	0	0.0002375	0.00360625	0.1786000	1422	0	0	0	0	0.0000	0.000	0.0000	0.0000	0.0000	0.0000	0.0000
47	51	1	1	1	0	0.0004375	0.00580000	0.0913600	1389	0	0	0	0	0.0000	0.000	0.0000	0.0000	0.0000	0.0000	0.0000
6	49	1	1	1	0	0.0002875	0.00415000	0.0840000	1422	0	0	0	0	0.0000	0.000	0.0000	0.0000	0.0000	0.0000	0.0000
121	119	1	1	1	0	0.0004062	0.00589688	0.1196000	1422	0	0	0	0	0.0000	0.000	0.0000	0.0000	0.0000	0.0000	0.0000
119	50	1	1	1	0	0.0004062	0.00589688	0.1196000	1853	0	0	0	0	0.0000	0.000	0.0000	0.0000	0.0000	0.0000	0.0000
48	9	1	1	1	0	0.0006375	0.01004380	0.1769600	1243	0	0	0	0	0.0000	0.000	0.0000	0.0000	0.0000	0.0000	0.0000
48	100	1	1	1	0	0.0003792	0.00554375	0.1115730	1422	0	0	0	0	0.0000	0.000	0.0000	0.0000	0.0000	0.0000	0.0000
100	101	1	1	1	0	0.0003792	0.00554375	0.1115733	1853	0	0	0	0	0.0000	0.000	0.0000	0.0000	0.0000	0.0000	0.0000
101	53	1	1	1	0	0.0003792	0.00554375	0.1115733	1853	0	0	0	0	0.0000	0.000	0.0000	0.0000	0.0000	0.0000	0.0000
8	11	1	1	1	0	0.0001500	0.00215625	0.0471200	1422	0	0	0	0	0.0000	0.000	0.0000	0.0000	0.0000	0.0000	0.0000
8	53	1	1	1	0	0.0004625	0.00674375	0.1356800	1422	0	0	0	0	0.0000	0.000	0.0000	0.0000	0.0000	0.0000	0.0000
8	104	1	1	1	0	0.0007531	0.01100625	0.2212000	1414	0	0	0	0	0.0000	0.000	0.0000	0.0000	0.0000	0.0000	0.0000
104	59	1	1	1	0	0.0007531	0.01100625	0.2212000	1414	0	0	0	0	0.0000	0.000	0.0000	0.0000	0.0000	0.0000	0.0000
49	12	1	1	1	0	0.0004938	0.00713125	0.1450400	1853	0	0	0	0	0.0000	0.000	0.0000	0.0000	0.0000	0.0000	0.0000
49	62	1	1	1	0	0.0007500	0.01075630	0.2185600	1414	0	0	0	0	0.0000	0.000	0.0000	0.0000	0.0000	0.0000	0.0000
11	61	1	1	1	0	0.0007125	0.01044370	0.2096800	1414	0	0	0	0	0.0000	0.000	0.0000	0.0000	0.0000	0.0000	0.0000
12	42	1	1	1	0	0.0004219	0.00617812	0.1218800	1853	0	0	0	0	0.0000	0.000	0.0000	0.0000	0.0000	0.0000	0.0000
42	51	1	1	1	0	0.0004219	0.00617812	0.1218800	1137	0	0	0	0	0.0000	0.000	0.0000	0.0000	0.0000	0.0000	0.0000
52	97	1	1	1	0	0.0004469	0.00650000	0.1304000	1853	0	0	0	0	0.0000	0.000	0.0000	0.0000	0.0000	0.0000	0.0000
97	53	1	1	1	0	0.0004469	0.00650000	0.1304000	1853	0	0	0	0	0.0000	0.000	0.0000	0.0000	0.0000	0.0000	0.0000
52	15	1	1	1	0	0.0004669	0.00693750	0.5196800	1422	0	0	0	0	0.0000	0.000	0.0000	0.0000	0.0000	0.0000	0.0000
52	96	1	1	1	0	0.0002334	0.00346875	0.2598400	1853	0	0	0	0	0.0000	0.000	0.0000	0.0000	0.0000	0.0000	0.0000
96	15	1	1	1	0	0.0002334	0.00346875	0.2598400	1422	0	0	0	0	0.0000	0.000	0.0000	0.0000	0.0000	0.0000	0.0000
52	56	1	1	1	0	0.0001156	0.00168437	0.1280000	2843	0	0	0	0	0.0000	0.000	0.0000	0.0000	0.0000	0.0000	0.0000
53	103	1	1	1	0	0.0006094	0.00891719	0.1765200	1422	0	0	0	0	0.0000	0.000	0.0000	0.0000	0.0000	0.0000	0.0000
103	102	1	1	1	0	0.0006094	0.00891719	0.1765200	1853	0	0	0	0	0.0000	0.000	0.0000	0.0000	0.0000	0.0000	0.0000
102	99	1	1	1	0	0.0006094	0.00891719	0.1765200	1853	0	0	0	0	0.0000	0.000	0.0000	0.0000	0.0000	0.0000	0.0000
99	54	1	1	1	0	0.0006094	0.00891719	0.1765200	1422	0	0	0	0	0.0000	0.000	0.0000	0.0000	0.0000	0.0000	0.0000
54	55	1	1	1	0	0.0003062	0.00451875	0.0884000	1422	0	0	0	0	0.0000	0.000	0.0000	0.0000	0.0000	0.0000	0.0000
55	95	1	1	1	0	0.0003062	0.00451875	0.0884000	1706	0	0	0	0	0.0000	0.000	0.0000	0.0000	0.0000	0.0000	0.0000
54	98	1	1	1	0	0.0003344	0.00491875	0.0975200	1422	0	0	0	0	0.0000	0.000	0.0000	0.0000	0.0000	0.0000	0.0000
98	56	1	1	1	0	0.0003344	0.00491875	0.0975200	1422	0	0	0	0	0.0000	0.000	0.0000	0.0000	0.0000	0.0000	0.0000
15	94	1	1	1	0	0.0003117	0.00461250	0.3531600	1414	0	0	0	0	0.0000	0.000	0.0000	0.0000	0.0000	0.0000	0.0000
15	59	1	1	1	0	0.0006234	0.00922500	0.7063200	1414	0	0	0	0	0.0000	0.000	0.0000	0.0000	0.0000	0.0000	0.0000
94	59	1	1	1	0	0.0003117	0.00461250	0.3531600	1414	0	0	0	0	0.0000	0.000	0.0000	0.0000	0.0000	0.0000	0.0000
57	58	1	1	1	0	0.0004062	0.00654375	0.1062400	1135	0	0	0	0	0.0000	0.000	0.0000	0.0000	0.0000	0.0000	0.0000
57	61	1	1	1	0	0.0005688	0.00825000	0.1657600	1414	0	0	0	0	0.0000	0.000	0.0000	0.0000	0.0000	0.0000	0.0000
58	63	1	1	1	0	0.0001412	0.00212500	0.1886400	1414	0	0	0	0	0.0000	0.000	0.0000	0.0000	0.0000	0.0000	0.0000
58	106	1	1	1	0	0.0000706	0.00106250	0.0943200	1414	0	0	0	0	0.0000	0.000	0.0000	0.0000	0.0000	0.0000	0.0000
106	63	1	1	1	0	0.0000706	0.00106250	0.0943200	1414	0	0	0	0	0.0000	0.000	0.0000	0.0000	0.0000	0.0000	0.0000
58	64	1	1	1	0	0.0012438	0.01818750	0.3652000	1414	0	0	0	0	0.0000	0.000	0.0000	0.0000	0.0000	0.0000	0.0000
59	105	1	1	1	0	0.0006719	0.00979063	0.1939200	1414	0	0	0	0	0.0000	0.000	0.0000	0.0000	0.0000	0.0000	0.0000
105	61	1	1	1	0	0.0006719	0.00979063	0.1939200	1414	0	0	0	0	0.0000	0.000	0.0000	0.0000	0.0000	0.0000	0.0000
59	93	1	1	1	0	0.0002742	0.00402312	0.3237600	1414	0	0	0	0	0.0000	0.000	0.0000	0.0000	0.0000	0.0000	0.0000
59	67	1	1	1	0	0.0005484	0.00804625	0.6475200	1414	0	0	0	0	0.0000	0.000	0.0000	0.0000	0.0000	0.0000	0.0000
93	67	1	1	1	0	0.0002742	0.00402312	0.3237600	1414	0	0	0	0	0.0000	0.000	0.0000	0.0000	0.0000	0.0000	0.0000
60	63	1	1	1	0	0.0001844	0.00269750	0.2164800	2828	0	0	0	0	0.0000	0.000	0.0000	0.0000	0.0000	0.0000	0.0000
61	65	1	1	1	0	0.0002812	0.00415625	0.0828000	1414	0	0	0	0	0.0000	0.000	0.0000	0.0000	0.0000	0.0000	0.0000
62	110	1	1	1	0	0.0003656	0.00522813	0.1099200	1414	0	0	0	0	0.0000	0.000	0.0000	0.0000	0.0000	0.0000	0.0000
110	65	1	1	1	0	0.0003656	0.00522813	0.1099200	1414	0	0	0	0	0.0000	0.000	0.0000	0.0000	0.0000	0.0000	0.0000
63	64	1	1	1	0	0.0011000	0.01590000	0.3215200	1414	0	0	0	0	0.0000	0.000	0.0000	0.0000	0.0000	0.0000	0.0000
63	70	1	1	1	0	0.0031688	0.04543750	0.9129600	1414	0	0	0	0	0.0000	0.000	0.0000	0.0000	0.0000	0.0000	0.0000
64	69	1	1	1	0	0.0007031	0.01055440	0.7951200	2828	0	0	0	0	0.0000	0.000	0.0000	0.0000	0.0000	0.0000	0.0000
66	69	1	1	1	0	0.0001719	0.00257813	0.1937600	3924	0	0	0	0	0.0000	0.000	0.0000	0.0000	0.0000	0.0000	0.0000

APPENDIX C. 129-BUS MODEL OF ITALIAN HV TRANSMISSION SYSTEM159

66	71	1	1	1	0	0.0009750	0.01426870	0.2855200	1962	0	0	0	0	0.0000	0.000	0.0000	0.0000	0.0000	0.0000	0.0000
66	72	1	1	1	0	0.0000219	0.00034375	0.0254400	3924	0	0	0	0	0.0000	0.000	0.0000	0.0000	0.0000	0.0000	0.0000
67	92	1	1	1	0	0.0009146	0.01350620	0.2647470	1422	0	0	0	0	0.0000	0.000	0.0000	0.0000	0.0000	0.0000	0.0000
92	91	1	1	1	0	0.0009146	0.01350620	0.2647470	1365	0	0	0	0	0.0000	0.000	0.0000	0.0000	0.0000	0.0000	0.0000
91	77	1	1	1	0	0.0009146	0.01350620	0.2647470	1365	0	0	0	0	0.0000	0.000	0.0000	0.0000	0.0000	0.0000	0.0000
68	71	1	1	1	0	0.0003006	0.00381000	0.2707360	3270	0	0	0	0	0.0000	0.000	0.0000	0.0000	0.0000	0.0000	0.0000
68	76	1	1	1	0	0.0006750	0.00790000	0.1104000	1308	0	0	0	0	0.0000	0.000	0.0000	0.0000	0.0000	0.0000	0.0000
68	112	1	1	1	0	0.0003950	0.00512500	0.3461520	1308	0	0	0	0	0.0000	0.000	0.0000	0.0000	0.0000	0.0000	0.0000
68	80	1	1	1	0	0.0007900	0.01025000	0.6923040	1422	0	0	0	0	0.0000	0.000	0.0000	0.0000	0.0000	0.0000	0.0000
112	80	1	1	1	0	0.0003950	0.00512500	0.3461520	1134	0	0	0	0	0.0000	0.000	0.0000	0.0000	0.0000	0.0000	0.0000
69	76	1	1	1	0	0.0008219	0.01239690	0.9364800	3327	0	0	0	0	0.0000	0.000	0.0000	0.0000	0.0000	0.0000	0.0000
69	77	1	1	1	0	0.0026750	0.03920620	0.7835200	1962	0	0	0	0	0.0000	0.000	0.0000	0.0000	0.0000	0.0000	0.0000
70	72	1	1	1	0	0.0011688	0.01298120	0.2033440	1308	0	0	0	0	0.0000	0.000	0.0000	0.0000	0.0000	0.0000	0.0000
70	107	1	1	1	0	0.0000744	0.00087000	0.0121680	1308	0	0	0	0	0.0000	0.000	0.0000	0.0000	0.0000	0.0000	0.0000
107	76	1	1	1	0	0.0006694	0.00783000	0.1095120	1308	0	0	0	0	0.0000	0.000	0.0000	0.0000	0.0000	0.0000	0.0000
71	111	1	1	1	0	0.0001375	0.00151250	0.0236368	1308	0	0	0	0	0.0000	0.000	0.0000	0.0000	0.0000	0.0000	0.0000
111	72	1	1	1	0	0.0012375	0.01361250	0.2127312	1308	0	0	0	0	0.0000	0.000	0.0000	0.0000	0.0000	0.0000	0.0000
22	73	1	1	1	0	0.0000500	0.00055469	0.0395200	4537	0	0	0	0	0.0000	0.000	0.0000	0.0000	0.0000	0.0000	0.0000
76	23	1	1	1	0	0.0014000	0.02048750	0.4094400	1702	0	0	0	0	0.0000	0.000	0.0000	0.0000	0.0000	0.0000	0.0000
77	90	1	1	1	0	0.0009406	0.01377190	0.2742400	1663	0	0	0	0	0.0000	0.000	0.0000	0.0000	0.0000	0.0000	0.0000
90	79	1	1	1	0	0.0009406	0.01377190	0.2742400	1422	0	0	0	0	0.0000	0.000	0.0000	0.0000	0.0000	0.0000	0.0000
78	79	1	1	1	0	0.0014188	0.01606250	0.2540000	1134	0	0	0	0	0.0000	0.000	0.0000	0.0000	0.0000	0.0000	0.0000
78	23	1	1	1	0	0.0007562	0.01112500	0.2236000	1702	0	0	0	0	0.0000	0.000	0.0000	0.0000	0.0000	0.0000	0.0000
78	85	1	1	1	0	0.0003750	0.00538750	0.1089440	1365	0	0	0	0	0.0000	0.000	0.0000	0.0000	0.0000	0.0000	0.0000
74	73	1	1	1	0	0.0000344	0.00045937	0.0484800	3404	0	0	0	0	0.0000	0.000	0.0000	0.0000	0.0000	0.0000	0.0000
74	75	1	1	1	0	0.0002775	0.00403563	0.0813920	1134	0	0	0	0	0.0000	0.000	0.0000	0.0000	0.0000	0.0000	0.0000
74	89	1	1	1	0	0.0013875	0.02017810	0.4069600	1066	0	0	0	0	0.0000	0.000	0.0000	0.0000	0.0000	0.0000	0.0000
89	79	1	1	1	0	0.0013875	0.02017810	0.4069600	1365	0	0	0	0	0.0000	0.000	0.0000	0.0000	0.0000	0.0000	0.0000
74	86	1	1	1	0	0.0006312	0.00916250	0.1845280	1365	0	0	0	0	0.0000	0.000	0.0000	0.0000	0.0000	0.0000	0.0000
73	118	1	1	1	0	0.0014812	0.02119688	0.4292000	1702	0	0	0	0	0.0000	0.000	0.0000	0.0000	0.0000	0.0000	0.0000
118	79	1	1	1	0	0.0014812	0.02119688	0.4292000	1702	0	0	0	0	0.0000	0.000	0.0000	0.0000	0.0000	0.0000	0.0000
73	82	1	1	1	0	0.0013625	0.01931250	0.3872000	1702	0	0	0	0	0.0000	0.000	0.0000	0.0000	0.0000	0.0000	0.0000
73	88	1	1	1	0	0.0007469	0.01101250	0.2217600	1702	0	0	0	0	0.0000	0.000	0.0000	0.0000	0.0000	0.0000	0.0000
88	86	1	1	1	0	0.0007469	0.01101250	0.2217600	1702	0	0	0	0	0.0000	0.000	0.0000	0.0000	0.0000	0.0000	0.0000
80	23	1	1	1	0	0.0003437	0.00498125	0.1010560	1702	0	0	0	0	0.0000	0.000	0.0000	0.0000	0.0000	0.0000	0.0000
80	113	1	1	1	0	0.0002153	0.00292006	0.2224720	1414	0	0	0	0	0.0000	0.000	0.0000	0.0000	0.0000	0.0000	0.0000
113	85	1	1	1	0	0.0002153	0.00292006	0.2224720	1365	0	0	0	0	0.0000	0.000	0.0000	0.0000	0.0000	0.0000	0.0000
80	114	1	1	1	0	0.0002153	0.00292006	0.2224720	1134	0	0	0	0	0.0000	0.000	0.0000	0.0000	0.0000	0.0000	0.0000
114	85	1	1	1	0	0.0002153	0.00292006	0.2224720	1365	0	0	0	0	0.0000	0.000	0.0000	0.0000	0.0000	0.0000	0.0000
81	82	1	1	1	0	0.0013000	0.01906250	0.3825600	1702	0	0	0	0	0.0000	0.000	0.0000	0.0000	0.0000	0.0000	0.0000
81	83	1	1	1	0	0.0007031	0.01022810	0.8224320	2843	0	0	0	0	0.0000	0.000	0.0000	0.0000	0.0000	0.0000	0.0000
81	24	1	1	1	0	0.0004281	0.00620625	0.5002880	2843	0	0	0	0	0.0000	0.000	0.0000	0.0000	0.0000	0.0000	0.0000
82	86	1	1	1	0	0.0007438	0.01095000	0.2197600	1702	0	0	0	0	0.0000	0.000	0.0000	0.0000	0.0000	0.0000	0.0000
83	85	1	1	1	0	0.0008250	0.01201870	0.2420000	1422	0	0	0	0	0.0000	0.000	0.0000	0.0000	0.0000	0.0000	0.0000
84	115	1	1	1	0	0.0011781	0.01702187	0.3413600	1702	0	0	0	0	0.0000	0.000	0.0000	0.0000	0.0000	0.0000	0.0000
115	24	1	1	1	0	0.0011781	0.01702187	0.3413600	1702	0	0	0	0	0.0000	0.000	0.0000	0.0000	0.0000	0.0000	0.0000
84	87	1	1	1	0	0.0015375	0.01275630	0.9529600	867	0	0	0	0	0.0000	0.000	0.0000	0.0000	0.0000	0.0000	0.0000
25	117	1	1	1	0	0.0007958	0.01133750	0.2583360	1365	0	0	0	0	0.0000	0.000	0.0000	0.0000	0.0000	0.0000	0.0000
117	116	1	1	1	0	0.0007958	0.01133750	0.2583360	1365	0	0	0	0	0.0000	0.000	0.0000	0.0000	0.0000	0.0000	0.0000
116	87	1	1	1	0	0.0007958	0.01133750	0.2583360	1365	0	0	0	0	0.0000	0.000	0.0000	0.0000	0.0000	0.0000	0.0000
28	1	1	1	1	0	0.0005750	0.01051870	0.1410880	2486	0	0	0	0	0.0000	0.000	0.0000	0.0000	0.0000	0.0000	0.0000
121	7	1	1	1	0	0.0000375	0.00027500	0.0508800	2502	0	0	0	0	0.0000	0.000	0.0000	0.0000	0.0000	0.0000	0.0000
121	120	1	1	1	0	0.0000375	0.00027500	0.0508800	1209	0	0	0	0	0.0000	0.000	0.0000	0.0000	0.0000	0.0000	0.0000
49	10	1	1	1	0	0.0000750	0.00079375	0.0124000	1235	0	0	0	0	0.0000	0.000	0.0000	0.0000	0.0000	0.0000	0.0000

APPENDIX C. 129-BUS MODEL OF ITALIAN HV TRANSMISSION SYSTEM160

```

50  13  1 1  1 0 0.0000078 0.00003906 0.0070400 3706      0      0      0 0 0.0000      0.000 0.0000 0.0000 0.0000 0.0000 0.0000
52  14  1 1  1 0 0.0002563 0.00250625 0.0368800  975      0      0      0 0 0.0000      0.000 0.0000 0.0000 0.0000 0.0000 0.0000
55  16  1 1  1 0 0.0002188 0.00230625 0.0407200 1235      0      0      0 0 0.0000      0.000 0.0000 0.0000 0.0000 0.0000 0.0000
57  17  1 1  1 0 0.0000063 0.00011094 0.0048800 2268      0      0      0 0 0.0000      0.000 0.0000 0.0000 0.0000 0.0000 0.0000
64  18  1 1  1 0 0.0001312 0.00146563 0.0912800 2268      0      0      0 0 0.0000      0.000 0.0000 0.0000 0.0000 0.0000 0.0000
66  19  1 1  1 0 0.0000313 0.00035425 0.0836000 5232      0      0      0 0 0.0000      0.000 0.0000 0.0000 0.0000 0.0000 0.0000
69  20  1 1  1 0 0.0000187 0.00027150 0.0815360 5459      0      0      0 0 0.0000      0.000 0.0000 0.0000 0.0000 0.0000 0.0000
72  21  1 1  1 0 0.0000531 0.00059206 0.0370400 2275      0      0      0 0 0.0000      0.000 0.0000 0.0000 0.0000 0.0000 0.0000
-999
LOSS ZONES FOLLOW                1 ITEMS
1 129-Bus
-99
INTERCHANGE DATA FOLLOW        1 ITEMS
1 1 Entracque      0.00 999.99 129Bus 129-Bus 167-Line System
-9
TIE LINES FOLLOW                0 ITEMS
-999
END OF DATA

```

The supply bids are shown in Tables C.1 and C.2, and the demand bids are shown in Tables C.3, C.4, C.5, C.6 .

Table C.1: Supply bids: I

Bus Number	Quantity (100MW)	Bid price (\$/MWh)
1	2.5167	30.0000
2	1.8500	34.1600
3	1.1667	33.6000
4	2.4667	32.5200
5	2.1333	30.0000
6	1.2333	37.9600
7	0.9333	34.0000
8	1.2333	35.2000
9	0.5167	30.0000
10	1.2333	36.5200
11	2.4667	35.0400
12	1.2333	34.8400
13	3.2833	34.1200
14	3.6833	33.6400
15	5.0000	33.0400
16	0.1542	39.0000
17	0.2733	30.0000
18	1.2333	37.7600
19	5.0000	32.8800
20	3.4333	32.8000
21	2.2167	35.5200
22	2.5000	36.6000
23	2.0000	30.0000

Table C.2: Supply bids: II

Bus Number	Quantity (100MW)	Bid price (\$/MWh)
24	3.4000	39.1200
25	1.1467	36.4400
32	1.2361	32.0000
34	0.9295	32.0000
87	0.3809	34.0000
95	0.3740	32.0000
108	0.2585	34.0000
120	0.7755	32.0000
129	0.0138	32.0000

Table C.3: Demand bids: I

Bus Number	Quantity (100MW)	Bid price (\$/MWh)
26	0.7938	34.8000
27	0.4979	36.0000
28	0.6167	36.4000
29	0.7292	34.8000
30	0.6312	36.4000
31	0.3417	37.2000
35	0.4437	35.2000
36	0.6167	34.8000
37	0.7708	34.8000
38	0.5604	36.4000
39	0.4667	35.2000
41	0.5062	36.0000
42	0.6979	35.6000
46	0.3000	36.4000
47	0.3375	34.4000
47	0.3375	34.4000
48	0.2208	36.0000
49	0.6937	35.2000
51	0.5833	34.0000
53	0.5333	35.2000
54	0.2500	34.0000
56	0.5125	34.0000
58	0.7312	37.6000

Table C.4: Demand bids: II

Bus Number	Quantity (100MW)	Bid price (\$/MWh)
59	0.5188	35.2000
60	0.6854	36.0000
61	0.9500	36.4000
62	0.9917	36.4000
63	1.0417	35.6000
64	0.1250	36.8000
65	0.6021	36.4000
67	0.0021	34.0000
68	0.4896	34.4000
69	0.2896	36.0000
70	1.1729	35.2000
71	1.2542	35.2000
72	1.0146	34.8000
74	0.4042	38.0000
76	0.5708	36.8000
77	0.5229	35.6000
78	0.4125	36.4000
79	0.4375	34.8000
80	0.2979	37.2000
81	0.2958	34.0000
83	1.2250	35.6000
84	0.5854	34.4000
85	0.8000	35.2000

Table C.5: Demand bids: III

Bus Number	Quantity (100MW)	Bid price (\$/MWh)
86	0.1375	34.4000
88	0.4979	34.8000
89	0.7479	37.2000
90	0.2313	36.4000
91	0.5896	34.0000
92	0.6875	36.4000
93	0.4646	37.2000
94	0.1042	34.8000
96	0.1812	36.4000
97	0.5917	38.0000
98	0.1917	34.8000
99	0.5333	36.0000
100	0.5271	36.8000
101	0.2354	37.6000
102	0.2500	34.4000
103	0.5458	35.6000
104	0.5292	37.6000
105	0.5479	34.8000
106	0.4542	38.0000
107	0.2313	36.8000
109	0.2375	34.4000
110	0.9667	35.2000
111	0.8604	34.8000

Table C.6: Demand bids: IV

Bus Number	Quantity (100MW)	Bid price (\$/MWh)
112	0.2000	35.6000
113	0.3458	36.8000
114	0.8750	37.2000
115	0.1146	36.4000
117	0.2396	35.2000
118	0.4958	36.8000
119	0.5563	36.0000
122	0.4479	34.4000
123	0.2188	36.8000
124	0.7062	34.8000
125	0.7417	37.2000
126	0.2812	34.0000
127	0.4354	36.0000
128	0.3667	37.6000